

2023-04-01

## Neurogenetic Function of Host Cell Factor-1

Victoria Lynn Castro  
*University of Texas at El Paso*

Follow this and additional works at: [https://scholarworks.utep.edu/open\\_etd](https://scholarworks.utep.edu/open_etd)



Part of the [Biology Commons](#), [Developmental Biology Commons](#), and the [Neuroscience and Neurobiology Commons](#)

---

### Recommended Citation

Castro, Victoria Lynn, "Neurogenetic Function of Host Cell Factor-1" (2023). *Open Access Theses & Dissertations*. 3772.

[https://scholarworks.utep.edu/open\\_etd/3772](https://scholarworks.utep.edu/open_etd/3772)

This is brought to you for free and open access by ScholarWorks@UTEP. It has been accepted for inclusion in Open Access Theses & Dissertations by an authorized administrator of ScholarWorks@UTEP. For more information, please contact [lweber@utep.edu](mailto:lweber@utep.edu).

# NEUROGENETIC FUNCTION OF HOST-CELL-FACTOR-1

VICTORIA LYNN CASTRO

Doctoral Program in Biosciences

APPROVED:

---

Anita M. Quintana, Ph.D. Chair

---

Marc B. Cox, Ph.D.

---

Sergio D. Iñiguez, Ph.D.

---

Sukla Roychowdhury, Ph.D.

---

Michael Kenney, Ph.D.

---

Stephen L. Crites, Jr., Ph.D.  
Dean of the Graduate School

# NEUROGENETIC FUNCTION OF HOST-CELL-FACTOR-1

by

VICTORIA LYNN CASTRO, B.S.

DISSERTATION

Presented to the Faculty of the Graduate School of  
The University of Texas at El Paso  
In Partial Fulfillment  
Of the Requirements  
For the Degree of

DOCTOR OF PHILOSOPHY

Department of Biological Sciences  
THE UNIVERSITY OF TEXAS AT EL PASO

May 2023

## ACKNOWLEDGEMENTS

First and foremost, I would like to praise and thank God, who has granted countless blessings, knowledge, and opportunity, to allow me to accomplish this thesis. I am thankful for my fiancé, Ruben who has supported my journey and every high and low moment throughout my entire professional career, from high school, undergraduate, to graduate school. I am most grateful to my mentor, Dr. Anita Quintana, for her invaluable advice, continuous support, and patience during my PhD study. Her extensive personal and professional guidance has taught me a great deal about both scientific research and life in general. I am grateful to all of those with whom I have had the pleasure to work with during this and other related projects. To each of the members of my Dissertation Committee, thank you for providing immense knowledge and encouragement during my academic research.

## ABSTRACT

Neural precursor cells (NPCs) are the stem-like cells of the developing brain. These cells differentiate into the differentiated cell types of the central nervous system. If disruption occurs in the number of total NPCs formed or their survival, various disorders including learning disabilities, behavioral problems, or epilepsy can occur. This dissertation describes how the *HCFC1* gene controls the proliferation and differentiation of NPCs. *HCFC1* encodes for a transcriptional co-factor that regulates the growth and metabolism of stem cells, including NPCs. Mutations in *HCFC1* cause *cbIX* syndrome, a neural developmental disorder that affects the nervous system and causes microcephaly, epilepsy, and intellectual disability. Since 2013, we have known that missense mutations in *HCFC1* cause *cbIX* syndrome with varied neurological impairments. However, since this finding there have been no studies to reveal a mechanism for how this occurs. Collectively, this dissertation describes independent studies using zebrafish as a model to study the function of HCFC1 and reveal a potential mechanism whereby HCFC1 regulates NPC proliferation and differentiation. Our first study describes how a loss of function (LOF) mutation in the *hcfc1a* gene in zebrafish results in increased numbers of proliferating NPCs and hypomotility. Subsequent RNA sequencing of these LOF mutants identified increased expression of *asx11*, a gene that encodes for a transcription factor that modulates cellular proliferation. We show that inhibition of *asx11* expression restored the number of NPCs to normal levels, demonstrating a potential mechanism by which *hcfc1a* regulates NPC proliferation and brain development. However, several questions remained to be addressed from this work. For example, RNA-sequencing was performed in whole brain homogenates which include a plethora of cells in addition to NPCs.

Therefore, we needed to address if *Asxl1* increases were directly involved in NPC development or an artifact of other cells such as endothelial or hematopoietic cell populations. Additionally, because of the transcriptional co-factor function of HCFC1, it is plausible that this protein bound to the promoter of *Asxl1* to increase mRNA expression, which was not fully investigated. Finally, protein validation of *Asxl1* was required to understand if the increases in mRNA also translated to changes in protein. Thus, in our following work, we sought to address these key questions. We used a missense mutant allele of *hcf1a* to further investigate the potential mechanism by which *Asxl1* might regulate abnormal brain development. We sought to use this allele because it was more representative of *cb1X* patients which inherit hemizygous missense mutations and have little to no protein changes in HCFC1. Using both the missense and nonsense alleles together, we sought to characterize the function of *Asxl1* in these two mutant backgrounds. We observed contrasting protein expression of two downstream target genes of HCFC1: *Asxl1* and *YWHAB*, a gene that encodes for the 14-3-3- $\beta/\alpha$  protein known to regulate AKT phosphorylation and activity. Interestingly, we found contrasting protein expression of Akt and downstream targets of mTor that correlated with contrasting numbers of radial glial cells produced. Based on these results we can conclude that mutations in *hcf1a* disrupt Akt/mTOR activity and glial cell development. These findings are the first to suggest a mechanism for how HCFC1 regulates different aspects of neurogenesis. Our data collectively provide a foundational understanding of how mutations in HCFC1 cause neurological impairments in humans and move the *cb1X* field forward by proposing possible therapeutic approaches that can be applied in the future.

## TABLE OF CONTENTS

ACKNOWLEDGEMENTS.....	iii
ABSTRACT.....	iv
TABLE OF CONTENTS.....	vi
LIST OF FIGURES.....	vii
LIST OF TABLES.....	viii
CHAPTER 1: LITERATURE REVIEW.....	1
CHAPTER 2: MANUSCRIPT PUBLICATION 1.....	21
CHAPTER 3: MANUSCRIPT PUBLICATION 2.....	59
CHAPTER 4: SUMMARY AND CONCLUSIONS.....	105
APPENDIX: LIST OF PUBLICATIONS.....	113
BIBLIOGRAPHY.....	114
BIOGRAPHICAL SKETCH.....	128

## LIST OF FIGURES

### CHAPTER I

Figure 1: HCFC1 Interacting Partners by domain.....	14
---	----

### CHAPTER II

Figure 1. Haploinsufficiency of the <i>hcfc1a<sup>co60/+</sup></i> allele ( <i>Co60/+</i> ).....	45
Figure 2: The <i>hcfc1a<sup>co60/+</sup></i> allele increases the number of Sox2+ cells in the developing brain.....	46
Figure 3: Increased Sox2+ cells are present in the <i>hcfc1a<sup>co60/+</sup></i> allele.....	47
Figure 4: The <i>hcfc1a<sup>co60/+</sup></i> allele is associated with increased cell proliferation and minimal cell death.....	48
Figure 5: The <i>hcfc1a<sup>co60/+</sup></i> allele increases the expression of differentiation markers.....	50
Figure 6: Over expression of HCFC1 decreases NPC number and differentiation...	51
Figure 7. The <i>hcfc1a<sup>co60/+</sup></i> allele regulates brain development and <i>asx1</i> expression.....	52
Figure 8: Inhibition of Asxl1 activity restores the NPC deficits in the <i>hcfc1a<sup>co60/+</sup></i> allele.....	54
Figure 9: Quantification of the number of NPCs after inhibition of Asxl1 activity.....	55
Figure 10: The <i>hcfc1a<sup>co60/+</sup></i> is associated with hypomotility.....	57

### CHAPTER III

Figure 1: Akt/mTor signaling is increased in the <i>hcfc1a<sup>co60/+</sup></i> allele.....	90
Figure 2: Missense and nonsense alleles of the <i>hcfc1a</i> gene differentially affect Hcfc1 expression.....	91
Figure 3: Differential regulation of Akt/mTor in the <i>hcfc1a<sup>co64</sup></i> allele.....	93
Figure 4: Neural precursors (NPCs) are increased in the <i>co64</i> allele.....	94
Figure 5: Radial glial cells (RGCs) are reduced in number and expression in the <i>co64</i> allele.....	96
Figure 6: <i>gfap</i> expression but not Sox2 cell number is mTor dependent.....	98
Figure 7: <i>cb1X</i> mutations differentially regulate <i>asx1</i> expression.....	100
Figure 8: Forced expression of Asxl1 does not drive NPC/RGC development but proteomics reveals differential expression of 14-3-3 $\beta\alpha$ in each <i>cb1X</i> allele.....	102
Figure 9: Proteomics demonstrates abnormal expression of ribosomal proteins and activation of Akt/mTor in the <i>Tg(hsp701:HCFC1<sup>c.344C&gt;T</sup>)</i> .....	104

## LIST OF TABLES

### CHAPTER I

Table 1: Summary of known HCFC1 variants with patient phenotype.....	13
--	----

## CHAPTER I

### SECTION I: REVIEW OF LITERATURE

Review manuscript: *The role of HCFC1 in syndromic and non-syndromic intellectual disability*

Castro, V., & Quintana, A. (2020). The role of HCFC1 in syndromic and non-syndromic intellectual disability. *Medical Research Archives*, 8(6). Doi:10.18103/mra.v8i6.2122

#### **Overview:**

This chapter presents a review manuscript written for publication to Medical Research Archives. Additional subheadings are included at the end of the manuscript to incorporate more recent findings and insight of the broader field.

#### **Abstract**

Mutations in the *HCFC1* gene are associated with syndromic (*cb1X*) and non-syndromic types of intellectual disability. Syndromic disorders present with severe neurological defects including intractable epilepsy, facial dysmorphism, and intellectual disability. Non-syndromic individuals have also been described and implicate a role for HCFC1 during brain development. The penetrance of phenotypes and the presence of an overall syndrome is associated with the location of specific mutations within the HCFC1 protein. Thus, one could hypothesize that the positioning of HCFC1 mutations lead to unique underlying cellular and molecular mechanisms. The HCFC1 protein is comprised of multiple domains that function in cellular proliferation/metabolism. Several reports of HCFC1 disease variants have been identified, but a comprehensive review of each

variant and its associated phenotypes has not yet been compiled. Here we perform a detailed review of HCFC1 function, model systems, variant location, and accompanying phenotypes to highlight current knowledge and the future status of the field.

## **History of Inborn Errors of Cellular Cobalamin Metabolism**

Cobalamin, also known as vitamin B12, is an essential molecule that is required for human metabolism. Once ingested from food, cobalamin undergoes various modifications that are required for the function of two enzymes in the body; methylmalonylCoA mutase (EC5.4.99.2) and methionine synthase (EC2.1.1.13)(1). The absorption of cobalamin requires multiple steps and is facilitated by many unique cobalamin-binding proteins, which are not the focus of this review. However, ultimately, intracellular cobalamin is reduced into two biologically active forms, 5'-deoxyadenosylcobalamin (AdoCbl) and methyl-cobalamin (MeCbl), these active forms function as co-factors in the mitochondria and cytosol, respectively.

Once in the cytoplasm, cobalamin binds to the enzymatic transport protein, MMACHC(2–4) and subsequently MMADHC.(5) Mutation of either *MMACHC* or *MMADHC* can cause an inborn error of cobalamin metabolism.(6,7) Inborn errors of cobalamin metabolism occur when the processing of cobalamin is defective, thus disrupting the functions of methylmalonylCoA mutase (EC5.4.99.2) and methionine synthase (EC2.1.1.13). Mutation of *MMACHC* causes methylmalonic aciduria and homocystinuria, cblC type (*cbIC*), while mutation of *MMADCH* results in methylmalonic aciduria and homocystinuria, cblD type (*cbID*). Additional sub-types exist and are associated with mutation in either intracellular transport (*cbIF* and *cbIE*) of cobalamin, the

conversion of homocysteine to methionine (*cbIG*), or additional enzymes within the mitochondrial pathway that cause similar disorders including *cbIA* and *cbIB*.(8,9)

Collectively, these inborn errors of cobalamin metabolism present as a multiple congenital anomaly syndrome. Depending on subtype, patients exhibit some form of methylmalonic aciduria or homocystinuria. However, other clinical phenotypes include megaloblastic anemia, leukopenia, thrombocytopenia, intellectual disabilities, and some degree of seizures.(1) The degree and onset of phenotypes varies with subtype and the mutation spectrum. Recently, clinical phenotypes that mirror specific subgroups have been observed, but these individuals do not have mutations in any of the genes associated with the complementation groups previously described. Such clinical cases fall into disorders of cobalamin metabolism that are of unknown genetic origin. One such example includes the recently described methylmalonic acidemia and homocysteinemia, *cbIX* type (*cbIX*) (MIM 309541).(10) *cbIX* is caused by mutations in the *HCFC1* gene, which encodes a transcriptional cofactor with nearly 5000 unique downstream target genes.(11) Interestingly, *HCFC1* has no known function in cobalamin metabolism, yet mutations in this gene cause a *cbIC* like disorder with metabolic defects, failure to thrive, craniofacial abnormalities, intractable epilepsy, and intellectual disabilities.

### ***cbIX* and related syndromes**

In 2013, *cbIX* was discovered using a trio based whole exome sequencing approach and was later confirmed in 14/18 total patients.(10) All patients had severe neurological defects that included intractable epilepsy and intellectual disability. Biochemical phenotypes in *cbIX* are present, but severity varies from patient to patient. In addition, mild to moderate craniofacial abnormalities are present in some *cbIX* patients.

In the original report, 5 unique mutations in the *HCFC1* gene were documented, each of which resides in the kelch protein interaction domain (Table 1). Of the five mutations, two affect amino acid 115, two affect amino acid 73, and one affects amino acid 68 (Table 1). Those that affect redundant amino acids do not cause the same missense change. For example, the p.Ala115Val and p.Ala115Thr variants both alter the amino acid at position 115, but with different amino acid substitutions. The effects of these two different mutations on protein function are not completely understood, but each cause overlapping clinical manifestations. Interestingly, additional studies have uncovered novel variants, some of which are not associated with cobalamin metabolism, but instead are associated with neural development and craniofacial abnormalities(12–16) (Table 1).

The mechanisms by which mutations in *HCFC1* cause such a myriad of clinical phenotypes are not completely understood. However, *HCFC1* is known to regulate genes that are essential for cell proliferation and metabolism.(17,18) For example, the metabolic deficits in *cbIX* syndrome are the result of defects in the expression of *MMACHC*, the gene associated with *cbIC* syndrome. The expression of *MMACHC* in patient derived fibroblasts is severely blunted and siRNA knockdown of *HCFC1* reduces *MMACHC* expression.(10) Subsequent reports have demonstrated that each mutation can have varying effects on *MMACHC* expression.(13) Some mutations including pSer225Asn and pGly876Ser (Table 1) moderately reduce the expression of *MMACHC*, while others have no effect on the level of *MMACHC* expression [(pAla1756Val and pArg2016Trp) (Table 1)].(13) These data strongly suggest that individual missense mutations disproportionately affect protein function. In support of this hypothesis, there are reports of individuals with mutations in *HCFC1* associated with intellectual disability,

microcephaly, and neural development defects in the absence(12,14) or presence(15,16) of cobalamin phenotypes.

HCFC1 regulates gene expression as part of a complex of other proteins including THAP11(19) and ZNF143.(11) Interaction with THAP11 and ZNF143 are essential to modulate the expression of *MMACHC*.(17) In accordance, a *cbIX*-like syndrome has been reported upon mutation of *THAP11* (20) and *ZNF143*. (21) Each of these disorders is associated with defects in *MMACHC* expression. These defects are likely the result of abnormal protein interactions as both THAP11 and ZNF143 have been shown to interact with the HCFC1 kelch domain (Figure 1), the site of mutations in HCFC1 that cause *cbIX* syndrome. However, the phenotypes of these syndromes are not limited to cobalamin metabolism and these individuals suffer from complex syndromes with hallmark neurological and neurodevelopmental defects.

### **Analysis of known *HCFC1* variants and corresponding phenotypes**

Previous studies have established that mutations in *HCFC1* are associated with a complex disorder that can include heterogeneous phenotypes spanning multiple body systems. *cbIX* syndrome is primarily associated with mutation of the kelch protein interaction domain of HCFC1.(10) These mutations appear to be unique because there are several other reports of mutations in other domains of HCFC1 that do not cause cobalamin deficiency.(12,14,16) For example, mutation in the promoter region of the *HCFC1* gene is associated with intellectual disability, but without cobalamin phenotypes.(12) Kelch domain mutations exclusively cause syndromic intellectual disability with cobalamin phenotypes,(10,15) with the exception of p.Ser225Asn reported by Huang and colleagues(12) (Table 1). However, the p.Ser225Asn was later shown to

regulate *MMACHC* expression(13) and was a presumed loss of function allele. However, whether this mutation is a loss of function allele has not been completely tested. There is one reported mutation within the fibronectin domain, the p.Ala477Asn variant, which is associated with intellectual disability and facial dysmorphism, but not cobalamin defects.(13) Mutations in the basic region have been described, which are generally associated with intellectual disability.(13,14,22,23) Of these, the p.Gly876Ser variant has been associated with mild regulation of the *MMACHC* promoter. Interestingly, other C-terminal variants including the p.Ala1756Val and p.Arg2016Trp variants are associated with intellectual disability and abnormal brain development, but not other phenotypes.

### **Known Functions of HCFC1**

The HCFC1 protein has several conserved protein domains including a kelch protein interaction domain, a fibronectin domain, and an HCF domain, which contains cleavage sites that facilitate protein processing and function(24–26) (Figure 1). The HCFC1 protein is cleaved into N and C-terminal fragments before functionality is unleashed.(25,27) The two cleavage products seemingly have different functions, but both individually regulate cell proliferation(26,28) and interact with one another.(29) HCFC1 lacks a true DNA binding domain, but regulates gene expression through interactions with transcription factors such as YY1, GABP, THAP11, ZNF143, and E2F(11,30) (Figure 1). Many of these interacting partners have a conserved HCFC1 binding motif (HBM) and this domain has been shown to interact with the kelch domain of HCFC1 (Figure 1). Of the interacting partners found in Figure 1, only GABP interacts in a protein domain outside of the kelch domain (Figure 1) and the specific binding site of YY1 has not been well established.

*HCFC1* is located on the X chromosome and has long been associated with Herpes Simplex Viral (HSV) infection where it is needed for the activation of early genes through its interactions with the VP16 transcription factor. (31) *HCFC1* interacts with VP16 via its kelch domain and mutation of the kelch domain *in vitro* causes defects in cell proliferation (32) and disrupts *HCFC1* binding with VP16. These data support the notion that cellular proteins behave in a similar fashion as does the VP16 protein. Notably, we identified at least five proteins in the literature that all interact with *HCFC1* via the kelch domain (Figure 1). Thus, mutations within the kelch domain are likely to interfere with protein: protein interactions and downstream functions. Such downstream functions include the regulation of *MMACHC* expression resulting in cobalamin deficiencies. Yet *cbfX* is complex and it is unclear whether other phenotypes are regulated via this same mechanism.

*HCFC1* is known to interact with various proteins, but the interaction with E2F and MLL (Figure 1) proteins drives cell proliferation.(30,33,34) Coordination of *HCFC1* interactions with the members of both protein families helps to facilitate the activation of S-phase promoter elements. For example, *HCFC1* can recruit MLL family members to E2F responsive promoters inducing transcriptional activation. However, some protein interactions that mediate cell proliferation are quite complex. *HCFC1* interacts with BAP1, a tumor suppressor that inhibits cell growth.(35) BAP is a deubiquitinating enzyme, thereby affecting protein stability. BAP1 interacts with the N-terminal domain of *HCFC1* resulting in deubiquitination (Figure 1), which promotes cell growth.(36,37) There are likely various unknown mechanisms by which the cell regulates *HCFC1* activity. Many of these are presumably via protein: protein interactions. Interestingly, a majority of these

protein interactions seem to regulate cell survival and DNA damage.(38) Based on these studies it is clear that HCFC1 function is complex, cell type specific, and highly reliant on the protein milieu. Consequently, missense mutations are highly likely to have distinct effects on protein function as they might interfere with distinct protein interactions.

### **Brain Development and HCFC1**

Mutation of *HCFC1*, either in *cbIX* or related syndromes, is associated with severe neurological defects, intractable epilepsy, and neural development defects.(10,12,13,20) *HCFC1* is expressed in fetal tissue (31), but the function of this gene in brain development is not completely understood and complex. Early *in vitro* assays performed by Huang and colleagues demonstrated that over expression of *Hcfc1* in mouse derived neurospheres reduced cell proliferation and biased differentiation of neural precursor cells (NPCs) towards an astrocyte lineage.(12) Supporting evidence for these observations was observed upon knockdown of *Hcfc1* in neurospheres, whereby decreased *Hcfc1* expression increased the numbers of NPCs, increased proliferation, and decreased differentiation.(13) Interestingly, disrupting the expression of *Hcfc1* does not recapitulate the effects of missense mutations. For example, over expression of wild type *Hcfc1* reduces proliferation, but the over expression of the p.Arg2016Trp variant (Table 1), a patient derived variant does not.(13) The function of each individual variant during brain development has not been described. However, it is highly likely that unique variants have specialized functions; consequently, causing heterogeneous syndromes of varied severity.

### **Murine models of Hcfc1 function**

In early 2016, a Cre-recombinase floxed allele of *Hcfc1* was created.(39) *Hcfc1* is required for embryonic development and therefore, deletion is lethal for hemizygous and homozygous carriers in mice.(40) Interestingly, female heterozygous carriers utilize compensatory mechanisms and X-linked inactivation to select for cells carrying the wild type allele, thus tolerating the mutation with only a temporary growth retardation. However, owing to the early lethality, this model was not appropriate for analysis of brain development. To circumvent this approach, a cell type specific conditional allele was created.(41) *Hcfc1* was conditionally deleted in a subpopulation of forebrain progenitors (Nkx2.1+) in the ventral telencephalon resulting in decreased numbers of GABAergic interneurons and glia, likely caused by increased cell death. Structural defects in brain development were also observed, which is consistent with the phenotypes reported in a subset of patients with *cbfX* syndrome.(10) These data are the first to implicate deletion of *Hcfc1* in the developing brain or in progenitor cells with increased apoptosis. Interestingly, similar strategies in murine hepatocytes demonstrated an increase in cell proliferation.(42) These data suggest a cell type specific function for *Hcfc1*. Moreover, deletion of *Hcfc1* in Nkx2.1+ cells contrasts with *in vitro* assays because knockdown *in vitro* causes increased NPCs, whereas cell type specific deletion causes a decrease in Nkx2.1+ cells. But these differences could be the result of the degree of knockdown, the brain microenvironment, and the influence of cell-type specific transcription factors that interact with HCFC1 protein. In addition, the marker used to track and follow cells is different across studies, which could affect overall interpretations.

### **Zebrafish models of *hcfc1* function**

While studies in mice have provided some understanding of Hcfc1 function, the early lethality and *in utero* gestation times have limited the effectiveness of these models. Consequently, additional model systems have been developed. Zebrafish are an alternative system for *in vivo* functional analyses.(43) They are externally fertilized, have a high fecundity, and easy to modify genetically by either transient knockdown or germline mutation. Zebrafish genome duplication has resulted in two *hcfc1* paralogs, *hcfc1a* and *hcfc1b*. These paralogs share approximately 70% identity and are conserved with both human and mouse *HCFC1*. Zebrafish do not have sex chromosomes and consequently the two genes are found on chromosomes 11 (*hcfc1a*) and 8 (*hcfc1b*). Knockdown of *hcfc1b* using anti-sense morpholinos is associated with reduced expression of the zebrafish *mmachc* gene,(44) suggesting this interaction is conserved across vertebrates. In addition, morphants present with craniofacial abnormalities owing to defects in the proliferation of neural crest cells (NCCs), a transient multi-potent progenitor cell population that gives rise to cartilage and bone of the head, neck, and face. More recently, additional analysis has demonstrated that knockdown of *hcfc1b* is associated with increased numbers of NPCs, consistent with *in vitro* assays, but contrasting with cell type specific murine models.(20) Similar facial and brain phenotypes were observed upon knockdown of the zebrafish *thap11* gene. Interestingly, these facial phenotypes can be restored by supplementing morphants with exogenous human MMACHC protein. In humans, THAP11, ZNF143, and HCFC1 interact to regulate *MMACHC* expression. Given the positive restoration of *hcfc1b* facial phenotypes by MMACHC, the presence of facial phenotypes upon deletion of *thap11*,(20) and the decreased *mmachc* expression in

*hcfc1b* morphants(44); it is plausible that the THAP11/ZNF143/HCF1 axis regulates facial development and NCCs in an MMACHC dependent manner.

Interestingly the effects of *hcfc1b* knockdown on NPCs is distinct from the effects on NCCs.(20,44) These differences are intriguing as both NPCs and NCCs are progenitor cell populations, albeit with different functions, microenvironments, and fate. Decreased *hcfc1b* expression causes increased numbers of NPCs and increased NPC proliferation; a phenotype that is consistent with knockdown of *thap11*. Interestingly, mutation of zebrafish *znf143* genes causes defects in brain development.(45) Recent *mmachc* mutants were created, but not characterized for NPC deficits; however, the presence of these germline mutants (46) would rapidly enable the characterization of NPCs in this system. While knockdown of *hcfc1b* results in increased NPCs, these data are not consistent with the observations by Minocha and colleagues, which suggest that deletion of *Hcfc1* in Nkx2.1+ precursors causes reduced cell proliferation.(41) However, these studies were performed by deleting *Hcfc1* (mouse) in a subset of precursors. In zebrafish, NPCs have primarily been analyzed according to the expression of Sox2, an NPC marker.(47) These cells are present across the entire brain and therefore are likely to include some Nkx2.1+ cells, which are restricted to the forebrain, but other subpopulations of precursors as well. During brain development, NPCs are likely to represent a heterogeneous cell population.

As discussed previously, zebrafish have two *hcfc1* paralogs. Thus far, most of the published literature has focused on *hcfc1b*. Knockdown of *hcfc1a* was performed in 2014, but the phenotypes associated with decreased *hcfc1a* were moderately relative to those observed in *hcfc1b* morphants. Both genes are ubiquitously expressed but appear to have

divergent functions. For example, *hcf1b* is essential for craniofacial development, but *hcf1a* appears to be dispensable for NCC function. In addition, *mmachc* expression is not significantly decreased in *hcf1a* morphants, but is dramatically reduced in *hcf1b* morphants. Whether *hcf1a* and *hcf1b* have an overlapping function in brain development is still unclear and has not been characterized to date.

### **Conclusions and Future Directions**

Human genetics has revealed approximately 13 variants of *HCFC1* associated with either non-syndromic or syndromic neurological impairment. Two other sequencing reports have demonstrated additional variants, including p.Thr239Met and pAla864Thr(22,23) associated with intellectual disability. These data collectively suggest an essential role for *HCFC1* during brain development. While N-terminal variants are primarily associated with syndromic versions of the disease, C-terminal variants appear to specifically disrupt brain development. Cobalamin deficits are likely the result of disrupted protein interactions with *ZNF143* and *THAP11*, as mutation of these genes causes a similar syndromic disease. Ultimately, these findings also suggest that each missense variant of *HCFC1* has a unique function, which based on current animal studies could be cell type specific. Thus, to comprehensively understand *cb1X* and related disorders, individual models of each variant are necessary for future therapeutic development and patient specific treatment options.

**Table 1: Summary of known *HCFC1* variants with patient phenotype.**

<b>Position of Mutation</b>	<b>Domain</b>	<b>Patient Phenotype</b>	<b>Citation</b>
p.Gln68Glu	K1	Cobalamin Disorder, Intellectual disability	10
p.Ala73Thr	K1	Cobalamin Disorder, Intellectual disability	10
p.Ala73Val	K1	Cobalamin Disorder, Intellectual disability	10
p.Tyr103His	K2	Intellectual Disability, Cobalamin Disorder, Craniofacial dysmorphism, Microcephalus, Intractable epilepsy, Profound neurocognitive impairment	15
p.Ala115Val	K2	Cobalamin Disorder, Intellectual disability	10
p.Ala115Thr	K2	Cobalamin Disorder, Intellectual disability	10
p.Ser225Asn	K4	Cobalamin Disorder (12), Intellectual Disability (13)	12 and 13
p.Thr239Met *(p.Thr142Met)	K4	Intellectual Disability	12 *(22)
p.Ala477Asn	FN3	Severe ID, absent speech and displayed frequent febrile seizures during infancy, elongated face, large ears, arachnodactyly and a lean body habitus.	13
p.Ala864Thr	Basic	No metabolic disorder, Intellectual Disability	23
p.Gly876Ser *(p.Gly779Ser)	Basic	No metabolic disorder, Autistic MMACHC expression changes	12 *(22)
p.Ala897Val	Basic	No metabolic disorder, Intellectual Disability	14
p.Ala1756Val	Acidic	Neural Development, Intellectual disability	12 and 13
p.Arg2016Trp	FN3	Neural Development	12 and 13

\*Originally annotated in Reference #22 and Corrected in reference #12.

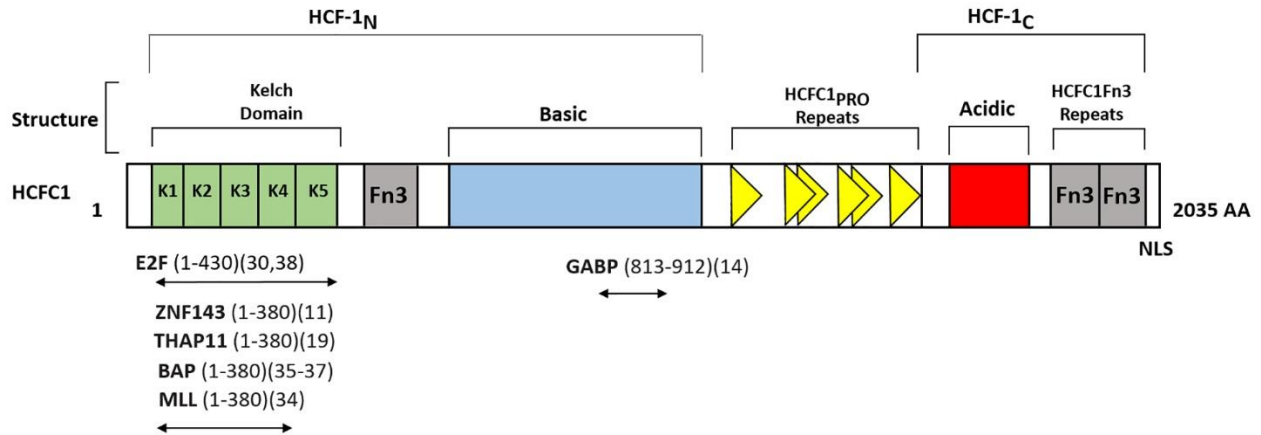


**Figure 1: HCFC1 Interacting Partners by domain.**

The HCFC1 protein structure is depicted from N to C terminus. The uncleaved protein is 2,035 amino acids in length. The primary conserved domains include the kelch domain (K1–5), the basic region (blue), multiple fibronectin domains (Fn3), an acidic domain (red), and the HCFC1 repeats that signal cleavage events (yellow). Of the interacting proteins discussed here, the vast majority bind to the kelch domain via conserved HBM domains. The binding domain of YY1 is not depicted and has not been characterized to our knowledge. Relative binding regions are shown based on literature review with citations associated. These represent the minimal region required for binding and are not drawn to scale.

## SECTION II: ADDITIONAL REVIEW OF LITERATURE

### **HCFC1 Function in Epigenetics**

There are several scientific studies and research papers that have explored the role of HCFC1 in histone modification and gene regulation and how this protein can impact epigenetic modifications depending on its interacting partners. Specifically, HCFC1 has been shown to interact with enzymes that add or remove chemical groups to histones, and it can also recruit these enzymes to specific regions of DNA. One example of HCFC1's role in histone modification is its interaction with the enzyme lysine-specific demethylase 1A (LSD1) (48). LSD1 is an enzyme that removes methyl groups from histones, and it has been shown to play a role in the regulation of gene expression. HCFC1 has been found to interact with LSD1 and recruit it to specific regions of DNA, which can result in the removal of methyl groups from histones and the subsequent activation of gene expression.

Another example of HCFC1's role in histone modification is its interaction with the enzyme histone acetyltransferase p300 (49). This enzyme adds acetyl groups to histones, which can result in the activation of gene expression. HCFC1 has been shown to interact with p300 and recruit it to specific regions of DNA, resulting in the acetylation of histones and the subsequent activation of gene expression. Overall, HCFC1 plays an important role in regulating histone modifications by interacting with enzymes that add or remove chemical groups to histones, and by recruiting these enzymes to specific regions of DNA. Dysregulation of HCFC1's function in histone modification can contribute to a range of health problems, including developmental disorders, cancer, and neurological conditions.

HCFC1 is associated with various additional histone-modifying proteins within larger multi-protein complexes. These include the *Sin3 histone deacetylase* (HDAC), the *mixed lineage leukemia* (MLL) (50), and the *human trithorax-related Set1 histone H3 lysine 4 methyltransferase* (H3K4 HMT) (51) complexes. Interestingly, HCFC1 selectively associates with H3K4 HMT and not HDACs when bound to the VP16 transcription factor, suggesting that HCFC1 can uniquely modulate chromatin structure to broadly regulate transcription. This is interesting as H3K4 methylation is associated with active chromatin, while HDACs are associated with heterochromatin or inactive states.

### **HCFC1 Role in Neurogenesis, Neural Stem Cell Fate, and Neural Circuitry**

HCFC1 can play an important role in regulating gene expression programs that are crucial for neural development. HCFC1 has the ability to regulate the expression of genes involved in neurogenesis (11), the process by which new neurons are generated in the developing brain. For example, HCFC1 interacts with ELAVL3, a neuron specific RNA binding protein essential for enhancing target gene expression to promote neuronal maturity. By recruiting histone-modifying enzymes to specific regions of DNA, HCFC1 can promote the activation of genes involved in neurogenesis and the differentiation of neural progenitor cells into neurons.

HCFC1 can also regulate the fate of neural precursors, which are responsible for generating all the different types of cells in the central nervous system. HCFC1 interacts with the transcription factor SOX2, which plays a key role in maintaining progenitor cell identity (52,53). By modulating histone modifications at the SOX2 promoter, HCFC1 may regulate the expression of SOX2 and control the fate of progenitor cells in the brain.

HCFC1 has also been implicated in the regulation of genes involved in the maintenance of neural circuitry. For example, HCFC1 interacts with the transcription factor MECP2 which is involved in the regulation of synaptic function and plasticity (54). By recruiting histone modifying proteins to the MECP2 promoter, HCFC1 can regulate the expression of MECP2 and contribute to the maintenance of neural circuitry.

Overall, HCFC1 can play an important role in regulating gene expression programs that are crucial for neural development, including neurogenesis, neural stem cell fate and neural circuitry. Dysregulation of HCFC1's function in these processes can contribute to a range of developmental disorders and neurological conditions. Studies which investigate the role of HCFC1 in these neural developmental processes are highly warranted and essential towards our understanding of its biological functions.

### **The Role of HCFC1 in Cell Cycle Control**

HCFC1 is required for a variety of biological processes including cell cycle progression (32,55) and maintenance of pluripotency (56). The function of HCFC1 during the cell cycle was discovered using a temperature sensitive mutation in a hamster cell line. A single proline to serine substitution in the kelch domain causes temperature induced cell growth arrest (55), cytokinesis defects (57), and the association of HCFC1 with chromatin. Together, these findings indicate that in addition to its role in viral gene expression, the kelch domain interactions in HCFC1 are essential for normal cell cycle progression and association with chromatin.

Many reports suggest that HCFC1 regulates various stages of the cell cycle (30,32,35,50,58,59). In animals, early embryonic development is associated with rapid

rounds of cell division, which allow the embryo to acquire the numbers of cells needed to support cell expansion and tissue development. The cell cycle can be divided into 4 distinct stages. The S-phase, or DNA synthesis phase, is the stage in which the cell's DNA is replicated, while the M-phase, or mitotic phase, is the stage in which the cellular contents are divided. There are growth phases called the G1 and G2 transient gap phases that occur before S- and M-phases (60). Additionally, there is a G0-phase that is often viewed together with G1 as a G0/G1-phase. This phase represents a sub-state of G1 in which growing cells deprived of growth factors exit the cycle and enter a long-term quiescent state from which they can be reactivated by growth factors to re-enter the cycle.

These rapid rounds of cellular division utilize cell-cycle regulator proteins particularly in the G1 phase. For example, the G1 to S-phase transition in mammalian cells is largely regulated by E2F transcriptional factor proteins, which regulate the expression of cyclins and genes involved in DNA synthesis. Previous studies have shown that the HCFC1 protein plays a large role in regulating aspects of cellular division. For example, following proteolytic cleavage of the HCFC1 precursor protein, two distinct and interacting subunits are generated: HCFC1<sub>N</sub> and HCFC1<sub>C</sub>. The HCFC1<sub>N</sub> subunit has been shown to promote passage through G1 phase, while the HCFC1<sub>C</sub> subunit ensures proper mitosis and cytokinesis during M-phase (61).

Interestingly, E2F and MLL interactions occur in the N-terminus domain of HCFC1 (30,50) and the most diverse and abundant interactions of HCFC1 are with the E2F family, specifically E2F's 1-8. E2F transcriptional factors can dictate activation of growth promoting genes during the G1 phase of the cell cycle. This ordered progression through the cell cycle is controlled by the sequential activation of cyclin-dependent kinases

(CDKs) that regulate phosphorylation of the retinoblastoma protein (Rb) and related Rb family pocket proteins. Because of these described interactions, HCFC1 has been well established as a regulator of cellular expansion and proliferation.

### **HCFC1 Role in Ribosomal Biogenesis**

Ribosome biogenesis is a phenomenon that happens inside cells to create ribosomes in order to maintain protein abundance in the cell, whereby without this process, cells are unable to proliferate or survive. Recent findings report that a genetic knock-in allele of the most common *cbfX* variant (p.Ala115Val) induced cranial facial phenotypes, consistent with *cbfX* patient phenotypes (62). However, neural developmental phenotypes associated with *cbfX* syndrome were not investigated in these mice, likely due to non-penetrant phenotypes or skewed mendelian ratios from perinatal lethality. Interestingly, a second knock-in was created in an HCFC1 interacting partner, THAP11, (p.F80L) which displayed astrocytic phenotypes that they attribute to defective ribosomal biogenesis.

Taken together, these data suggest that THAP11 and potentially HCFC1 mediate astrocytic phenotypes. However, this has yet to be proven in a viable HCFC1 mutant model system. Therefore, a model system that circumvents lethality and which allows for the study of brain development is significantly warranted.

### **Conclusions and Future Directions**

This section provides a review for the biological functions of the HCFC1 transcriptional co-factor, which include roles in cell cycle, cellular metabolism, and stem cell maintenance. Mutations in HCFC1 cause *cbfX* syndrome, but because of early

embryonic lethality of mouse models with mutations in HCFC1, no direct mechanism for how this protein regulates neural development has been proposed. Model systems *in vitro* highlight a role for HCFC1 in neural precursor cell development, but because of limitations in mouse lethality, we do not fully understand how HCFC1 regulates NPC development *in vivo*. Therefore, *in vivo* model systems like zebrafish, which can circumvent lethality and provide insight into the gene function of HCFC1 in brain development are warranted. This dissertation seeks to address these questions using zebrafish as a model system to elucidate the putative mechanisms by which HCFC1 regulates neural precursor cell (NPC) development and differentiation.

## CHAPTER II

### RESEARCH MANUSCRIPT I

Section I: Hcfc1a regulates neural precursor proliferation and *asx1* expression in the developing brain.

Castro, V.L., Reyes, J.F., Reyes-Nava, N.G. *et al.* Hcfc1a regulates neural precursor proliferation and *asx1* expression in the developing brain. *BMC Neurosci* **21**, 27 (2020).

<https://doi.org/10.1186/s12868-020-00577-1>

#### **Background**

Neural precursor cells (NPCs) give rise to the differentiated cells of the central nervous system and defects in the number produced, their proliferation, and/or survival can result in a variety of neural developmental disorders. These disorders include intellectual disability (63), cognitive dysfunction (64), behavioral impairment (65), microcephaly (66), epilepsy (67), autism spectrum disorders (68), and cortical malformations (69). Previous studies have demonstrated a complex network of transcription factors that are responsible for modulating NPC function including SOX2 (70), SOX1 (71), NESTIN (72), and PAX transcription factors (73). Recent evidence suggests that the *HCFC1* gene, which encodes a transcriptional cofactor, is essential for stem cell proliferation and metabolism (18,74) in a variety of different tissue types, including NPCs (12,13,41,75). These data strongly suggest that HCFC1 is part of a more global transcriptional program modulating NPC proliferation and differentiation.

HCFC1 regulates a diverse array of target genes and has been shown to bind to the promoters of more than 5000 unique downstream target genes (76). Consequently,

the molecular mechanisms by which HCFC1 regulates NPC proliferation and differentiation are complex. Mutations in *HCFC1* cause methylmalonic acidemia and homocysteinemia, *cbIX* type (*cbIX*) (309541). *cbIX* is an X-linked recessive disorder characterized by defects in cobalamin (vitamin B12) metabolism, nervous system development, neurological impairment, intractable epilepsy, and failure to thrive (10). Functional analysis of *cbIX* syndrome has provided a platform whereby the function HCFC1 in discrete organs and tissues can be elucidated. For example, *in vitro* analysis has demonstrated that HCFC1 regulates metabolism indirectly by regulating the expression of the *MMACHC* gene (10,12,13,18). These data are further supported by *in vivo* analysis using transient knockdown in the developing zebrafish (44,75). Additional mouse models exist and have demonstrated a function for HCFC1 in diverse cell populations (40,77), including a subset of NPCs (41). However, although it is clear that HCFC1 is essential for NPC function (41), previous studies have not yet determined a mechanistic basis for the cellular phenotypes observed. Thus, additional studies examining the function of HCFC1 in NPCs are warranted.

We have created a zebrafish harboring a mutation in the *hcfc1a* gene (*hcfc1a<sup>co60/+</sup>* allele) using CRISPR/Cas9. Zebrafish have two orthologs of HCFC1 and in previous studies, we demonstrated that *hcfc1b* is associated with increased NPC production (75). The two zebrafish paralogs have been shown to have divergent functions, as the knockdown of *hcfc1b* causes facial dysmorphia, but knockdown of *hcfc1a* does not (44). Therefore, we asked whether germline mutations in the *hcfc1a* gene cause defects in neural development. Our results demonstrate that the *hcfc1a<sup>co60/+</sup>* allele results in increased numbers of proliferating NPCs (Sox2+) and hypomotility. Subsequent RNA

sequencing on whole brain homogenates obtained from the *hcfc1a<sup>co60/+</sup>* allele identified increased expression of *asx11*, which encodes a transcription factor known to modulate the cell cycle (78,79). Furthermore, inhibition of *asx11* expression in larvae carrying the *hcfc1a<sup>co60/+</sup>* allele restored the number of NPCs to normal levels. Collectively, our study demonstrates a molecular mechanism by which *hcfc1a* regulates NPC proliferation and brain development.

## **Methods**

### **Experimental Model and Subject Details**

The experimental model used in this study is the zebrafish, *Danio rerio*. Zebrafish were obtained from the University of Colorado, School of Medicine, or the Zebrafish International Resource Center (ZIRC). The *hcfc1a<sup>co60/+</sup>* allele was produced using CRISPR/Cas9 methodology as described (80). The *hcfc1a<sup>co60/+</sup>* allele was produced at the University of Colorado, School of Medicine by the corresponding author and obtained according to protocols from the University of Texas El Paso. Briefly, a guide RNA (GGTTCATACCAGCCGTTTCGT) was designed using publicly available software (ZiFit) (81). Oligonucleotides from the forward and reverse strand were annealed and ligated into the DR274 vector as described (82). Guide template DNA was synthesized using PCR amplification with primers (DR274 FWD: TTTGAGACGGGCGACAGAT and DR274 Rev: TTCTGCTATGGAGGTCAGGT) and RNA was synthesized using the MEGAscript T7 *in vitro* transcription kit. Cas9 was synthesized using the T7 mMessage machine after linearization with PmeI (New England Biolabs) of the Cas9 vector (pMLM3613). A solution (0.2M KCl with phenol red indicator) containing a final concentration of 500ng Cas9 and 70 ng of guide RNA was injected at a volume of 2nL at the single cell embryos were grown

to adulthood. The *hcfc1a<sup>co60/+</sup>* allele was generated from a single founder (F<sub>0</sub>), which was outcrossed with 3 independent wildtype (AB) fish to generate 3 families of F1 carriers. Each family consisted of approximately 20 total fish with equal numbers of males and females. To generate subsequent generations, we outcrossed a minimum of 3 F1 individuals with wildtype (Tupfel Long Fin) to obtain a minimum of 3 families of F2 carriers. We subsequently outcrossed F2 carriers (minimum of 3) with wildtype (AB) fish to produce an F3 generation of approximately 3 total families with equal numbers of males and females. Sanger sequencing confirmed mutation and experiments were initiated in the F3 generation.

The *Tg(hsp701:HCFC1)* was created using Gateway cloning technology. Briefly, the p5e-*hsp701*, pME-*HCFC1* (created from pcDNA6.1 reported in (44)), p3E-polyA, and the pDestTol2PA were recombined via LR recombination. The resultant vector was co-injected with transposase mRNA synthesized from the pCS2FA vector as previously described (83). The experiments described herein were performed in the F2 generation, which was produced from a single founder (F<sub>0</sub>). The positive F<sub>0</sub> carrier was outcrossed with wildtype (AB) to produce 2 families of F1 individuals and a minimum of 3 carriers of the F1 generation were outcrossed to produce 3 families of F2 carriers that were utilized for the experiments described.

For all experiments, embryos (prior to sexual dimorphism) were obtained by crossing AB wildtype, Tupfel Long Fin wildtype, *Tg(hsp701:HCFC1)*, or *hcfc1a<sup>co60/+</sup>*. Experiments were performed at developmental stages only [0-5 days post fertilization (DPF)]. All embryos were maintained in embryo medium at 28° C. All adults beyond the age of peak breeding age (>1.5 years) were euthanized using a 10g/L buffered solution

of pharmaceutical grade MS 222 (Tricaine). Fish were submerged in solution for 30 minutes at room temperature. All euthanized adults underwent secondary euthanasia using a cold ice bath (2-4 degrees C). Fish were monitored for operculum movement during euthanasia and cessation of movement was indicative of euthanasia. Embryos (<7 days old) were euthanized using 1-10% sodium hypochlorite solution after being anesthetized in cold ice bath. Prior to fin clipping and before fixation, all fish, adults and larvae, respectively, were anesthetized using MS 222 (150mg/L for adults and 300mg/L for embryos). The degree of anesthesia was monitored by operculum movement of adults and cessation of movement for larvae. These techniques are approved and advised by the American Veterinary Medical Association and approved by the University of Texas El Paso Institutional Animal Care and Use Committee.

### **Genotyping**

Genotyping of the *hcfc1a<sup>co60/+</sup>* allele was performed by lysing excised larval tissue or fin clips (adults) in lysis buffer (10mM Tris pH 8.2, 10mM EDTA, 200mM NaCl, 0.5% SDS, and 200ug/ml proteinase K) for 3 hours at 55° C. DNA was isolated according to standard phenol chloroform : ethanol precipitation procedures. Primers pairs were developed that specifically bind to and amplify the mutated allele, which did not amplify the wildtype allele. The fragment of interest was amplified by standard PCR at an annealing temperature of 64° (FWD: CCAGTTCGCCTTTTTGTTGT and REV: ACGGGTGGTATGAACCACTGGC). Positive amplification indicates positive carriers of the allele (Figure 1). Genotyping of the *Tg(hsp701:HCFC1)* allele was performed with the following primers: forward primer (TGAAACAATTGCACCATAAATTG) located in the *hsp701* promoter and reverse primer in the *HCFC1* open reading frame

(CGTCACACACGAAGCCATAG). Amplification indicates the genotype of interest.

### ***Immunohistochemistry***

Embryos/larvae were fixed in 4% paraformaldehyde (Electron Microscopy Sciences) for minimum of 1 hour at room temperature (RT). For each time point, a small piece of caudal tissue was excised for genotyping and the remaining rostral tissue was embedded in 1.5% agarose (Fisher) produced in 5% sucrose (Fisher) and embryo medium. Embedded blocks were incubated overnight in 30% sucrose (Fisher) and then snap frozen with dry ice and cryosectioned (12-20 $\mu$ M). Sections were washed twice in 1X phosphate buffered saline (PBS) pH 7.4 at RT for 30 minutes each and blocked for 1 hour in blocking buffer (2mg/ml bovine serum albumin (Fisher), 2% goat serum (Fisher) diluted in 1X PBS). Primary antibody (1:200 anti-Sox2 (Abcam) or 1:500 anti-HuC/D (Fisher) was incubated overnight at 4°C and then washed twice in 1X PBS for 30 minutes each at RT. Alexa fluor antibodies (Fisher) were diluted 1:200 and incubated on each slide for 1 hour at RT. All slides were cover slipped using Vectashield (Vector Laboratories) and imaged on a Zeiss LSM 700 at 20X-63X magnification. For cell proliferation, larvae were pulsed in 20mM 5-ethynyl-2'-deoxyuridine (EdU) (Fisher) diluted in 10% dimethyl sulfoxide (DMSO) (Fisher) for 30 minutes at RT prior to fixation. EdU was detected using the EdU Click-It technology (Fisher) according to manufacturer protocol.

### **Cell Quantification**

For cell quantification, sections were first divided into forebrain, midbrain, and hindbrain regions using two zebrafish brain atlases; 1) Atlas of Zebrafish Development (84) and 2) Atlas of Early Zebrafish Brain Development (85). To specify brain regions,

major hallmark sub-divisions of each brain section were separated based on age of larvae and the published sections and demarcations present in (85). For example, sections of the developing brain are organized by letters: A-F indicates forebrain sections, G-L are midbrain, and M-R are hindbrain according to the zebrafish brain atlas. After standardization of the brain region by atlas, cells from each section (12-20uM) were counted using the ImageJ cell counter. The ImageJ cell counter allows for the manual counting of cells by marking each cell with a colored square and adds the tallied cell to the quantification sheet. The cell counter allows for the tally of 4 independent groups separately with a different color square. Cells were easily visible across all replicates. Only biological replicates with high tissue integrity were quantified. For comparison of representative images, equivalent sections are shown to ensure that minor changes in tissue geometry do not affect the overall conclusion. These sections are standardized from the zebrafish brain atlas. For bar graphs, the average number of cells across each brain region were utilized for quantification using approximately 10-20 equivalent sections/brain region/fish. The number of animals per group is described in each figure legend. To determine the relative increase/decrease in total cell number, the number of total cells/section was divided by the average number of cells present in wildtype siblings for each brain region analyzed and multiplied by 100. All statistical analysis was performed using total numbers of cells/section/brain region. All immunohistochemistry was validated with quantitative real time PCR (QPCR) of each gene analyzed.

### ***QPCR and in situ hybridization***

Whole mount *in situ* hybridization (ISH) was performed as described by Thisse and Thisse (86). Briefly, embryos were harvested and dechorionated at the indicated time

point and fixed in 4% paraformaldehyde (PFA) (Electron Microscopy Sciences) for 1 hour at RT. Embryos were permeabilized with proteinase K (10ug/ml) for the time indicated (87). Permeabilized embryos were prehybridized in hybridization buffer (HB) (50% deionized formamide (Fisher), 5X SSC (Fisher), 0.1% Tween 20 (Fisher), 50 $\mu$ g ml<sup>-1</sup> heparin (Sigma, St. Louis), 500 $\mu$ g ml<sup>-1</sup> of Rnase-free tRNA (Sigma), 1M citric acid (Fisher) (460 $\mu$ l for 50ml of HB)) for 2-4 hours and then incubated overnight in fresh HB with probe (50-100ng) at 70°C. Samples were washed, blocked in 2% sheep serum, and incubated with anti-DIG Fab fragments (1:10,000) (Sigma) overnight at 4°C. Samples were developed with BM purple AP substrate (Sigma) and images were collected with a Zeiss Discovery Stereo Microscope fitted with Zen Software. *The asx11* cDNA probe sequence was amplified using the following primers: FWD: CATCAACACACGGACCTTTG and REV: CAGTGAGTGGGGTGGAAAGTT, purified using a DNA purification kit (Fisher), then ligated into the pGEM-T easy vector using the pGEM T-easy Plasmid Ligation Kit (Promega).

For QPCR, RNA was isolated from embryos at the indicated time point using Trizol (Fisher) according to manufacturer's protocol. Reverse transcription was performed using Verso cDNA synthesis (Fisher) and total RNA was normalized across all samples. PCR was performed in technical triplicates for each sample using an Applied Biosystem's StepOne Plus machine with Applied Biosystem's software. Sybr green (Fisher) based primer pairs for each gene analyzed are as follows: *mmachc* fwd: GCTTCGAGGTTTACCCCTTC, *mmachc* rev: AGGCCAGGGTAGGGTCCTG, *hcf1a* fwd: ACAGGGCCTAACACAGGTTG, *hcf1a* rev: TCCTGTGACTGTGCCAAGAG, *asx11* fwd: CCAGAGCTGGAAAGAACGTC, *asx11* rev: ACATCTCCAGCTTCGCTCAT, *rp113a*

fwd: TCCCAGCTGCTCTCAAGATT, *rpl13a* rev: TTCTTGGAATAGCGCAGCTT, *sox2*  
fwd: AACTCCTCGGGAAACAACCA, *sox2* rev: ATCCGGGTGTTCTTCATGT, *elav13*  
fwd: TAACGGCCCTGTCATTAGCA, *elav13* rev: CGTGTTGATAGCCTTGTCGG, *gfap*  
fwd: GGCCAACTCTAACATGCAGG, *gfap* rev: ATTCCAGGTCACAGGTCAGG, *olig2*  
fwd: TTCTGTAGGCCACACACCAG, and *olig2* rev: TTAACTCCGGTGGAGAATCG.  
Analysis was performed using  $2^{\Delta\Delta Ct}$ .

For RNA sequencing analysis, total RNA was isolated from brain homogenates (N=12/group from 3 biological replicates), analyzed for RNA integrity, and sequenced at The University of Texas El Paso Border Biomedical Research Center Genomics Core Facility. RNA sequencing was performed in biological triplicate. RNA integrity was assessed with a TapeStation 2200 and the library was prepared with a TruSeq stranded mRNA library preparation kit. Sequencing was performed on a NextSeq500 (Illumina) using a high output kit V2 (150 cycles). For analysis, the sequences were quality trimmed using Trimmomatic (88) and aligned to the *Danio rerio* genome (build GRCz11) obtained from Ensembl v95 using Tophat2 (89). Cufflinks (90) was used to determine the differential expression patterns between mutant and wildtype samples.

### ***Tg(hsp701:HCFC1)* analysis and rescue experiments.**

F2 carriers of the *Tg(hsp701:HCFC1)* were incrossed and grown at 28° for 24 hours and then split into two groups, non-heat shock and heat shock. Heat shock was performed for 30 minutes at 38° and then allowed to acclimate at RT for 20 minutes. Heat shock was initiated at 24 hours post fertilization (HPF) and performed every 8 hours until 2 or 5 DPF. For LY294002 (Selleck Chemicals) rescue, the drug was dissolved in 100% DMSO (Fisher) and embryos were treated at 24 HPF with a 12uM concentration for a period of

24 hours. Media was removed and embryos were dechorionated (if necessary) and fixed for immunohistochemistry.

For morpholino rescue, 2 nL of a 0.1 mM solution of *asx1* targeting translation inhibiting morpholinos (GTTTGTCCTTCATTTCCTCAGTGTT) or random control morpholinos (Gene-Tools) were injected into offspring of the *hcfc1a<sup>co60/+</sup>* allele. Injected embryos were fixed at 2 DPF and simultaneously stained for the number of Sox2+ and/or EdU+ positive cells. Cells were counted as described above.

### **Larval Behavioral Assay**

Embryos were obtained from an outcross of the *hcfc1a<sup>co60/+</sup>* allele and raised to 5 DPF. Behavioral quantification was performed using the Zebbox (ViewPoint Behavior Technology) as previously described (91). Larvae were individually tracked for swim speed and total distance swam in a 96 well plate. The behavioral protocol was a total of 15 minutes divided into 5-minute intervals of dark/light/dark conditions. All larvae were acclimated to the dish and housing conditions for 1 hour prior to analysis. Settings for the program include a threshold of 16 and integration period of 300 seconds. Data was measured as total distance traveled (mm) and total swim speed (mm/sec) ( $\text{Swim Speed} = \frac{\{\text{Total distance traveled in large and small movements}\} (\text{Sml} + \text{Lard})}{\{\text{Total duration spent by the animal in small and large movements}\} (\text{sml} + \text{lard})}$ ). Statistical significance was determined according to a T-test. All experiments were performed in biological triplicate.

### **Quantification and Statistical Analysis**

For all assays, statistical significance was calculated using a T-test to compare the

means of two groups. All assays were performed in biological duplicate and triplicate and all QPCR was performed in technical and biological triplicate or duplicate, respectively. For each assay, the total number of animals (N) is indicated in the figure legend. The number of animals was determined based on power analysis conducted from preliminary studies. For all graphs, statistical significance between groups and the P-value is shown in the figure legend. For cell quantification, the number of Sox2+ or EdU+ cells were counted per section and normalized according to the methods section above. All sections were sub-divided based on landmarks in the Atlas of Early Zebrafish Brain Development, 2<sup>nd</sup> Edition and then separated into specific brain regions (forebrain, midbrain, and hindbrain). All graphs represent error bars as standard error of the mean (SEM).

## **Results**

### **Production of the *hcfc1a*<sup>co60/+</sup> allele.**

Previous studies suggest that HCFC1 regulates the number of NPCs *in vitro* and in mouse models (12,13,41,75). *HCFC1* is highly conserved across species (10) and zebrafish have been used as a model system to understand the mechanisms by which mutations in *HCFC1* cause disease (44,75). Therefore, we developed a zebrafish harboring a germline mutation in the *hcfc1a* gene using CRISPR/Cas9 technology. We developed a specific guide RNA (sgRNA) that targets exon 3 of the *hcfc1a* gene (Figure 1A). The sgRNA was injected at the single cell stage and resulted in the net insertion of 13 nucleotides (Figure 1A). The introduction of these nucleotides is predicted to introduce a premature stop codon and encode a peptide of 94 amino acids in length (Supplemental Figure 1). Full length Hcfc1a is approximately 1778 amino acids in length. Genotyping of the *hcfc1a*<sup>co60/+</sup> allele was developed according to the materials and methods section,

using a reverse primer unique to the mutant allele in the amplification strategy (Figure 1A). Positive amplification was indicative of positive carriers (Figure 1B), as the primers did not bind to or amplify the wildtype allele. Initial crosses between heterozygous carriers of the *hcfc1a<sup>co60/+</sup>* allele failed to generate homozygous progeny and did not obey Mendelian inheritance patterns. These results indicate that Hcfc1a is required for early development, which is consistent with previously published studies (40,77), however the mechanism for embryonic lethality of the homozygous allele was not explored further here. Importantly, heterozygous carriers survived to adulthood with a lifespan equivalent to wildtype adult zebrafish. Adult heterozygous carriers did not show any gross morphological phenotypes associated with the allele. Larval heterozygous carriers did not show overt morphological phenotypes during early development, which is consistent with previous studies using anti-sense morpholinos targeting the *hcfc1a* gene (44). However, based on previous studies (12,13) we surmised that heterozygous carriers of the *hcfc1a<sup>co60/+</sup>* allele would have defects in overall *hcfc1a* expression and potential defects in brain development. Therefore, we measured the expression of *hcfc1a* in carriers of the *hcfc1a<sup>co60/+</sup>* allele and their wildtype siblings using QPCR. We designed primers to detect *hcfc1a* expression downstream of Exon 3 that span exons 15 and 17 to ensure that the primers were capable of detecting changes in total mRNA expression and not truncated N-terminal transcripts. As shown in Figure 1C, at 2 DPF carriers of the *hcfc1a<sup>co60/+</sup>* allele had a 50% decrease in total *hcfc1a* mRNA ( $P < 0.05$ ).

### **Hcfc1a regulates NPC number *in vivo*.**

Several studies suggest that mutation or abnormal expression of *Hcfc1* (mouse) mRNA disrupts the number of NPCs, their proliferation, and/or their differentiation.

Moreover, we have previously published that *hcfc1a* is expressed in the developing brain across the forebrain, midbrain, and hindbrain (44). Therefore, we asked whether the decrease in *hcfc1a* mRNA expression in carriers of the *hcfc1a<sup>co60/+</sup>* allele resulted in abnormal numbers of NPCs *in vivo*. To test this, we first measured the expression of *sox2* and *pax6* using QPCR at 5 DPF. We used *sox2* and *pax6* as a readout for NPCs because they are co-localized and established markers of NPCs in the field (47,92,93). At 5 DPF, the expression of both *sox2* and *pax6* were up-regulated in *hcfc1a<sup>co60/+</sup>* larvae relative to their wildtype siblings (Figure 2A). We next compared the total number of Sox2+ cells in *hcfc1a<sup>co60/+</sup>* larvae and their wildtype siblings over the course of development at 1 (Figure 2B), 2, and 5 DPF. Increased NPCs were not observed until 2 DPF (Figure 2C), but this increase was sustained until 5 DPF (Figure 2D). *hcfc1a<sup>co60/+</sup>* larvae had increased numbers of NPCs in the forebrain, midbrain, and hindbrain regions, with NPCs highly enriched in the ventricular region of the developing brain (Figure 3A-D and A'-D', arrowheads indicate cells). There were approximately 25-30% more Sox2+ cells per brain region based upon our quantification (Figure 2&3).

***The *hcfc1a<sup>co60/+</sup>* allele disrupts cell proliferation.***

Mutation of *Hcfc1* in mice is associated with increased cell death in a subpopulation of NPCs (41), therefore, we hypothesized that the excess NPCs produced undergo cell death. To measure cell death, we performed immunohistochemistry with anti-active caspase 3 antibodies and anti-Sox2 antibodies at 5 DPF. As shown in Figure 4A and 4A', we detected approximately 1-2 Caspase+ Sox2+ cells in sibling controls (white arrowhead), however larvae harboring the *hcfc1a<sup>co60/+</sup>* allele had on average approximately 4-5 co-localized cells per/section (white arrowheads in 4A'). As we

detected very few total caspase+ NPCs, we next quantified the total number of NPCs in each group to determine the total number of NPCs surviving. As shown in Figure 4B, while the *hcfc1a<sup>co60/+</sup>* allele led to an increase in the number of caspase positive NPCs (red bars), the vast majority of NPCs in both wildtype and *hcfc1a<sup>co60/+</sup>* larvae were not caspase positive (gray bars), indicating that a significant fraction of NPCs survive. Because of this survival, we next analyzed cell proliferation in *hcfc1a<sup>co60/+</sup>* larvae and their wildtype siblings using EdU click-it technology. The *hcfc1a<sup>co60/+</sup>* allele resulted in a statistically significant increase in the number of EdU positive cells in both the midbrain and hindbrain regions (Figure 4C-D & 4C'-D' and quantified in Figure 4E). We observed an increase in the number of EdU positive cells in the forebrain, although the increase in the forebrain was not significant across multiple biological replicates (P=0.06). Collectively, these data suggest the *hcfc1a<sup>co60/+</sup>* allele results in an increase in NPC proliferation, whereby a sub-population of these NPCs undergo cell death, while the majority of those NPCs produced, survive.

**The *hcfc1a<sup>co60/+</sup>* allele is associated with abnormal expression of pro-neural and pro-glial genes.**

The *hcfc1a<sup>co60/+</sup>* allele is associated with increased proliferation and an increased number of NPCs. Importantly, the majority of these cells do not undergo cell death and therefore, we asked if the expression of genes associated with either neuronal or glial differentiation was abnormal. We measured the expression of two established markers of neurons and radial glial cells, *elavl3* and *gfap*, by immunohistochemistry. As shown in Figure 5A'&B', the expression of both Gfap and Elavl3 expression was increased in *hcfc1a<sup>co60/+</sup>* larvae at 5 DPF. Next, we quantified the level of expression of each marker

and one additional marker of differentiation (*olig2*) using QPCR at 5DPF. QPCR demonstrated an increase in the level of mRNA expression of each marker (Figure 5C) in *hcfc1a<sup>co60/+</sup>* larvae relative to their wildtype siblings ( $P < 0.05$ ).

### **Overexpression of HCFC1 reduces the number of NPCs and decreases neural and glial gene expression.**

Our data demonstrates that haploinsufficiency of *hcfc1a* is associated with increased proliferation and increased numbers of Sox2+ cells. Previous studies have shown that over-expression of *Hcfc1* (mouse) *in vitro* is associated with reduced NPC proliferation/growth and reduced NPC proliferation (12). We tested the effects of HCFC1 over expression in zebrafish by creating a transgenic zebrafish expressing human HCFC1 under the control of the heat shock promoter, *hsp701*. The efficacy of the *hsp701* promoter in zebrafish has been widely established in previous studies (83,94–98). We activated expression of HCFC1 by performing a heat shock as described in the methods section for a period of 5 days. We first measured the mRNA expression of *sox2*, *elavl3* (HuC/D), *gfap*, and *olig2* by QPCR. Activation by heat shock of the *Tg(hsp701:HCFC1)* allele resulted in decreased expression of all markers analyzed (Figure 6A;  $P < 0.05$ ). We next analyzed the number of Sox2+ cells in the presence and absence of heat shock. Activation of the *Tg(hsp701:HCFC1)* was associated with a decreased number of NPCs across the forebrain ( $P = 4.88568E-05$ ), midbrain ( $P = 0.004359$ ), and hindbrain ( $P = 0.0776$ ) (Figure 6B, 6C-C').

**Asxl1 is overexpressed in animals with the *hcfc1a<sup>co60/+</sup>* allele.**

HCFC1 is known to regulate metabolism and craniofacial development via the modulation of *MMACHC* expression (10,13,44). Therefore, we hypothesized the neural phenotypes associated with mutations in *hcfc1a* were the direct consequence of defects in *mmachc* expression. We measured the expression of *mmachc* in *hcfc1a* mutants and their wildtype siblings. As shown in Figure 7A, QPCR analysis demonstrated that *mmachc* expression was unchanged by the *hcfc1a<sup>co60/+</sup>* allele. Based upon these data, we hypothesized that mutation of *hcfc1a* does not regulate brain development by modulating *mmachc* expression. To better understand the mechanisms downstream of *hcfc1a*, we performed RNA-sequencing at 2 DPF using whole brain homogenates from wildtype and *hcfc1a<sup>co60/+</sup>* larvae (Supplemental Table 1). Using literature analysis, we identified the *asx1* gene as one possible downstream effector of Hcfc1a in the developing brain. *Asx1* encodes a transcriptional regulator that is essential for proper cell proliferation and whose deletion causes cellular senescence (79,99). More importantly, mutations in *ASXL1* have been associated with Boring Opitz Syndrome (605039), which has been characterized by profound intellectual disability (100). According to *in situ* hybridization, *asx1* expression is restricted to the developing zebrafish brain as indicated by the purple stain in panel B' (Figure 7B&B'). The sense negative control was absent of this purple stain as shown in Figure 7B. Additionally, QPCR analysis of brain homogenates validated a 14-fold increase of *asx1* expression at 2 DPF in *hcfc1a<sup>co60/+</sup>* larvae relative to wildtype siblings (Figure 7C).

#### **Inhibition of *asx1* restores the NPC phenotype in *hcfc1a<sup>co60/+</sup>* larvae.**

Deletion of *Asx1* in mouse embryonic fibroblasts (MEFs) causes growth retardation because *Asx1* regulates the cell cycle via activation of the AKT-E2F axis (79).

Based upon these data, we hypothesized that over-expression of *asx1* in *hcf1a<sup>co60/+</sup>* larvae promotes proliferation of NPCs. To test this hypothesis, we designed a translational blocking morpholino to inhibit *asx1* expression in *hcf1a<sup>co60/+</sup>* larvae. We determined the concentration for injection empirically and selected the highest concentration that promoted >70% survival of injected embryos. We injected *asx1* morpholinos or random control morpholinos into *hcf1a<sup>co60/+</sup>* larvae and their wildtype siblings at the single cell stage and then analyzed the number of EdU positive cells at 2 DPF. As shown in Figure 7D, the injection of random control morpholinos into *hcf1a* mutants and their wildtype siblings had no detrimental effects and recapitulated the NPC phenotype previously observed (i.e. increased NPCs, Figure 2 and 3). However, the injection of *asx1* morpholinos completely restored the number of NPCs to wildtype levels in all brain regions (Figure 7D, red bars).

Morpholinos can display off-target effects (101) and therefore we sought an alternative route of *asx1* inhibition in *hcf1a<sup>co60/+</sup>* larvae. Youn and colleagues have demonstrated that ASXL1 (mouse) expression promotes cell proliferation by binding to AKT kinase and promoting AKT phosphorylation (79). However, this function can be inhibited with PI3K/AKT inhibitors. Therefore, we treated *hcf1a<sup>co60/+</sup>* larvae and their wildtype siblings with LY294002, a PI3K inhibitor as described in (79). *Hcf1a<sup>co60/+</sup>* embryos were treated at 24HPF with 12uM LY294002 or vehicle control (DMSO). Vehicle treatment of wildtype and *hcf1a<sup>co60/+</sup>* larvae recapitulated the NPC phenotype (i.e. increased NPCs) present in *hcf1a<sup>co60/+</sup>* larvae (Figure 8A-A", 8B-B", and 8C-C", white arrowheads), which was consistent across all brain regions as both the number of Sox2+ cells (Figure 9A-A") and the number of EdU+ cells (Figure 9B-B") were increased in

*hcfc1a<sup>co60/+</sup>* larvae. In contrast, treatment with LY294002 reduced the number of cycling cells (EdU+) and the number of NPCs (Sox2+) in *hcfc1a<sup>co60/+</sup>* larvae, consistent with our hypothesis (Figure 9A&B, red bars). To complement these data, we next performed mRNA expression analysis of *sox2*, *asx1/1*, and cyclin E (*ccne1*) in treated and untreated *hcfc1a<sup>co60/+</sup>* larvae at 5 DPF. As shown in Figure 9C, treatment with LY294002 resulted in decreased expression of *sox2* and *asx1/1*, which was correlated with decreased *ccne1* expression (P<0.05).

### **Defects in neural development are associated with larval hypomotility.**

The functional consequences of the defects in brain development in the *hcfc1a<sup>co60/+</sup>* allele are not completely understood. However, mutation of HCFC1 in patients with *cbIX* syndrome is associated with movement disorders (10). Therefore, we performed larval behavioral assays to determine if defects in the number of NPCs were associated with abnormal swim patterns. To test this, we monitored swim behavior of 5 DPF larvae using Zebrafish technology. Carriers of the *hcfc1a<sup>co60/+</sup>* allele exhibited reduced overall distance swam in response to light stimulus as described in (91), but overall speed was not affected (Figure 10A&B). These behavioral deficits are consistent with a hypomotility phenotype (102). Importantly, *hcfc1a<sup>co60/+</sup>* responded normally to dark-light-dark transitions (Figure 10C) as has been previously demonstrated (103).

### **Discussion**

Here we demonstrate that the *hcfc1a<sup>co60/+</sup>* allele results in an increase in the number of NPCs during early brain development. This increase in NPC number is a direct consequence of over proliferation of NPCs. Mutations in *HCFC1* cause *cbIX* syndrome,

a multiple congenital anomaly syndrome, associated with cobalamin deficiencies and significant neurological deficits, among other phenotypes (10,12). *HCFC1* encodes for a transcriptional co-activator that regulates genes important for metabolism and proliferation (18). It is suggested that HCFC1 binds to and regulates the expression of >5000 different genes (76), with various different interacting partners including THAP11 (74) and ZNF143 (104), where mutation of either can cause a *cbIX* like disorder (21,75).

Previous reports suggest that HCFC1 regulates NPC function (12,13,41,75). *In vitro*, decreased *Hcfc1* (mouse) expression increases the number of NPCs and reduces the expression of markers associated with differentiation (13). These data are consistent with the known function of *Hcfc1* in cell proliferation (28,105,106). Mutation of *Hcfc1* (mouse) is embryonically lethal (77) and consequently, the *in vivo* function of HCFC1 has been difficult to characterize. Our results are consistent with this observation, as we did not detect viable homozygous larvae or adults. We genotyped larvae from an incross of *hcfc1a<sup>co60/+</sup>* adults at 2, 4, and 8 HPF and even at the earliest time points, we detected few to zero homozygous larvae. We did not explore this mechanism further, however in previous studies the murine *Hcfc1* mutant allele was subject to compensatory mechanisms and only the paternally inherited allele was viable (77). Zebrafish do not have sex chromosomes, but future studies are warranted that characterize the inheritance of the *hcfc1a<sup>co60/+</sup>* allele as well as the embryonic lethality.

Recently a cell-type specific mutant allele was created in which *Hcfc1* (mouse) was deleted from a subpopulation of neural precursors (NKX2.1+). This cell type specific deletion of *Hcfc1* (mouse) induces cell death and defects in differentiation without affecting proliferation. These results differ from *in vitro* assays, whereby decreased *Hcfc1*

(mouse) results in an increase in the number of precursors. The discrepancy between these results might be explained by many factors, including the propagation of neurospheres *in vitro* and the inability to decipher how the developing microenvironment affects normal physiology. However, some studies have helped to shed light on the latter explanation because the *in vivo* knockdown of *hcfc1b*, one of the zebrafish orthologs of *HCFC1*, resulted in increased NPC proliferation (75). Thus, the function of *HCFC1* is complex, with several unknown cell-type specific functions that can be affected by the surrounding microenvironment.

Here we developed a zebrafish harboring a germline mutation in the *hcfc1a* gene. We analyzed the effects of this mutation on NPC number and proliferation. Consistent with the literature (12,13,75), our allele resulted in an increase in the number of Sox2+ cells and increased cellular proliferation without significant deficits in cell survival. Increased cell proliferation was observed across all brain regions. However, our studies were limited to detection of NPCs using the Sox2 marker. A significant fraction of these cells co-localize with EdU positive cells in the *Co60/+* allele, but not all of them. These data strongly suggest that *hcfc1a* is important for the proliferation of Sox2 positive NPCs. However, the NPC population is heterogeneous in nature and can include Sox2+ and Sox2- cells. We do not yet understand the effects of *hcfc1a* mutations on the Sox2- population or other NPC sub-populations (actively proliferating versus not proliferating). However, we did observe increased *pax6* expression. *Sox2* and *Pax6* are known to be co-expressed in a subpopulation of NPCs so it is possible these two markers label similar populations of NPCs (93).

The increased numbers of NPCs in the *hcfc1a*<sup>co60/+</sup> allele was not associated with increased apoptosis of NPCs, but instead was associated with increased expression of markers associated with neurons and glia. The effects of this increased expression are yet to be elucidated, however studies that provide information on brain volume and the ratio of gray and white matter in the central nervous system are warranted; particularly given that the increases in neurons and glia we observed are unique from the differentiation defects observed in previous studies (13,41). However, we suspect the difference in phenotype between previous studies and our own is likely associated with the type of mutation introduced, the brain microenvironment, the cell population analyzed, and the region of the brain of interest. For example, Minocha and Herr (41) deleted exons 2 and 3 of *Hcfc1* using a Cre-Lox system with a cell type specific promoter. The resulting approach introduces the formation of a truncated protein, whereas our system results in decreased overall expression (Figure 1), which may be more consistent with previous *in vitro* assays and haploinsufficiency. However our haploinsufficient allele advances the field because unlike the previous *in vitro* assays (12,13), our allele accounts for the broad expression of *Hcfc1* which was recently documented by Minocha and colleagues (41).

HCFC1 regulates a myriad of downstream target genes (18,76) and therefore, the mechanisms by which HCFC1 regulates NPC function are not clear. The majority of the literature focuses primarily on the function of HCFC1 at the *MMACHC* promoter in the human syndrome, *cbIX*. *cbIX* disorder is the result of mutations in the *HCFC1* gene and these mutations disrupt protein function causing a decrease the expression of *MMACHC* and a metabolic disorder (10,13). Interestingly, mutations in *MMACHC* cause *cbIC* disorder, which has many overlapping phenotypes with *cbIX* including

neurodevelopmental defects (107). These data led us to hypothesize that HCFC1 regulates NPC function by modulating MMACHC expression. However, the *hcfc1a<sup>co60/+</sup>* allele did not disrupt *mmachc* expression. However, whether our allele causes other metabolic deficits is not known and was not explored further here. For example, mutation of the human *HCFC1* gene has been associated with non-ketotic hyperglycinemia (16). Collectively the data presented here suggests that the *hcfc1a<sup>co60/+</sup>* allele disrupts NPC proliferation by a novel molecular mechanism. In addition, these data suggest some divergent function between *hcfc1a* and *hcfc1b*, as the latter has been shown to regulate *mmachc* expression and craniofacial development (44).

Our results strongly suggest an *mmachc* independent mechanism underlying the neural developmental phenotypes associated with the *hcfc1a<sup>co60/+</sup>* allele, but we cannot completely rule out that *hcfc1b* regulates brain development via *mmachc* expression or that other factors including cobalamin, homocysteine, or methylmalonic acid accumulation. However, RNA-sequencing of brain homogenates provided a list of potential downstream effectors of *hcfc1a*. Of those candidates, the *asx1* gene was afforded high priority because of its known role regulating cellular proliferation (79,99,108) and for its documented function in mouse embryonic stem cells and neural differentiation (78). Interestingly, the *hcfc1a<sup>co60/+</sup>* allele causes a 14-fold induction of *asx1* expression. In mouse embryonic fibroblasts, the deletion of *Asx1* causes cellular senescence. We observed increased cellular proliferation and therefore, postulated that an increased level of Asx1 protein was promoting NPC proliferation in *hcfc1a* mutant larvae. Consistent with the known function of *asx1* and our hypothesis, knockdown of *asx1* in *hcfc1a* mutant

larvae restored the defects in cellular proliferation, resulting in normal numbers of Sox2+ cells.

Interestingly, *ASXL1* has been shown to regulate cell proliferation in other cell types (108,109) and this activity has been associated with activation of AKT. Based upon these data, we attempted to restore the phenotypes present in the *hcfc1a<sup>co60/+</sup>* allele by inhibiting ASXL1 activity downstream of PI3K (79). Consistent with this role, the inhibition of ASXL1 activity using pharmacological inhibition completely restored the NPC deficits present in *hcfc1a* mutants. Thus, our data suggest a mechanism whereby *hcfc1a* regulates the expression of *Asxl1* and the cell cycle during early brain development. However, whether *hcfc1a* regulates *asxl1* by directly binding to the *asxl1* promoter is still not known, but interestingly ASXL1 and HCFC1 interact with one another in myeloid cells to regulate proliferation and differentiation (110). Thus, these two proteins may regulate the activity of one another at multiple levels.

We observed changes in the expression of various markers of neurons and glia. However, the physiological consequences of these changes are not currently known. Zebrafish have emerged as a model for neurodevelopmental disorders (111) and behavioral assays for seizure (112) and motor deficits (113) have been described. Therefore, we characterized the locomotion of *hcfc1a* mutants in response to light stimulus (114). Our results, using Zebrabox technology, demonstrated reduced motility as indicated by decreased distance travelled. Importantly, the decreased motility during a light stimulus was not due to an overall defective response to light, as our analysis demonstrated that carriers of the *hcfc1a<sup>co60/+</sup>* allele responded to normally to light stimulus, as indicated by the “V” like pattern in dark-light-dark conditions (115).

Decreased distance travelled has been previously defined as hypolocomotion and is associated with motor incoordination (116). Hypolocomotion has been demonstrated in zebrafish models of ALS (113,117) and fetal akinesia (118), two disorders characterized by motor deficits. Interestingly, the hypolocomotion we observed was correlated with increased NPCs and defects in the expression of various markers associated with differentiation. We did not observe short convulsions or whirlpool like behaviors in mutant larvae, which would have been indicative of a seizure phenotype and it is likely that the protocol we used to detect behavioral deficits does not stimulate a seizure like phenotype. Future studies that use multiple stimuli, including low dose convulsants will likely shed light on the epileptic phenotypes associated with mutations in *hcfc1a*.

## **Conclusions**

Our study focuses on the function of *hcfc1a*, one ortholog of *HCFC1*, during brain development. Specifically, we focus on the function of *hcfc1a* in modulating NPC number and proliferation. We demonstrate that *HCFC1* is essential for the proliferation of NPCs. Importantly we connect these cellular deficits to a molecular mechanism whereby *hcfc1a* indirectly or directly regulates *asx1* expression to control cellular proliferation. Thus, we propose that our system has the potential to inform about the transcriptional program regulating NPC function.

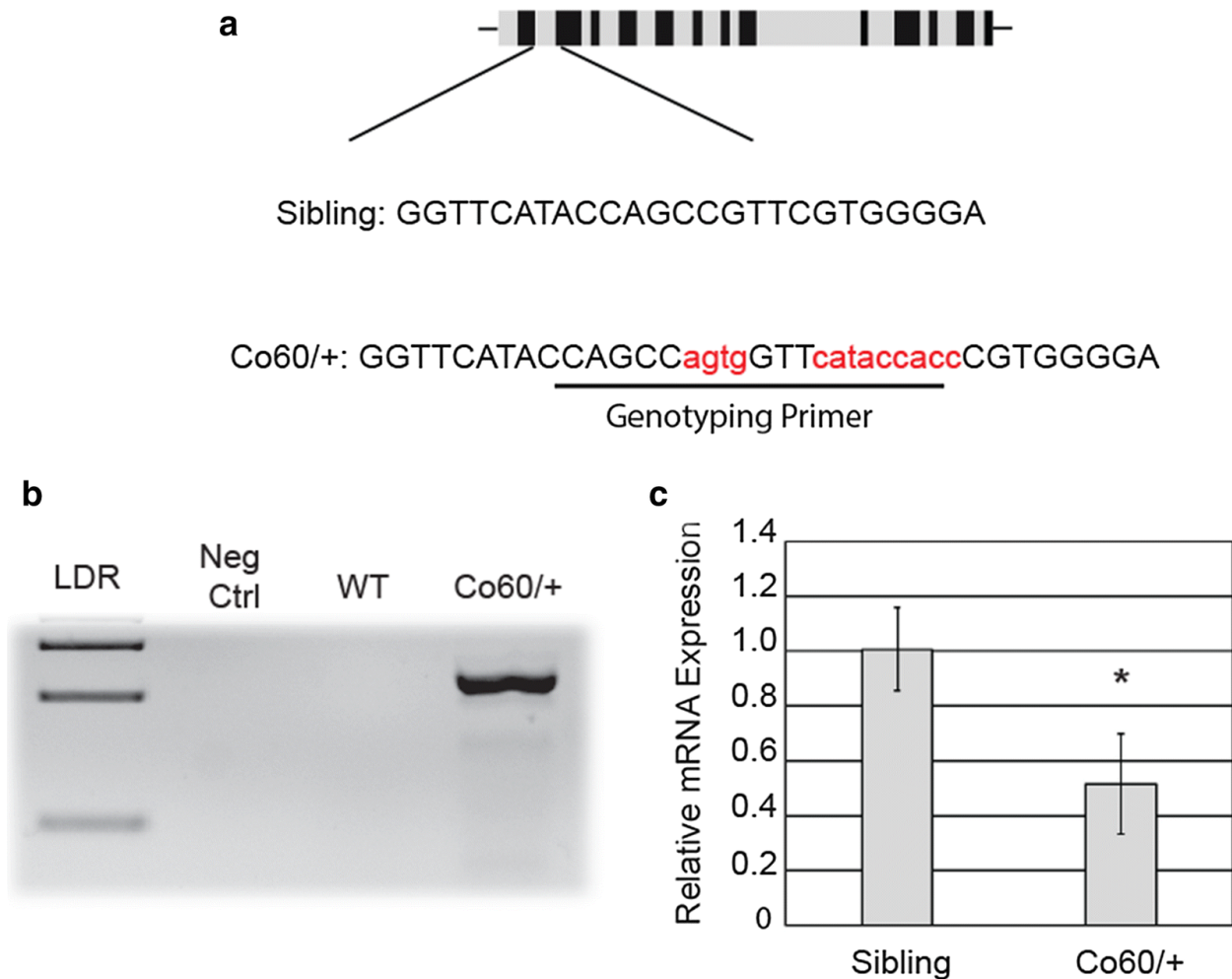


**Figure 1. Haploinsufficiency of the *hcf1a*<sup>co60/+</sup> allele (Co60/+).** A. Schematic of the exon structure of the *hcf1a* gene (not drawn to scale). The gRNA produced targets the sequence shown within exon 3 (Sibling). The Co60 allele results in an insertion of 13 nucleotides (Red). B. Primers were designed to specifically amplify the Co60 allele. The specific primer is underlined and bolded in the sequence presented in (A). Positive amplification is indicative of heterozygous carriers (Co60/+) with no amplification of the wildtype allele (WT). C. Quantitative real time PCR analyzing the relative expression of *hcf1a* in wildtype siblings (Sibling) and the *hcf1a*<sup>co60/+</sup> allele (Co60/+) at 2 days post fertilization. N=16 larvae per group with 3 biological replicates. \**p*<0.05

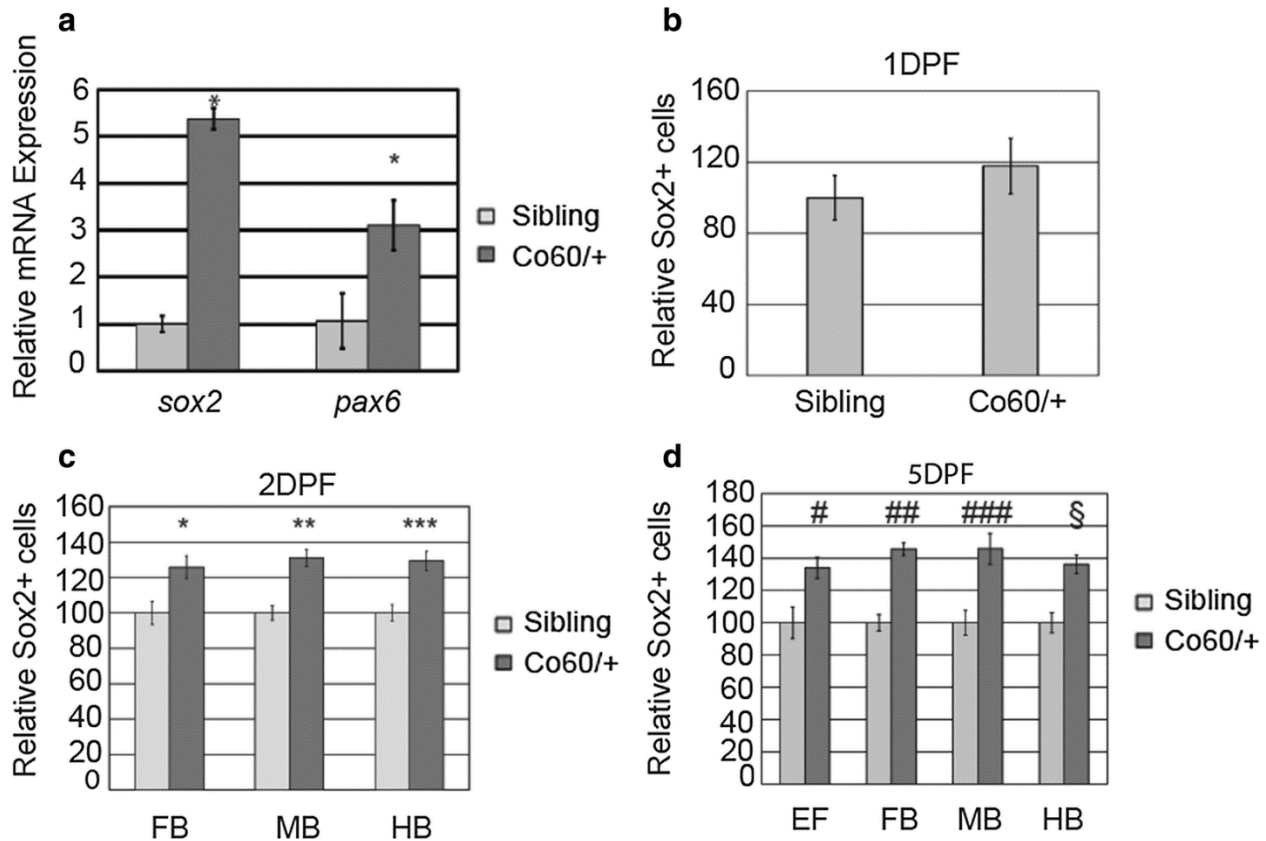


**Figure 2: The *hcfc1a<sup>co60/+</sup>* allele increases the number of Sox2+ cells in the developing brain.** A. Quantitative real time PCR analyzing the relative expression of *sox2* and *pax6* in wildtype siblings (Sibling) and the *hcfc1a<sup>co60/+</sup>* allele (Co60/+). N=7 larvae per group/biological replicate \*p<0.05. B-D. Quantification of the number of Sox2+ cells at 1 day post fertilization (DPF) (B), 2 DPF (C), and 5 DPF (D) in the early forebrain (EF), forebrain (FB), midbrain (MB), and hindbrain (HB). \*p=0.006828, \*\*p= 1.13873E-05, \*\*\*p= 0.000107, #p= 0.010168, ##p= 4.55E-06, ###p= 1.97E-07, and §p= 0.005476. In B, total number of animals is Sibling (N=6) and *hcfc1a<sup>co60/+</sup>* (N=6), C total animals is Sibling (N=7) and *hcfc1a<sup>co60/+</sup>* (N=7), and D total animals is Sibling (N=4) and *hcfc1a<sup>co60/+</sup>* (N=4). All error bars represent standard error of the mean.

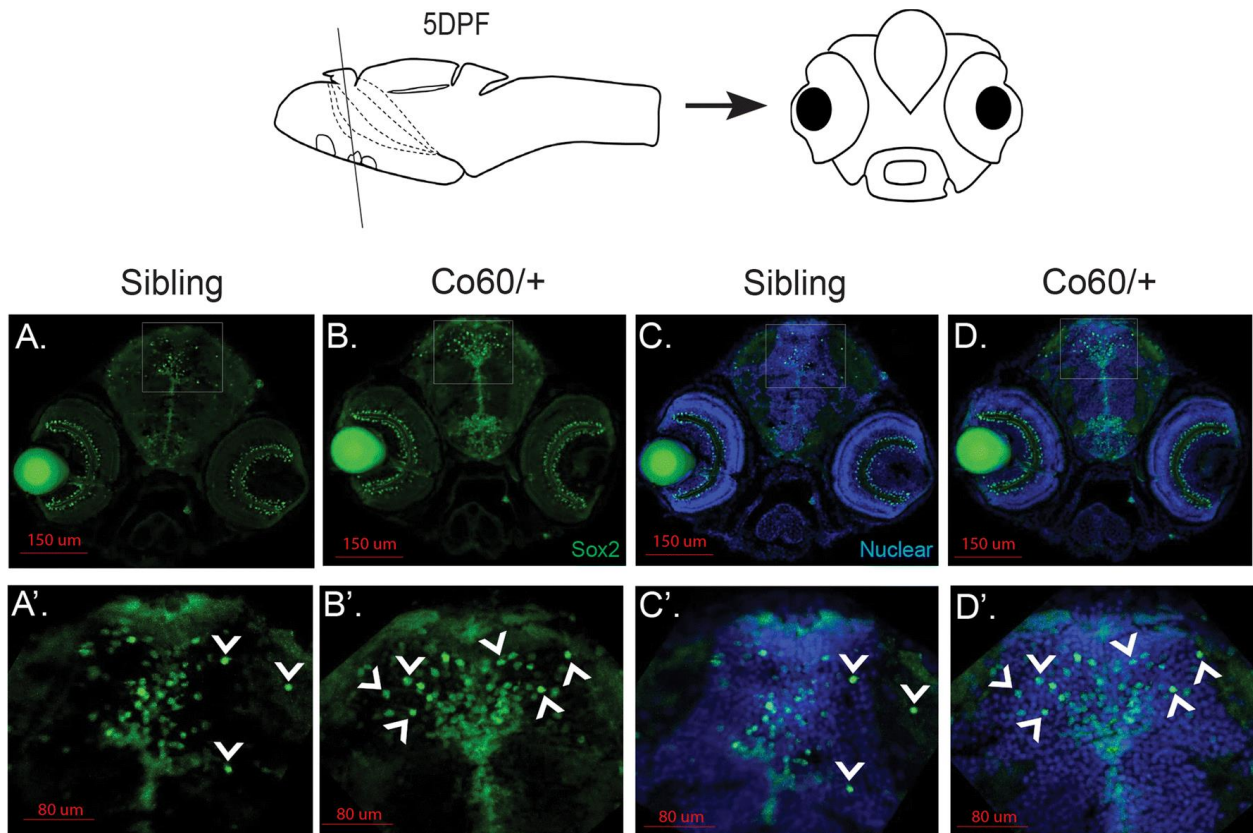


**Figure 3: Increased Sox2+ cells are present in the *hcf1a<sup>co60/+</sup>* allele.** A-D&A'-D'. Representative images of brain sections from larvae at 5 days post fertilization (DPF) stained with Sox2 antibodies (green) and Hoechst DNA content dye. The whole brain (20X) and the ventricular zone (63X) are shown. Images were captured from sections on a confocal microscope. A schematic of the zebrafish at 5 DPF is shown above representative images with a line to indicate the cross section below.

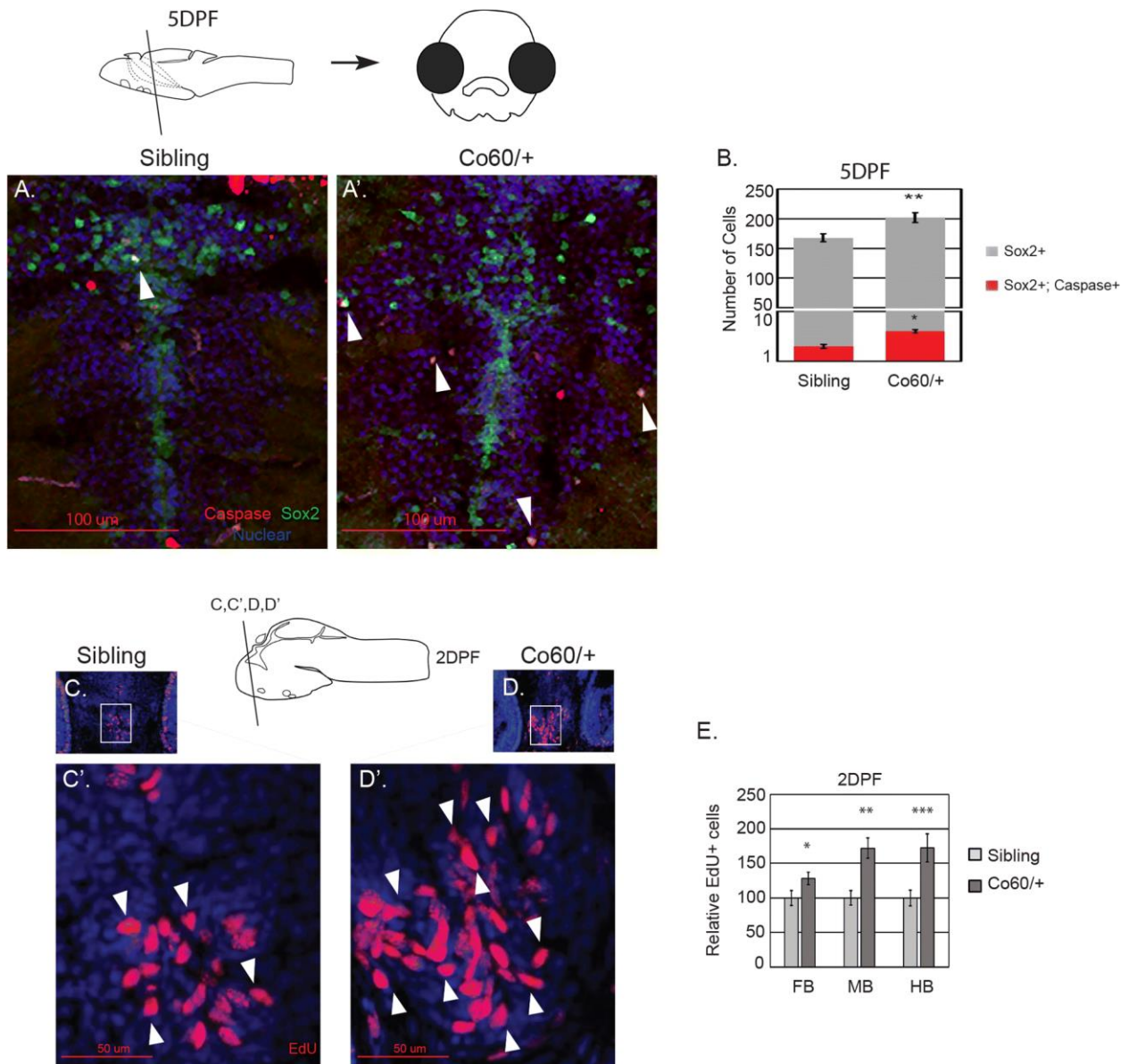


**Figure 4: The *hcf1a*<sup>co60/+</sup> allele is associated with increased cell proliferation and minimal cell death.** A-A'. Apoptosis of Sox2<sup>+</sup> neural precursor cells was assessed using anti-caspase 3 and anti-Sox2 antibodies at 5 days post fertilization (DPF). Representative images are depicted from sibling wildtype (Sibling) or the *hcf1a*<sup>co60/+</sup> allele (Co60/+). Arrows indicate Sox2<sup>+</sup> caspase<sup>+</sup> neural precursors. B. The total number of Sox2<sup>+</sup> Caspase<sup>+</sup> cells was quantified in wildtype siblings and the Co60/+ allele. Independently, the total number of Sox2<sup>+</sup> was also quantified and the graph depicts the total number of

Caspase positive NPCs (red bars; \* P= 1.47822E-16) present within the entire Sox2<sup>+</sup> population (gray bars; \*\*P<0.05). Due to the small number of total Sox2<sup>+</sup> Caspase<sup>+</sup> cells present, the data is depicted as total numbers of cells in the entire brain. N=3/group. C-D&C'-D'. Representative images of larvae (Sibling or Co60/+) pulsed with ethynyl-deoxyuridine (EdU) to monitor cell proliferation at 2DPF. C&D are 20X magnifications and C'&D' represent region in the inset at 63X magnification. E. Quantification of the total number of EdU positive cells in forebrain (FB), midbrain (MB), and hindbrain (HB) of siblings and *hcf1a<sup>co60/+</sup>* larvae at 2 DPF. \*p= 0.060553, \*\*p= 0.00108, \*\*\*p= 0.006642, N=9 per group. All error bars represent standard error of the mean.

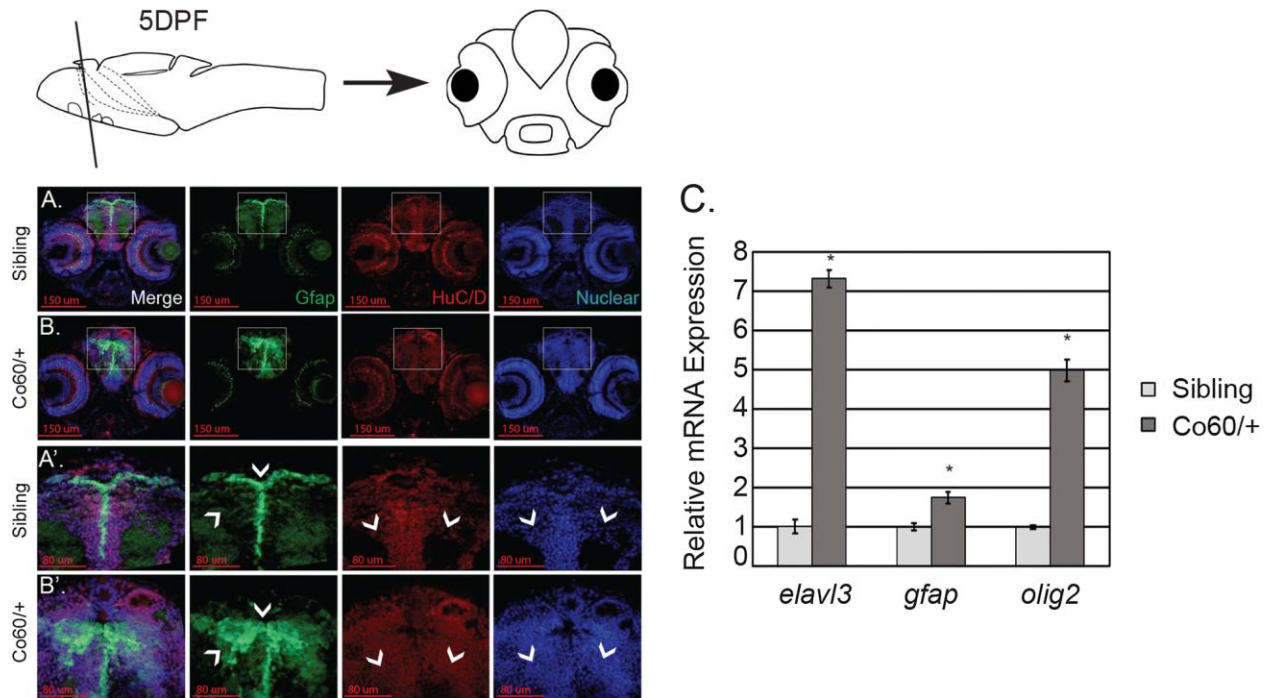


**Figure 5: The *hcfc1a*<sup>co60/+</sup> allele increases the expression of differentiation markers.**

A, A', B,&B'. Representative images of brain sections from *Tg(gfap:EGFP)* larvae harboring the *hcfc1a*<sup>co60/+</sup> allele (Co60/+) at 5 days post fertilization (DPF) stained with Elavl3 (HuC/D) antibodies and Hoechst DNA content dye. 20X representatives of the entire brain (A-B) and 63X sub-regions (A'-B') are shown. Wildtype siblings (N=6) and *hcfc1a*<sup>co60/+</sup> larvae (N=6). Arrowheads indicate regions of increased expression/localization of protein. Arrowheads of Hoechst (Nuclear) images demonstrate regions with cell bodies. The top schematic demonstrates a 5 DPF larval brain with a line to demonstrate the region depicted below. C. Quantitative real time PCR analysis of the expression of *elavl3*, *gfap*, and *olig2* in siblings and *hcfc1a*<sup>co60/+</sup> larvae (N=8/group/biological replicate). Error bars represent standard error of the mean. \* P<0.05.

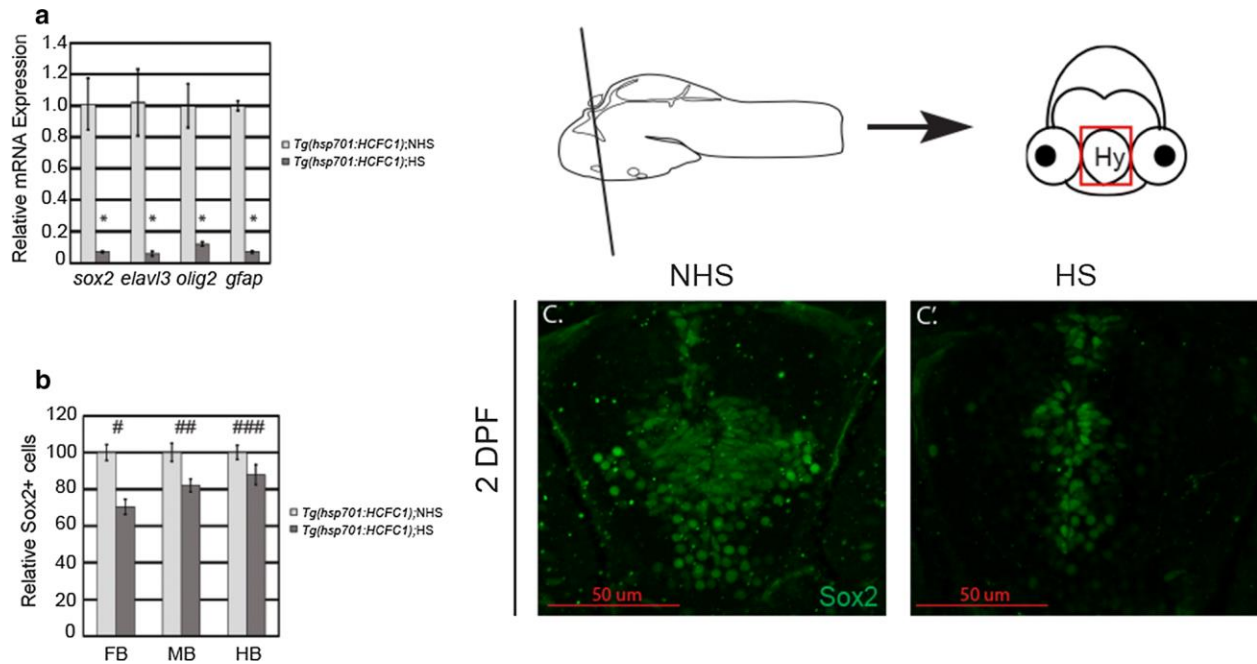


**Figure 6: Over expression of HCFC1 decreases NPC number and differentiation.** A. *Tg(hsp701: HCFC1)* were heat shocked according to the methods section and total RNA was isolated from control (No heat shock (NHS)) and heat shock larvae (HS). Quantitative PCR was performed to test the expression of *sox2*, *elavl3*, *olig2*, and *gfap*. Error bars represent standard error of the mean. N=28/group/biological replicate. \*P<0.05. B. The total number of Sox2 cells was quantified across forebrain (#P= 4.88568E-05), midbrain (##P= 0.004359), and hindbrain (##P=0.077). Error bars represent standard error of the mean. N=5/group. C&C'. Representative images of 2 days post fertilization (DPF) *Tg(hsp701:HCFC1)* larvae (NHS or HS) stained with anti-Sox2 antibodies. Schematic demonstrates 2 DPF larval brain section with graphical inset of hypothalamus (Hy) to specify region shown.

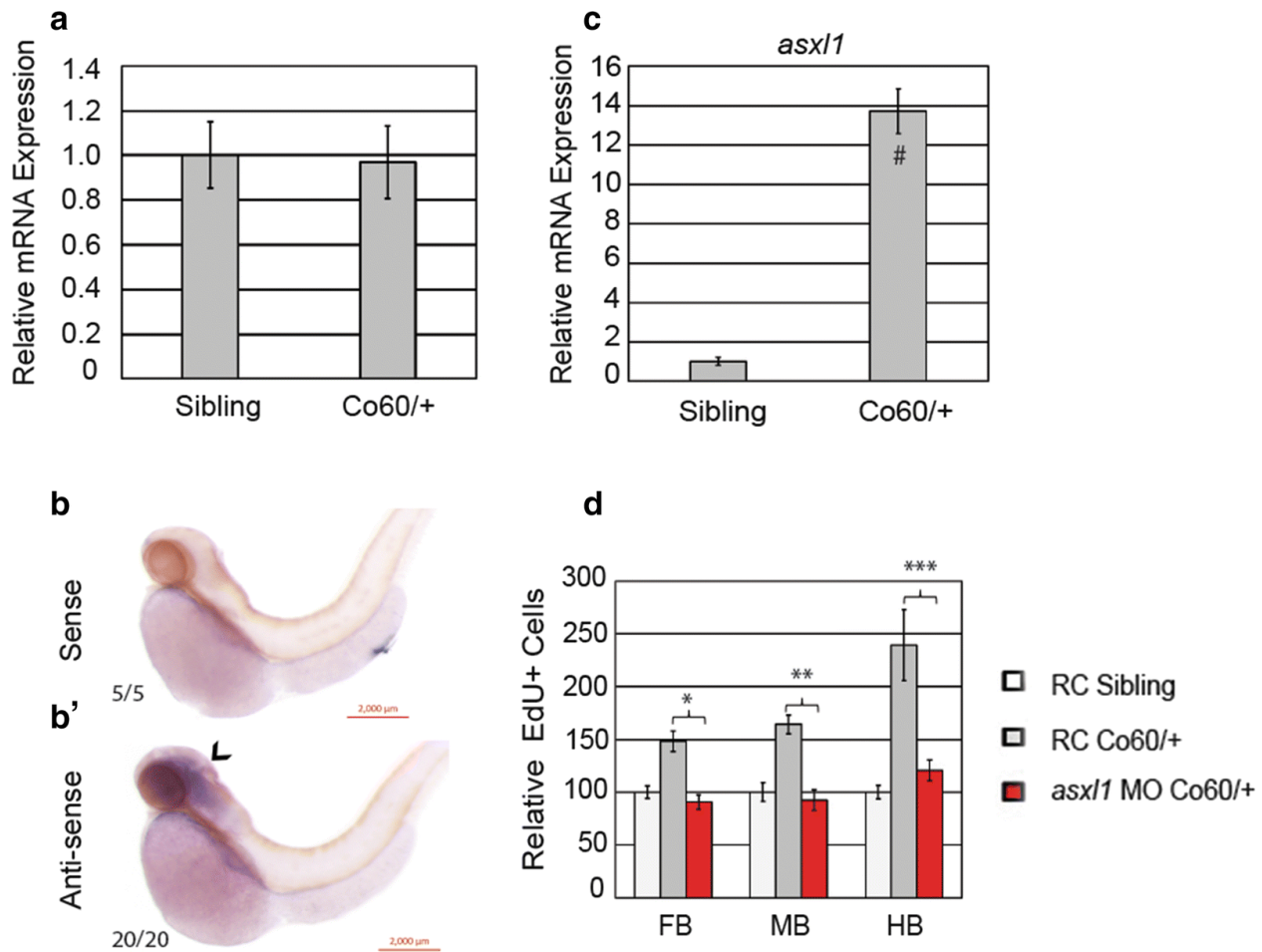


**Figure 7. The *hcfc1a*<sup>co60/+</sup> allele regulates brain development and *asx1* expression.**

A. Quantitative real time PCR (QPCR) analyzing the relative expression of *mmachc* in wildtype siblings (Sibling) and *hcfc1a*<sup>co60/+</sup> larvae (Co60/+). N=16 larvae per group with 3 biological replicates. (B&B') Whole mount *in situ* hybridization (ISH) was performed at 2 days post fertilization (DPF) using a riboprobe targeting *asx1* mRNA. ISH was performed with sense control (B) and anti-sense specific probe (B'). Purple demonstrates positive staining in the developing brain. N= 21. C. QPCR analyzing the relative expression of *asx1* in wildtype siblings (Sibling) and the *hcfc1a*<sup>co60/+</sup> allele. N=16 larvae per group with 3 biological replicates. # p<0.05. D. *hcfc1a*<sup>co60/+</sup> larvae (Co60/+) and their wildtype siblings (Sibling) were injected with translation inhibiting morpholinos targeting *asx1* (*asx1* MO)

or random control (RC) morpholinos. At 2 DPF, larvae were pulsed and stained for EdU incorporation and the number of EdU positive cells was counted per brain section. The total number of cells in the forebrain (FB), midbrain (MB), and hindbrain (HB) was calculated. \*p=0.000127, \*\*p=0.000407, \*\*\*p=0.00712. N=6/group.

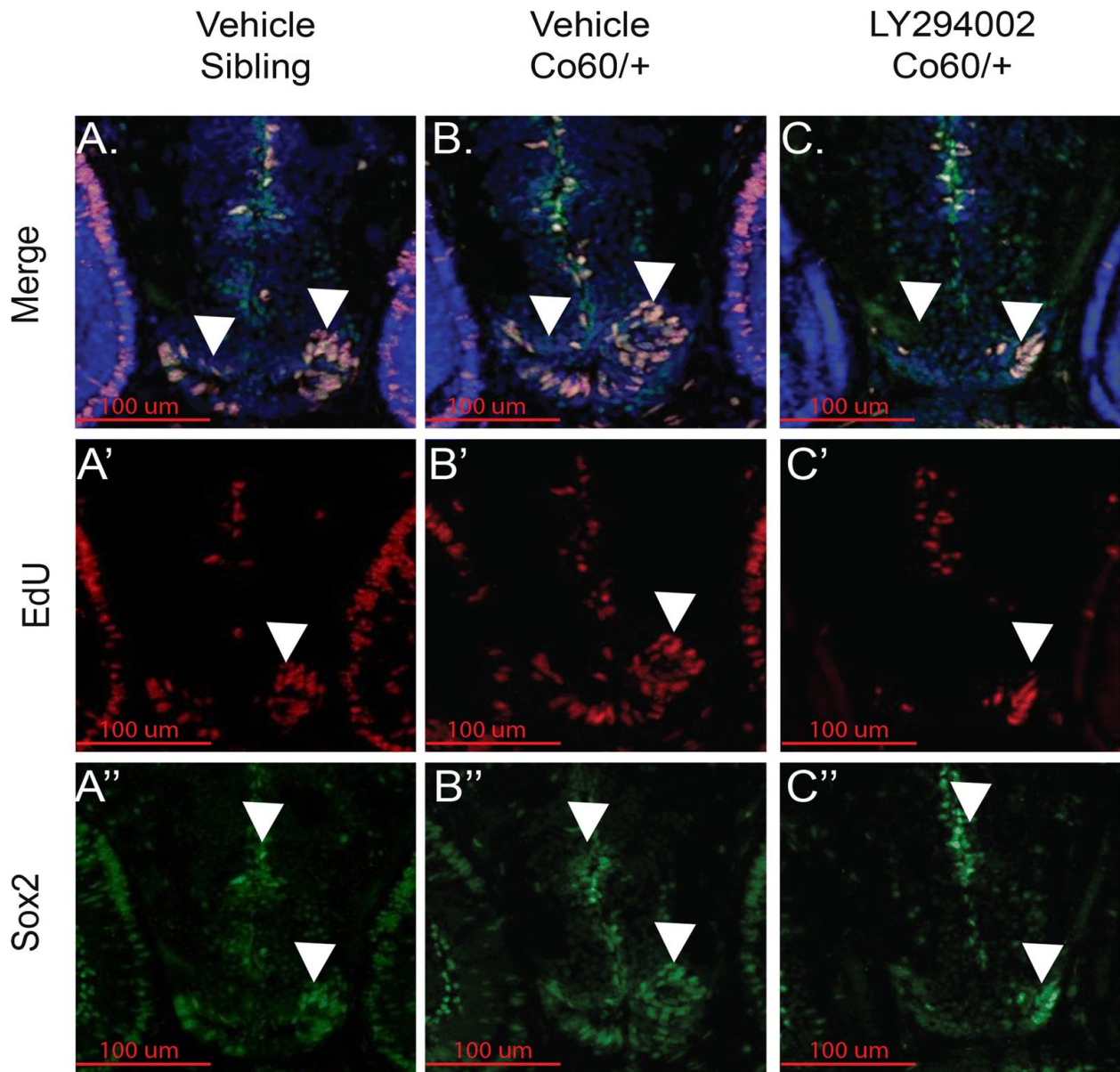


**Figure 8: Inhibition of *Asx1* activity restores the NPC deficits in the *hcf1a<sup>co60/+</sup>* allele.** A-A'', B-B''&C-C''. Representative 20X images of Sibling wildtype (A-A''), *hcf1a<sup>co60/+</sup>* larvae (Co60/+) (B-B''), or Co60/+ larvae treated with 12uM LY294002 (C-C'') at 2 days post fertilization (DPF).

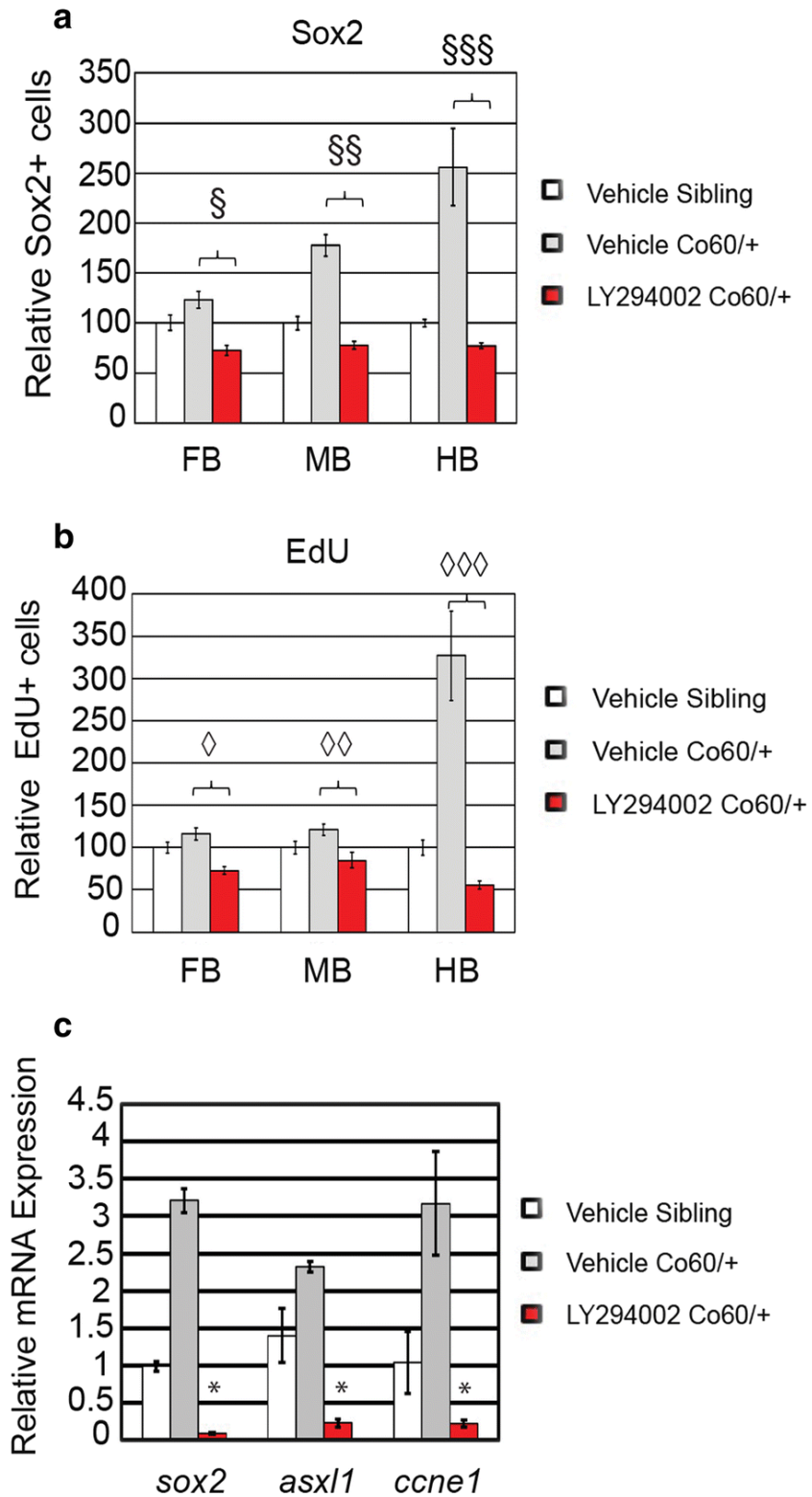


**Figure 9: Quantification of the number of NPCs after inhibition of Asxl1 activity.**

A&B. Quantification of the number of Sox2+(A) or EdU (B) positive cells in vehicle treated

and larvae treated with LY294002 at 2 days post fertilization (DFP). N= 4 Vehicle Sibling, 6 Vehicle *hcfc1a<sup>co60/+</sup>* larvae, and 4 LY294002 *hcfc1a<sup>co60/+</sup>* larvae. §p=0.000168, §§p=2.08852E-09, §§§p=0.000153. ◇p=7.22142E-07, ◇◇p=0.000997, ◇◇◇p=0.00014. All error bars represent standard error of the mean. C. *hcfc1a<sup>co60/+</sup>* larvae and their wildtype siblings (Sibling) were treated at 24-hour intervals with 12uM LY294002 until 5 DPF and then total RNA was isolated from brain homogenates. Quantitative real time PCR was performed to test the expression of *sox2*, *asx1*, and cyclin E (*ccne1*). N=10/group/biological replicate. Error bars represent standard error of the mean. \*P<0.05

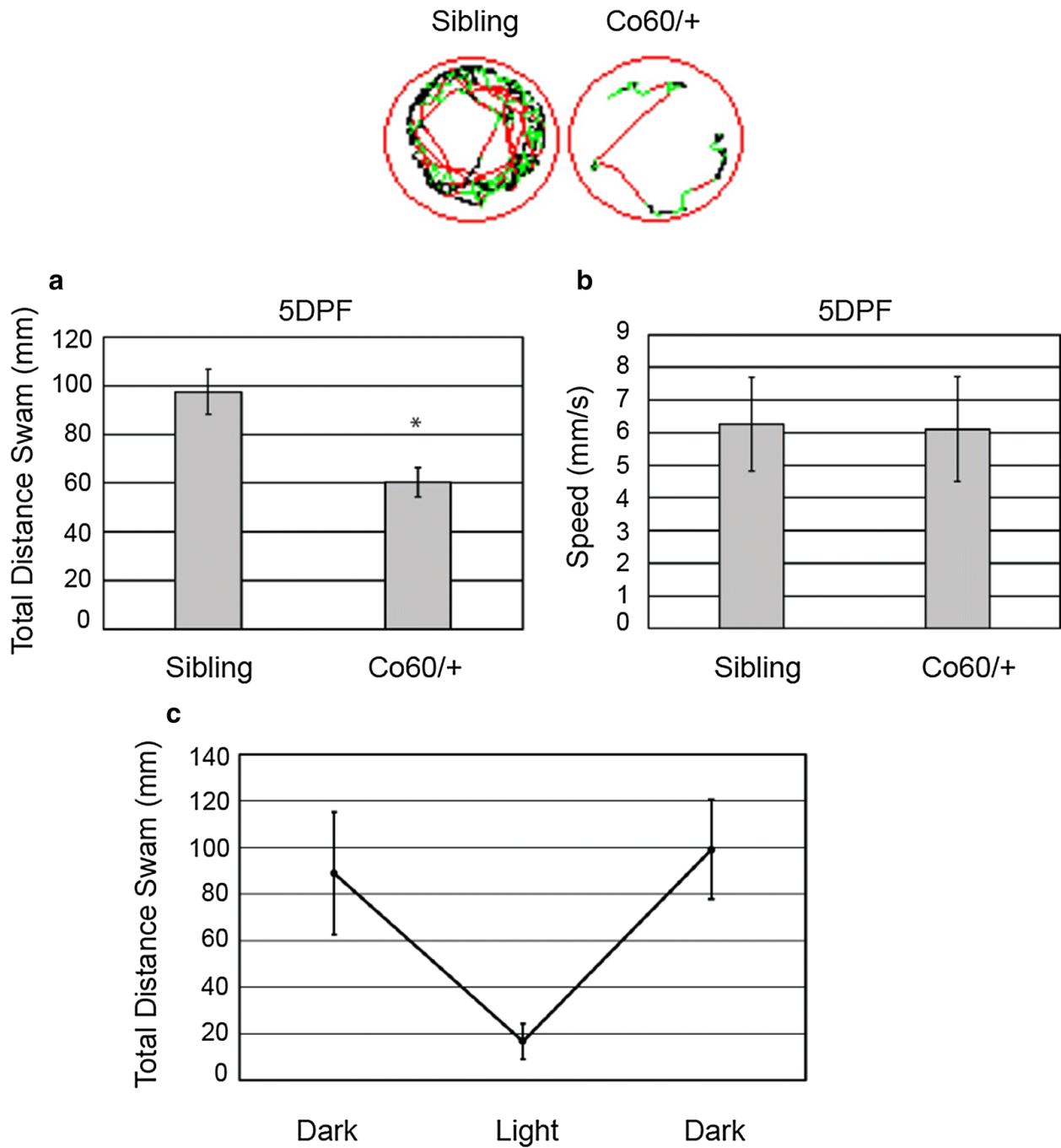


**Figure 10: The *hcfc1a*<sup>co60/+</sup> is associated with hypomotility.** Total distance (A) and average speed (B) of wildtype (Sibling) and heterozygous carriers of the *hcfc1a*<sup>co60/+</sup> (Co60/+) allele were tracked at 5 days post fertilization (DPF) using ZebraBox technology. Distance and speed were monitored during light stimulus for a 5-minute duration. Top

panel shows representative tracking patterns from Sibling wildtype and heterozygous carriers of the Co60/+ allele. \* $p < 0.001$ . N=52 Sibling wildtype and 56 Co60/+ individual larvae. C. 5 DPF larvae were monitored for total distance swam in alternating dark-light conditions.

## CHAPTER III

### RESEARCH MANUSCRIPT II

Section I: Missense and nonsense mutations of the zebrafish *hcfc1a* gene result in contrasting mTor and radial glial phenotypes.

Castro, V. L., Paz, D., Virrueta, V., Estevao, I. L., Grajeda, B. I., Ellis, C. C., & Quintana, A. M. (2023). Missense and nonsense mutations of the zebrafish *hcfc1a* gene result in contrasting mTor and radial glial phenotypes. *Gene*, *864*, 147290. <https://doi.org/10.1016/j.gene.2023.147290>

#### **Abstract**

Mutations in the HCFC1 transcriptional co-factor protein are the cause of *cbIX* syndrome and X-linked intellectual disability (XLID). *cbIX* is the more severe disorder associated with intractable epilepsy, abnormal cobalamin metabolism, facial dysmorphism, cortical gyral malformations, and intellectual disability. *In vitro*, murine *Hcfc1* regulates neural precursor (NPCs) proliferation and number, which has been validated in zebrafish. However, conditional deletion of mouse *Hcfc1* in *Nkx2.1+* cells increased cell death, reduced *Gfap* expression, and reduced numbers of GABAergic neurons. Thus, the role of this gene in brain development is not completely understood. Recently, knock-in of both a *cbIX* (*HCFC1*) and *cbIX*-like (*THAP11*) allele were created in mice. Knock-in of the *cbIX*-like allele was associated with increased expression of proteins required for ribosome biogenesis. However, the brain phenotypes were not comprehensively studied due to sub-viability. Therefore, a mechanism underlying increased ribosome biogenesis was not described. We used a missense, a nonsense, and two conditional zebrafish

alleles to further elucidate this mechanism during brain development. We observed contrasting phenotypes at the level of Akt/mTOR activation, the number of radial glial cells, and the expression of two downstream target genes of HCFC1, *asx1* and *ywhab*. Despite these divergent phenotypes, each allele studied demonstrates with a high degree of face validity when compared to the phenotypes reported in the literature. Collectively, these data suggest that individual mutations in the HCFC1 protein result in differential mTOR activity which may be associated with contrasting cellular phenotypes.

## **Introduction**

Mutations in the human HCFC1 transcriptional co-factor protein cause *cbIX* syndrome (MIM 309541) (119,120) and X-linked intellectual disability (XLID) (121–125). *cbIX* is a multiple congenital anomaly syndrome characterized by abnormal cobalamin metabolism, neurodevelopmental defects, cortical gyral malformations, intractable epilepsy, craniofacial dysmorphic features, and movement disorders. However, XLID is milder and associated only with intellectual disability. The clinical phenotypes of the patients are heterogeneous and varied in severity. Multiple systems and approaches have been undertaken to understand the function of human HCFC1 during development. *in vitro* over expression assays first revealed decreased neural precursor cell (NPC) proliferation with abnormal differentiation and a bias towards the astrocyte lineage in mouse neurospheres (121). Later we demonstrated that mutation or knockdown of the zebrafish paralogs of *HCFC1* caused increased proliferation of NPCs, but these changes were associated with increased expression of radial glial (RGC) and neuronal markers (126,127). Global deletion of *Hcfc1* in mice was embryonic lethal (128), but tissue specific deletion in *Nkx2.1*+ progenitors caused increased death in the cells of the sub-ventricular

zone and mantle, which was associated with a decrease in GABAergic interneurons and glia (129). Thus, while model system specific, previous studies collectively demonstrate a function for human HCFC1 in brain development and neural precursors.

Recently, a patient derived *cbIX* mutation (p.A115V) was knocked into the mouse *Hcfc1* loci to produce the first *in vivo cbIX* model, but the brain phenotypes were not comprehensively studied. However, these studies suggested a mechanism by which mutations in mouse *Hcfc1* cause abnormal development. Concurrently, Chern and colleagues uncovered increased expression of proteins essential for ribosome biogenesis in a *cbIX*-like disorder (62) caused by mutations in the mouse THAP11 (p.F80L) protein, a protein that interacts with HCFC1 in human cells and in the mouse (130). These data are described by previous *in vitro* studies which have shown that human and mouse HCFC1 regulate genes essential for metabolism and stem cell maintenance (131,132). What remains uncharacterized is the mechanism by which *in vivo* mutations in the HCFC1 protein promote increased ribosome biogenesis as well as the effects of this biogenesis on brain development.

The mechanistic target of rapamycin (mTOR) pathway is a well-known regulator of protein translation and cell growth, particularly as it relates to stem cell regulation (133). Interestingly, the mTOR pathway is a common pathway dysregulated in neurodevelopmental disorders (134). Zebrafish harbor one mTOR ortholog, which is expressed in the brain throughout development (135). mTOR is regulated at many levels, but one positive regulator of this pathway is PI3K/AKT. Activation of PI3K leads to AKT activation, which in turn drives activation of mTOR signaling and promotes ribosomal biogenesis and protein synthesis. We have previously demonstrated that inhibition of

PI3K can restore the NPC deficits present in a zebrafish with a nonsense mutation in *hcfc1a* (co60 allele) (126). These data, combined with recent literature, indirectly link regulation of PI3K/AKT signaling with phenotypes that occur in *cbfX* syndrome. PI3K/AKT signaling is conserved in zebrafish, so we characterized this pathway in two germline mutant alleles of the zebrafish *hcfc1a* gene. In addition, we previously identified a driver of AKT signaling, the zebrafish *Asxl1* polycomb group protein, which was up-regulated in the co60 allele, one germline mutant of zebrafish *hcfc1a* (126). These data implicate *Asxl1*, as an HCFC1 downstream target gene, and a putative mediator of Akt/mTor in zebrafish. Therefore, we hypothesized that mutations in human HCFC1 drive ribosomal biogenesis and disrupt brain development through regulation of AKT/mTOR.

Here we identified divergent activity of the zebrafish Akt/mTor signaling pathway in two independent zebrafish *hcfc1a* germline mutant alleles. Contrasting Akt/mTor activity was correlated with divergent RGC phenotypes. In addition, we identified disparate expression of two downstream effectors of the human HCFC1 protein in each allele: *Asxl1* and 14-3-3 $\beta$ , both of which are known to regulate PI3K/AKT/mTOR activity, and brain development in mouse and human cells (136–139). Further, restoration experiments revealed that zebrafish *gfap* expression is mTor dependent. Thus, our analysis of distinct zebrafish *hcfc1a* mutant alleles raises the possibility that unique patient variants can have different effects on human HCFC1 protein dosage/function and may lead to individual cellular and molecular phenotypes.

## **Materials and Methods**

### ***Experimental model and subject details.***

For the experiments described, embryos were produced from natural spawning's of the following lines: *hcfc1a<sup>co64/co64</sup>*, *hcfc1a<sup>co60/+</sup>*, *Tg(sox2:2A:EGFP)*, *Tg(gfap:EGFP)*, *Tg(hsp701:HCFC1)*, *Tg(hsp701:HCFC1c.344C>T)*, AB, or Tupfel long fin. Embryos were maintained in E3 media as described by the protocols on the Zebrafish Information Network (ZFIN) at 28° with a 14/10 light:dark cycle. All procedures were approved by the Institutional Animal Care and Use Committee at the University of Texas El Paso, protocol number 811869-5. Methods for euthanasia and anesthesia were performed according to guidelines from the 2020 American Veterinary Medical Association guidebook.

The *hcfc1a<sup>co64/co64</sup>* allele was created as previously described (126) with an identical guide RNA and with equivalent CRISPR/Cas9 editing technology as described. The *hcfc1a<sup>co64/co64</sup>* was created at the same time as the afore published *hcfc1a<sup>co60/+</sup>* allele except that the insertion/deletion introduced produced a second allele with the sequences described. The offspring of the *hcfc1a<sup>co64/co64</sup>* allele were generated from a single founder (F<sub>0</sub>), which was outcrossed with 3 independent wildtype fish to generate a minimum of 3 families of F1 carriers. Each family consisted of approximately 20 total fish with equal numbers of males and females. To generate subsequent generations, we outcrossed a minimum of 3-F1 individuals with wildtype to obtain a minimum of 3 families of F2 carriers. We subsequently outcrossed F2 carriers (minimum of 3) with wildtype (AB) fish to produce an F3 generation of approximately 3 total families with equal numbers of males and females. Sanger sequencing confirmed mutation of the allele and experiments were initiated in the F3 generation. The *Tg(hsp701:HCFC1c.344C>T)* was created using Gateway cloning technology as previously described (126,140). Vectors utilized for the HCFC1 open reading frame were previously described (127,141). The experiments described

herein were performed in the F2 generation, which was produced from a single founder (F<sub>0</sub>). The positive F<sub>0</sub> carrier was outcrossed with wildtype (AB) to produce 2 families of F1 individuals and a minimum of 3 carriers of the F1 generation were outcrossed to produce 3 families of F2 carriers that were utilized for the experiments described. All shared resources will be shared via ZFIN.

### ***Genotyping of indicated zebrafish lines.***

Genotyping was performed with DNA from excised larval tissue or fin clips (adults). Tissue was lysed in 50 millimolar (mM) sodium hydroxide (Fisher Scientific) for 15 minutes at 95° Celsius and pH adjusted with 1M Tris-HCl. Primers pairs were developed for each allele that specifically bind to and amplify the mutated allele and will not amplify the wildtype allele (126). For the *hcfc1a*<sup>co60/+</sup> the primers specific to the mutated allele are FWD: CCAGTTCGCCTTTTTGTTGT and REV: ACGGGTGGTATGAACCACTGGC. PCR annealing was performed at 64°. For the *hcfc1a*<sup>co64/co64</sup> allele, the mutant allele was amplified by standard PCR at an annealing temperature of 64° with FWD: CCAGTTCGCCTTTTTGTTGT and REV: CTGGAGGGATGTTTCATAACGG). For identification of the wildtype allele, the following primers were utilized: FWD: CCAGTTCGCCTTTTTGTTGT and REV: TCCCCACGAACGGCTGGTAT.

Genotyping of the *Tg(hsp701:HCFC1)* allele was performed with the following primers: FWD: TGAAACAATTGCACCATAAATTG present in the *hsp701* promoter and REV: CGTCACACACGAAGCCATAG in the *HCFC1* open reading frame. PCR for *HCFC1* genotyping was performed at 60° annealing temperature with standard extension times. The two heat shock alleles were genotyped with overlapping primer pairs. Genotyping and validation of this allele was previously described (126).

### ***Protein Isolation and western blotting***

Protein was isolated from the excised brains of larvae at 5 DPF. Brains were homogenized using a pestle in 1X Radio-Immuno-Precipitation-Assay (RIPA) (Fisher Scientific) or 1X Cell Lysis Buffer (Cell signaling). Protease inhibitors were added at a final 1X concentration (Fisher Scientific). Supernatant was collected after a 10-minute centrifugation at 10,000XG in a cold centrifuge. Protein concentration was quantified using Precision Red (Cytoskeleton) according to manufacturer's instructions. Western blots were performed using standard techniques using the Novex Tris-Glycine-SDS system (Fisher Scientific). Protein loading was quantified using Ponceau S (Fisher Scientific) and membranes were blocked with 5% ECL Prime Blocking Agent (Fisher Scientific). Primary antibody concentrations are as follows: *pAkt* (Thr308) (Cell Signaling Cat. # D25E6) (anti-rabbit) 1:3000, *Akt* (pan) (Cell Signaling Cat. # C67E7) (anti-rabbit) 1:3000, 14-3-3-beta/alpha (Cell Signaling Cat # 9636S) (anti-rabbit) 1:3000, S6 Ribosomal (5G10) (Cell Signaling Cat # 2217S) (anti-rabbit) 1:3000, P-S6 Ribosomal Protein (S235/236) (Cell Signaling Cat # 4858S) (anti-rabbit) 1:3000, *Asx1* (Cell Signaling Cat # 52519S) (anti-rabbit) 1:3000, Beta-Actin (Sigma/Millipore Cat # A5441 clone AC-15) (anti-mouse) 1:5000, N-terminal HCFC1 (Sigma/Millipore Cat # QC10816) (anti-rabbit) 1:500, C-terminal HCFC1 (Bethyl labs Cat # 50-156-0286 purchased through Fisher Scientific) (anti-rabbit) 1:100. Secondary antibodies were utilized at a concentration of 1:20,000 and chemiluminescence was performed with ECL Primer Western Blotting detection reagent (Fisher Scientific). Imaging was performed using an iBright chemiblot system.

### ***RNA isolation and quantitative real time PCR***

RNA was isolated from embryos at the indicated time points using Trizol (Fisher Scientific) according to manufacturer's protocol. Reverse transcription was performed using Verso cDNA synthesis (Fisher Scientific) and total RNA was normalized across all samples. For each biological replicate (2-5/experiment) PCR was performed in technical triplicates using an Applied Biosystem's StepOne Plus machine with Applied Biosystem's software. Analysis was performed using  $2^{-\Delta\Delta ct}$ . Sybr green (Fisher Scientific) based primer pairs for each gene analyzed are as follows: *hcfc1a fwd*: ACAGGGCCTAACACAGGTTG, *hcfc1a rev*: TCCTGTGACTGTGCCAAGAG, *hcfc1b fwd*: GGATGGGTCCCTCTGGTTAT, *hcfc1b rev*: CGGTAACCATCTCGTCCACT, *mmachc fwd*: CACACTGTCTGCCTGCATCT, *mmachc rev*: CGGATTGTGGATGTCTGATG, *asx1 fwd*: CCAGAGCTGGAAAGAACGTC, *asx1 rev*: ACATCTCCAGCTTCGCTCAT, *rpl13a fwd*: TCCCAGCTGCTCTCAAGATT, *rpl13a rev*: TTCTTGGAATAGCGCAGCTT.

### ***Proteomics sample preparation***

Samples were isolated from the whole brain as described above and proteins were precipitated from lysis buffer using trichloroacetic acid (TCA) as follows: 50 microliters ( $\mu$ l) of 100% TCA (Sigma/Millipore – cat# T6399-5G) was added to 200  $\mu$ l of protein sample at a final concentration of 20%, then incubated at 4°C for 10 minutes. The mixture was centrifuged at 14,000 relative centrifugal force (rcf) for 5 minutes. The pellet was resuspended in 200  $\mu$ l of 100% liquid chromatography-mass spectrometry (LC/MS) grade acetone (Fisher Scientific) and centrifuged at 14,000 rcf for 5 minutes and supernatant was discarded. This process was repeated two more times to ensure removal of residual detergents. After the third wash, the pellet was heated on a heating block at 95°C for 2

minutes to ensure acetone evaporation. Samples were stored at -80°C and resuspended in 8M Urea prior enzymatic digestion.

Enzymatic tryptic digestion of proteins was obtained by using iST Sample preparation kit from PreOmics (catalog no. iST 96x 00027) according to manufacturer's instructions. Briefly, 10 µl of LYSE buffer was added per 1 microgram (µg) of protein from larvae brains and placed in a heating block (80°C for 20 min, mixing every 5 min) for protein denaturing, alkylation, and reducing disulfide bonds within it. Droplets were subject to brief centrifugation (300 rcf; 10 sec, room temperature). Samples were sonicated using 10-cycles; 30 sec on/off. After sonication, 50 µL of DIGEST buffer was added, gently vortexed, and placed in a heating block at 37°C for 90 minutes. Samples were gently vortexed every 10-minutes during the 90-minute incubation period. One hundred microliters of STOP solution was added and thoroughly mixed by pipetting up and down 10-times. Samples were transferred to cartridges using 1.5 milliliters (mL) microcentrifuge tubes with collar adapters and centrifuged for 1-minute at 3,800 rcf. Loaded peptides were washed once with 200 µL of Wash-1 and Wash-2 solutions, with 1-minute 3,800 rcf centrifugation in between each wash step. Peptides were eluted in a fresh 1.5 mL microcentrifuge tube using 100 µL of ELUTE solution for 1-minute at 3,800 rcf each. Two elution rounds were performed. Eluted peptides were dried completely in a speed vacuum centrifugation at 45°C, 100 mTorr, for 90 min (Savant; Thermo Fisher Scientific). Dried peptides were stored at -80°C until ready for LC-MS/MS data acquisition.

### ***Liquid chromatography–tandem mass spectrometry (LC/MS)***

Digested peptide mixtures were resuspended in LC/MS grade 4% acetonitrile (ACN) (Fisher Scientific), 0.1% formic acid (FA), at a concentration of 1 µg/µL. One microliter of

resuspended samples was loaded onto an Acclaim PepMap rapid separation LC column (75 $\mu$ m x 50cm nanoViper, PN 164942, Thermo Scientific), which had been previously equilibrated with 4% solvent B (100% acetonitrile, 0.1% formic acid), and 96% solvent A (100% H<sub>2</sub>O, 0.1% formic acid). The multi-step gradient started with peptides being loaded with a flow rate of 0.5 $\mu$ L/min for 15 minutes using a Dionex Ultimate 3000 RSLCnano (Thermo Scientific). The flow rate was decreased to 0.3 $\mu$ L/min over 15 min, and the solvent B increased to 20% at 115 minutes, then increase to 32% at 135 minutes, and finally increased to 95% solvent B over 1 minute. To elute any additional remaining peptides, 95% solvent B was held for 4 minutes at a flow rate of 0.4 $\mu$ L/min. The flow rate was increased to 0.5 $\mu$ L/min over 1 minute. The column was re-equilibrated at 4% solvent B for 39 minutes and maintained a flow rate of 0.5  $\mu$ L/min for a total of 180 minutes total runtime for each technical duplicate. The column was maintained at 55°C throughout the entire data acquisition. One blank injection was performed between biological samples using a 60-minute two sawtooth gradient at 4-95% solvent B and re-equilibrated at 4% solvent B for the next sample injection.

Eluted peptide information was acquired with a Q-Exactive Plus Hybrid Quadrupole-Orbitrap Mass Spectrometer (Thermo Scientific) in positive mode, set to data dependent MS<sup>2</sup>. Full MS ions were collected at resolution of 70,000, AGC target of 3e<sup>6</sup>, with a scan range of 375 to 1500 *m/z*. Ions were fragmented with NCE set to 27 and collected at a resolution of 17,500 with AGC target at 1e<sup>5</sup>, 2 *m/z* isolation window, maximum IT set to 60 ms, loop count 10, TopN 10. Charged exclusion ions were set to unassigned, 1, 6 – 8, >8.

### ***Bioinformatics data analysis***

After LC/MS analysis, Proteome Discover (PD) 2.5.0.400 (Fisher Scientific) was utilized to identify the proteins from each peptide mixture. The database for *Danio rerio* was downloaded from UniProtKB; <http://www.uniprot.org/> on 21 October 2021 with a database 61,623 sequences. A contaminant dataset was run in parallel composed of trypsin autolysis fragments, keratins, standards found in CRAPome repository and in-house contaminants. PD analysis parameters are as follows: false-discovery rate (FDR) of 1%, HCD MS/MS, fully tryptic peptides only, up to 2 missed cleavages, parent-ion mass of 10 ppm (monoisotopic); fragment mass tolerance of 0.6 Da (in Sequest) and 0.02 Da (in PD 2.1.1.21) (monoisotopic). Two-high confidence peptides per protein were applied for identifications. PD dataset was processed through Scaffold Q+S 5.0.1. Scaffold (Proteome Software, Inc., Portland, OR 97219, USA) was used to probabilistically validate protein identifications derived from MS/MS sequencing results using the X!Tandem and Protein Prophet computer algorithms. Data was transferred to Scaffold Lfq (Proteome Software, Portland, Oregon, USA) which was used to validate and statistically compare protein identifications derived from MS/MS search results. A protein threshold of 95%, peptide threshold of 95%, and a minimum number of 2 peptides were used for protein validation. Normalized weighted spectral counts were used when comparing the samples. To ascertain p-values, Fisher's Exact was run with a control FDR level  $q * .05$  with standard Benjamini-Hochberg correction.

### ***Flow cytometry***

To identify mutants, we adapted a protocol whereby tissue was excised from caudal most tip of the tail from larvae at 2-3 DPF (142). Tissue was collected on a filter paper and genotyped as described in the sections above. Equal numbers of mutants and wildtype

larvae were euthanized according to standard procedures, then heads were excised from tails to create a whole brain homogenate. Dissociation of heads was followed exactly according to previous protocol (143). Briefly, tissue was dissociated using Trypsin-EDTA (0.25%) (Fisher Scientific) with collagenase (100mg/mL) (Fisher Scientific), applying heating at 30° Celsius and disturbing tissue by pipetting up and down. The reaction was stopped by adding lamb serum (Fisher Scientific) and cells were harvested through centrifugation (5 minutes at 700g at room temperature). The cells were resuspended in 1X phosphate buffered saline (Fisher Scientific) and filtered through 40-70µM filter before performing flow cytometry. Analysis was performed with Kaluza software at a fixed rate of 10,000 cell events for a maximum of 3 minutes.

### ***Immunohistochemistry***

The larvae were fixed at the indicated time points in 4% paraformaldehyde (Electron Microscopy Sciences) for minimum of 1 hour at room temperature. Genotyping was performed as described (142). Brain tissue was embedded in 1.5% agarose (Fisher Scientific) produced in 5% sucrose (Fisher Scientific). Embedded blocks were incubated overnight in 30% sucrose (Fisher Scientific) and then frozen with dry ice before cryosectioning (20-30µM). Validated transgenic reporter animals were utilized for visualization of Sox2<sup>+</sup> and Gfap<sup>+</sup> cells (ZDB-TGCONSTRCT-070410-2). For DNA content staining, Hoechst (2ug/ml) (Fisher Scientific) dye was utilized. Hoechst stain was performed according to manufacturer's protocol available as part of the EdU Click-It technology kit (Fisher Scientific). All slides were cover slipped using Vectashield (Vector Laboratories) and imaged on a Zeiss LSM 700 at 20x–63x magnification.

### **Chromatin Immunoprecipitation (ChIP)**

ChIP was performed as previously described (144) except that larvae were disassociated into a single cell homogenate prior to cell fixation with formaldehyde. Briefly, equal numbers of non-heat shocked (NHS) and heat-shocked (HS) larvae in either line, *Tg(hsp701:HCFC1)* or *Tg(hsp701:HCFC1<sup>c.344C>T</sup>)*, were euthanized according to standard procedures, then heads were excised from tails to create a whole brain homogenate. Tissue was dissociated as described above for flow cytometry. Shearing was performed in a 200 µl volume of 50 mM Tris pH 8.0 (Millipore/Sigma) by adding 40 units of micrococcal nuclease (Fisher Scientific) for 10 minutes at 37°C. Ethylenediaminetetraacetic acid (EDTA-Fisher Scientific) (10 mM) was used to stop the reaction and nuclei were lysed in 1% sodium dodecyl sulfate (SDS-Fisher Scientific). ChIP was performed with anti-HCFC1 antibodies (Millipore Sigma AV38600) or anti-IgG antibodies (Santa Cruz Biotechnology, sc-2025). The collected precipitates were washed and de-crosslinked and the DNA was purified using standard protocols (144). qPCR was used to determine enrichment using primers designed to the 1 kilobase region upstream of each start site/gene of interest. Primers to *gapdh* putative promoter were used as a negative control and each set of enrichment was normalized to *gapdh* PCR or input as described (144). Primers used for SYBR green (Fisher Scientific) based PCR are as follows: *gapdh* fwd: GCCTGATTTGGTTGTGTCCT, *gapdh* rev: CCAATTGGGAAATGCTTGAG, *asx1* fwd: GGCTGTAGGAGCGACTGAAG, *asx1* rev: TAAACACACACAGGGCGAAG.

### **Heat shock and drug treatment assays**

Heat shock was performed as previously described (126,145). Briefly, heat shock was initiated at 24 hours post fertilization (HPF) and performed twice daily every 8-12 hours

until 5 DPF. Heat shock was performed for a duration of 30-45 minutes by incubating dishes at 38°. For rapamycin treatment (Selleck Chemicals), the drug was dissolved in 100% DMSO (Fisher Scientific) and embryos were treated at 24 HPF and 72 HPF with a 0.8  $\mu$ M concentration for a period of 24 hours. Concentration was determined empirically using a gradient coupled with gene expression of *ccne1*. The concentration utilized reduced *ccne1* expression, without any effect on larval viability. Media was removed and no treatment was applied at 48 and 96 HPF. Total treatment time during the 5-day period is 48 hours. Total time with treatment off is 72 hours.

## **Results**

### **Akt/mTor signaling is increased in the *co60* allele.**

We have previously established that nonsense mutation of zebrafish *hcfc1a* (*co60* allele) causes an increase in *asx1* expression, which is associated with increased proliferation of NPCs (126). In mice, ASXL1 promotes AKT phosphorylation (139) and we established that inhibition of zebrafish PI3K, an upstream regulator of AKT, is sufficient to restore NPC numbers to normal levels in the *co60* allele. Thus, we hypothesized that nonsense mutation of *hcfc1a* leads to increased activation of zebrafish Akt kinase. We performed western blot analysis using anti-phospho-Akt threonine 308 (pAkt308) and total Akt antibodies. We detected increased expression of total Akt, which was associated with hyperphosphorylation of pAkt308 (Fig. 1A). Since total Akt was routinely higher in the *co60* allele, we used  $\beta$ -actin as an additional loading control to validate increased expression of total Akt protein (Fig 1A). We observed equal  $\beta$ -actin expression, which correlated with Ponceau S staining of the membrane. We did not analyze phosphorylation

of Serine 473, as we could not identify an antibody that would cross react with zebrafish Akt at this location.

AKT kinase is an upstream regulator of the mTOR pathway in mice and humans, which subsequently promotes growth, proliferation, translation, and ribosomal protein synthesis. Chern and colleagues published that *cb1X* is associated with increased expression of proteins required for ribosome biogenesis (62). Therefore, we performed western blot analysis to detect phosphorylation of S6 kinase (pS6), which is phosphorylated by active mTOR signaling in humans and mice. We observed increased pS6 kinase in carriers of the *co60* allele with equivalent levels of total S6 protein (Fig 1B).  $\beta$ -actin was used to validate protein loading in addition to total S6. Ponceau S was used to confirm protein loading and concentration. In addition, we did not detect differences in total S6 in any biological replicate. These data demonstrate that nonsense mutation of *hcfc1a* is associated with increased zebrafish Akt/mTor signaling.

### **Missense mutation of the N-terminal kelch domain does not change the expression of *hcfc1a*.**

Nonsense mutation of zebrafish *hcfc1a* results in increased Akt/mTor (Fig 1). However, nonsense mutation of *hcfc1a* (*co60* allele) is haploinsufficient in zebrafish and reduces *hcfc1a* expression by 50%, which does not accurately reflect the types of mutations present in *cb1X* syndrome. *cb1X* syndrome is caused by missense mutations that do not reduce overall protein expression (120). We generated an additional *hcfc1a* allele (*hcfc1a<sup>co64/co64</sup>* or *co64*) which results in an insertion deletion that causes an in-frame deletion of arginine at amino acid position 75 with two missense mutations p.G76M and

p.D77N within the kelch protein interaction domain (Fig 2A). The co64 allele is homozygous viable into adulthood (the only model to date) and homozygous offspring obey Mendelian inheritance patterns. As shown in Fig 2B, we did not detect any significant difference in the expression of *hcfc1a* or *hcfc1b*, a second zebrafish ortholog of *HCFC1* in the co64 allele. Since *hcfc1b* expression is unchanged, we do not anticipate any compensatory mechanisms present in the co64 allele, but we cannot fully rule out the possibility at this time.

### **The co60 and co64 alleles have unique effects on Hcfc1a protein expression.**

The two zebrafish orthologs, *hcfc1a* and *hcfc1b*, are ubiquitously expressed throughout the developing embryo (141). Human HCFC1 is synthesized as a large preprotein that is cleaved into N and C-terminal fragments (146). We used two independent antibodies which detect conserved epitopes in the N or C-terminal domains of the human HCFC1 protein. We compared the expression of Hcfc1a using both N and C-terminal specific antibodies in the co60 and co64 alleles using western blot. The co60 allele (nonsense) showed decreased Hcfc1 expression utilizing both N- and C-terminal specific antibodies (Fig 2C&D). In contrast, the co64 allele (missense) did not markedly reduce overall protein expression (Fig 2C&D). The conserved N- and C terminal epitopes analyzed are present in both Hcfc1a and Hcfc1b. Therefore, the expression of the bands in Figure 2C&D indicates levels of both Hcfc1a and Hcfc1b. These data provide evidence that the co64 allele does not reduce overall protein expression, but the co60 allele affects the expression level of Hcfc1a.

### **The co64 allele is associated with decreased Akt/mTor signaling.**

We observed increased Akt/mTor in the co60 allele, but since the co64 and co60 alleles differentially affect protein expression, we hypothesized that dosage changes in Hcfc1a expression (co60) would affect brain development and Akt/mTor signaling differently than missense mutations in the kelch domain. We used western blot analysis to determine the level of Akt/mTor signaling in the co64 allele. We observed hypophosphorylation of Akt at threonine 308 with equivalent levels of total Akt (Fig 3A). We used total Akt and  $\beta$ -actin as loading controls and did not detect changes in the expression of total Akt or  $\beta$ -actin in any of the biological replicates performed. This contrasts with the co60 allele, which demonstrated consistently with increased total Akt. Decreased Akt phosphorylation was associated with decreased pS6 in the co64 allele (Fig 3B). Total S6 protein and  $\beta$ -actin were unchanged across multiple biological replicates. These data reveal differential regulation of Akt/mTor in the co60 and co64 alleles, which we confirmed have unique effects on Hcfc1a protein expression (Fig. 2).

### **NPC number is increased in *cb1X*-like syndromes.**

We have previously demonstrated that the co60 allele causes increased numbers of Sox2+ NPCs (126). We sought to determine the number of NPCs in the co64 allele given the differential regulation of Akt/mTor. To quantify the number of NPCs, we first crossed the co64 allele into the *Tg(sox2:2A:EGFP)* reporter. We then produced a single cell homogenate and performed flow cytometry to detect EGFP positive cells. We detected an increase in the number of GFP+ cells by flow cytometry at 6 days post fertilization (DPF) (Fig 4A&A') and validated this increase using immunohistochemistry at 2 DPF

(Figure 4B&B', arrows indicate regions of increased cell number). We performed flow cytometry on two independent occasions and found a statistically significant ( $p < 0.05$ ) increase in NPCs in heterozygous and homozygous carriers of the *co64* allele (Fig 4C). These data suggest that both the *co60* and *co64* allele have increased NPCs. The presence of overlapping phenotypes provides face validity for the effectiveness of each allele as a putative model system to inform as to the function of human HCFC1 in NPC development.

### **The *co60* and *co64* alleles differentially disrupt RGC number.**

We have previously shown that the *co60* allele increases the expression of zebrafish *gfap* and *elavl3*, markers of RGCs and neurons, respectively (126). Therefore, we measured the expression of both genes in the *co64* allele. We observed a statistically significant decrease in zebrafish *gfap* expression at 2 DPF (Fig 5C), which we validated by immunohistochemistry at 6 DPF (Fig 5A&B). We next crossed the *co64* allele into the *Tg(gfap:EGFP)* reporter and performed flow cytometry to quantify the total number of RGCs. We observed a statistically significant decrease in the total number of RGCs (Fig 5D). Decreased RGC number in the *co64* allele contrasted with the number of RGCs in the *co60* allele, as we detected equivalent numbers of RGCs using flow cytometry in the *co60* allele (Fig 5E). Interestingly, we validated an increase in the expression of zebrafish *gfap* in the *co60* allele (Fig 6F, yellow bars,  $p = 0.06$ ). This display of increased mRNA with no change in cell number can be owed to similar number of RGCs producing increased levels of zebrafish *gfap* transcript and protein (126). These data demonstrate that 1) the *co64* allele reduces the number of RGCs, 2) the *co60* allele increases *gfap*

expression, but has no effect on total RGC number, and 3) the different *hcfc1a* alleles studied have unique effects on RGC development.

### **NPC number is mTor independent in the co60 allele.**

Both the co60 and co64 alleles cause an increase in the number of NPCs but demonstrate divergent regulation of Akt/mTor. Based on these data, we surmised that NPC number was Akt/mTor independent. To test this, we treated co60 embryos/larvae with rapamycin (Fig 6 Schematic) and measured the number of Sox2+ NPCs in whole brain homogenates using flow cytometry. We observed a statistically significant increase in the number of NPCs by flow cytometry in the co60 allele (Fig 6A-A''&B). These data are consistent with previous studies, which find a higher percentage increase of NPCs in a region specific manner across the forebrain, midbrain, and hindbrain (126). Treatment of rapamycin did not reduce the number of NPCs at 5 DPF (Fig. 6A-A''&B) and exacerbated the phenotype leading to an even higher number of total EGFP Sox2+ cells in specific replicates. We validated these results with immunohistochemistry (Fig 6C-E & C'-E').

### ***gfap* expression is partially regulated by mTor in the co60 allele.**

The co60 and co64 alleles demonstrated with differential expression of *gfap* as documented in Fig 5C and (126). In the co60 allele, increased *gfap* expression is not due to increased numbers of cells (Fig 5E). We validated the increased expression of *gfap* expression in the co60 allele in Fig 6F (yellow bars,  $p=0.06$ ). Since *gfap* and mTor activity were differentially regulated in the co60 and co64 alleles, we sought to determine if *gfap* expression was mTor dependent. Wildtype and co60 carriers were treated with rapamycin

as shown in Fig 6 schematic and the expression of *gfap* was analyzed by qPCR analysis. Treatment with rapamycin caused a statistically significant decrease in the expression of *gfap* in mutant animals (co60) (Fig 6F), red bars). These data suggest that *gfap* expression is partially regulated by mTor signaling in the co60 allele.

### ***Asx1* expression correlates with Akt/mTor activity in the co60 and co64 alleles.**

We have previously established that the co60 allele caused increased expression of zebrafish *asx1*, a mediator of AKT signaling in mice (126,139). Thus, we hypothesized that differential expression of *asx1* was mediating contrasting Akt/mTor signatures in each allele. We measured the expression of *asx1* in the co64 and observed it to be significantly decreased relative to sibling wildtype (Fig 7A). Human HCFC1 protein has been shown to bind to the human *ASXL1* promoter (147) and therefore, we hypothesized that the expression of zebrafish *asx1* was reduced in the co64 allele due to abnormal binding of mutated Hcfc1a to the zebrafish *asx1* promoter. To test this hypothesis, we utilized the *Tg(hsp701:HCFC1)* transgene (126). After performing a heat shock protocol (126,145), we performed chromatin immunoprecipitation (ChIP) and used PCR to detect binding of wildtype human HCFC1 protein to the zebrafish *mmachc* and *asx1* promoters. Human and mouse *MMACHC* is a known downstream target gene of HCFC1 and used here as a positive control (132). Semi-quantitative PCR was performed in technical triplicate and demonstrated amplification of the zebrafish *mmachc* and *asx1* promoter regions (Fig 7B). We did not detect amplification after 40 cycles in the IgG antibody control lanes, except in one sample designed to amplify the *asx1* promoter region. However, this amplification was far less than the enrichment detected using HCFC1 specific antibodies.

These results indicate putative binding to the zebrafish *mmachc* and *asx1* promoters by human HCFC1. Positive binding was associated with increased mRNA expression of zebrafish *mmachc* and *asx1* following heat shock protocol (Fig 7C).

We next produced a heat shock transgene that would express the human *cb1X*(c.344C>T) variant (*Tg(hsp701:HCFC1<sup>c.344C>T</sup>)*) located in the kelch domain and previously described (120). Interestingly, this patient variant is the same variant produced in mice by Chern and colleagues. We performed ChIP using anti-IgG or anti-HCFC1 antibodies but did not detect binding of HCFC1 to the zebrafish *asx1* promoter by qPCR (Fig 7D). Loss of enrichment was not the result of an inability of the antibody to bind the c.344C>T mutant variant, as western blot was used to validate the specificity of the HCFC1 antibody to the *cb1X* variant protein (Fig 7E). Importantly, endogenous zebrafish Hcfc1 was detected in the no heat shock control as the antibody cross reacts with zebrafish Hcfc1 protein. Consistent with a loss of binding, we did not detect up-regulation of *asx1* mRNA after heat shock protocol (Figure 7F). Collectively, these data suggest that human HCFC1 binds to and activates the zebrafish *asx1* promoter and that this function may be disrupted in *cb1X*.

### **NPC/RGC number are independent of murine *Asx1* over-expression.**

Our data uncovered contrasting activity of Akt/mTor and differential *gfap* expression in the co60 and co64 alleles. These phenotypes correlate with unique signatures of *asx1* expression, whereby high Akt/mTor activity is associated with increased *asx1* expression. Furthermore, *cb1X* mutations, including the c.344C>T variant, disrupted binding and activation to the zebrafish *asx1* promoter. Therefore, we hypothesized that

the mTor dependent phenotypes in the *co60* allele were *Asx1* dependent. To test this, we injected mRNA encoding mouse *Asx1* into single cell embryos harboring either the *Sox2* or *Gfap* EGFP reporters. We then monitored the number of total NPCs and RGCs by flow cytometry. As shown in Figure 8A, we did not detect any significant change in the number of *Sox2*<sup>+</sup> or *Gfap*<sup>+</sup> cells after over expression of *Asx1*. We did not anticipate changes in the number of *Sox2*<sup>+</sup> cells after *Asx1* injection because this is an overlapping phenotype present in the *co60* and *co64* alleles. Furthermore, we were not surprised that the number of *Gfap*<sup>+</sup> cells was normal after injection because the *co60* allele disrupts the expression of *gfap* and not cell number (Fig. 5E and 6F). However, we did not detect increased expression of *gfap* or *sox2* relative to non-injected control (Fig 8B). Importantly, injection of *Asx1* encoding mRNA induced blood cell phenotypes consistent with a previously described function for this gene in hematopoiesis (148,149) (Supplemental Fig 1). The presence of blood cell phenotypes indicates the functional translation of *Asx1* mRNA after injection.

### **Proteome analysis reveals abnormal expression of ribosomal proteins and 14-3-3 $\beta\alpha$ in the *co60* allele.**

Over-expression of mouse *Asx1* did not alter RGC expression or number and therefore, we used proteomic analysis to identify novel mediators of Akt/mTor in the *co60* allele. Our analysis identified a total of 2172 proteins that were differentially expressed with 159 of those proteins statistically different in the *co60* allele. We identified many proteins belonging to biological processes such as hematopoiesis, erythrocyte development, the ribosome, and/or structural constituents of the ribosome. After secondary Benjamini-

Hochberg correction, only 20 proteins were significantly different in the co60 allele relative to sibling control. Zebrafish Asxl1 protein was not detected as abnormal. Literature analysis of the 20 significant proteins demonstrated increased expression of ribosomal proteins: Rpl36a, Rpl38a, Rps7, Rpl18, Rpl9, Rpl30, Rpl18a, and Rpl3 (Supplementary Data File 1). Our identification of increased expression of proteins required for ribosome biogenesis is consistent with results obtained from a patient derived *cb1X*-like knock-in allele (human *THAP11* gene), which adds additional face validity to our model system (62). Additional literature characterization of the remaining proteins revealed a statistically significant decrease in the expression of 14-3-3  $\beta\alpha$  (Fig. 8C). 14-3-3 proteins are a family of signaling proteins that bind to phosphorylated serine and threonine residues. They are known to regulate brain development (137) and have been shown to reduce AKT phosphorylation at threonine 308 in human cell lines (138). Based on the function of 14-3-3 proteins, we surmised that the co60 and co64 alleles would have opposite expression profiles as it relates to 14-3-3  $\beta\alpha$ . We used western blotting to determine the expression of 14-3-3  $\beta\alpha$  in the co64 allele and observed increased expression relative to sibling wildtype (Figure 8D), which contrasts with reduced expression in the co60 allele (Figure 8C). We next used the *Harmonizome* and The *Encyclopedia of DNA Elements* (ENCODE) databases to determine if human HCFC1 binds to and regulates the expression of 14-3-3  $\beta/\alpha$ . 14-3-3  $\beta/\alpha$  is encoded by the *YWHAB* gene and we validated by database that human HCFC1 binds to the *YWHAB* promoter (150,150–152). Thus, 14-3-3  $\beta/\alpha$  is an HCFC1 target gene and we detected abnormal expression in the co60 and co64 alleles indicating conservation of this regulatory mechanism.

**Phenotypes in the co60 allele overlap with phenotypes in the c.344C>T *cb1X* variant.**

We observed two independent mTor signatures in the co60 and co64 alleles. One of which is associated with increased mTor and increased expression of proteins required for ribosome biogenesis. Thus, we questioned which of our alleles, and which mTor signature most closely resembles the molecular mechanisms underlying *cbIX* syndrome. To begin to address this, we performed proteomics analysis using the *Tg(hsp701:HCFC1<sup>c.344C>T</sup>)* at 5 DPF. We observed a statistically significant up regulation of proteins essential for ribosome biogenesis and elongation initiation factors which are required for protein translation (Fig 9A and Supplemental File 2). These data support and align with previous literature and therefore, provided additional face validity of heat shock HCFC1 transgenes as systems to help understand *cbIX* syndrome. We plotted the average spectral count from biological replicates for each of those proteins whose function is linked to ribosome biogenesis and translation. Each protein was increased in expression after induction of the c.344C>T patient variant (Figure 9A and Supplemental File 2). We next hypothesized that an increase these proteins was a consequence of increased mTor signaling in the *Tg(hsp701:HCFC1<sup>c.344C>T</sup>)*. We compared pS6 phosphorylation in heat shocked induced and non-heat shock control samples. We observed increased pS6 kinase and increased total S6, with equivalent levels of  $\beta$ -actin as a loading control (Fig 9B). We used  $\beta$ -actin as a control because we observed an increase in total S6 in multiple biological replicates. These data suggest that *cbIX* mutations induce defects in the synthesis of proteins important for ribosomal biogenesis, consistent with previous literature.

## **Discussion**

Mutations in the human *HCFC1* gene cause *cbIX* syndrome and XLID (119–123,153). Various model systems have been developed and suggest that human HCFC1 is critical for the function of NPCs (62,121,122,126–129,154). Most recently, Chern and colleagues characterized the cellular and molecular phenotypes associated with a *cbIX* patient knock-in allele (62). These analyses focused on craniofacial development and demonstrated only limited characterization of brain development, likely due to sub-viability. Despite limitations associated with viability, analysis of a related disorder caused by mutations in human THAP11 protein (p.F80L), which interacts with HCFC1, revealed increased expression of proteins associated with ribosome biogenesis. These studies complement existing work in the zebrafish in which Castro and colleagues found brain phenotypes to be *mmachc* independent (126).

We sought to build on these findings by comparing the molecular and cellular phenotypes present in 2 zebrafish *hcfc1a* germline mutant alleles. We have previously characterized the cellular and molecular phenotypes present in a nonsense allele of *hcfc1a* (*co60*). However, *cbIX* is the result of missense mutations and therefore, we created the *co64* allele, the first homozygous viable germline mutant *in vivo*. We demonstrated that the *co60* and *co64* alleles differentially affect Hcfc1a protein expression. The *co60* allele reduces total protein expression whereas the *co64* allele does not, producing a protein with a missense mutation in the kelch domain. Multiple different mutations in human HCFC1 have been reported in the literature including those that affect dosage and cause XLID (121). The *co60* reduces protein expression and the dosage of zebrafish Hcfc1a resulting in cellular and molecular phenotypes that are unique from the *co64* allele. Protein analysis confirmed the *co64* allele did not affect dosage and

genomic sequencing confirmed that the co64 allele resulted in a 2 amino acid modification in the N-terminal kelch domain. It is not surprising that mutations affecting dosage have distinct and overlapping phenotypes when compared with those that alter protein function rather than dosage. Particularly as it is related to human HCFC1, as the protein is proteolytically cleaved and each fragment is known to have unique functions (155–158). In addition, previous studies have established that unique mutations in other genes (*Gli3*) can cause different diseases (159).

Our comparison of the co60 and co64 alleles revealed contrasting phenotypes at the level of Akt/mTor activation. Nonsense mutation of *hcfc1a*, which reduced expression of total Hcfc1a protein, resulted in hyperphosphorylation and activation of Akt and mTor. These data strongly support the observations from Chern and colleagues, as activation of mTor promotes translation and ribosome biogenesis, which was elevated in a mouse knock-in allele of *Thap11* (*cbIX*-like) (62). Thus, the co60 is a valid model system to study the mechanisms by which changes in protein dosage affect brain development and understand the mechanisms driving increased expression of ribosome biogenesis. Mutation of human THAP11 causes a *cbIX*-like syndrome (127), but whether the underlying mechanisms associated with mutation of THAP11 are identical to *cbIX* syndrome has not been elucidated. The expression level of proteins associated with ribosome biogenesis was not directly tested in *cbIX*, but genetic complementation assays with germline mutants that cause ribosomopathies were performed. Here we more directly tested the role of ribosome biogenesis using the *Tg(hsp701:HCFC1<sup>c.344C>T</sup>)* transgene. This allele conditionally, but ubiquitously expresses the human patient variant previously modeled by Chern and colleagues (62). We observed increased expression of

proteins associated with ribosome biogenesis and translation. Therefore, we provide face validity for the *Tg(hsp701:HCFC1<sup>c.344C>T</sup>)* as a model of *cbIX* syndrome.

Interestingly, we observed hypophosphorylation of Akt/mTor after missense mutation of *hcfc1a*. These data contrast with the *co60* allele and the *Tg(hsp701:HCFC1<sup>c.344C>T</sup>)* allele. We anticipate that the mechanisms present in the *co64* allele also differ from the genetic knock-in created by Chern and colleagues (62). This is because the *co64* deletes an in-frame arginine and results in two amino acid changes within the kelch domain. Interestingly, despite differences in Akt/mTor signaling, the *co60* and *co64* have overlapping effects on the number of NPCs. These overlapping phenotypes provide evidence that *Hcfc1a* is essential for proper control of the NPC compartment and that the presence of similar phenotypes across different alleles is indicative that these phenotypes are a direct result of mutation in *Hcfc1a* and not due to any unknown off-target effect. The two zebrafish orthologs, *Hcfc1a* and *Hcfc1b*, contain >75% sequence identity with human HCFC1 (141). Knockdown of *hcfc1a* and *hcfc1b* by morpholino resulted in an increase in the number of NPCs (127), providing additional validity for both the *co60* and *co64* alleles. While these two genes have overlapping NPC functions, they have divergent craniofacial functions (141). Therefore, future studies will be aimed to characterize the functions of both paralogs in NPC development. For example, we observed differential expression of the zebrafish *asx1/1* gene in the *co60* and *co64* alleles. These data warrant additional studies as to the function of *asx1/1* in both alleles. Our zebrafish studies are supported by *in vitro* knockdown of *Hcfc1*, which resulted in an increase in NPCs (122). Given the strong validity of each allele, our data raise the possibility that unique mutations in *hcfc1a* can lead to overlapping and individual

phenotypes. We do not yet understand if individual human disease variants will have differential regulation of mTOR, but such studies are underway and may reveal unique signatures of AKT/mTOR across disease variants. A role for human mTOR signaling in *cb/X* is further supported by a recent review that suggests the phenotypes of multiple neurodevelopmental disorders converge on the mTOR pathway (134).

Previously studies in the *co60* allele uncovered increased expression of *asx/1*, which encodes a chromatin binding protein capable of interacting with Akt in the cytoplasm and promoting Akt phosphorylation (126,139). Interestingly, *asx/1* transcript was increased at the transcriptional level, but not elevated according to proteomics analysis. This can be attributed to unknown post-transcriptional mechanisms, or the stringency of bioinformatics performed at the protein level. Additionally, whole brain homogenates were analyzed, which can cause limited sensitivity or ability to detect protein levels above background. We previously used inhibitors of PI3K, an upstream regulator of AKT phosphorylation to indirectly link the NPC phenotypes present in the *co60* allele to zebrafish Akt signaling (126). Castro and colleagues suggest that PI3K regulates NPC number, therefore we followed up on analyzing the role of AKT/mTOR, a common downstream target of PI3K. However, inhibition of Akt/mTor activity in zebrafish did not restore NPCs. To note, downstream targets of PI3K are vast and therefore, additional studies with which inhibition of other targets are underway. Here we uncovered differential expression of *asx/1* in the *co60* and *co64* alleles. Most interesting was the fact that *asx/1* expression was correlated with hyper or hypo activation of Akt/mTor in each allele. We hypothesized that dysregulation of *asx/1* in *cb/X* was the mechanism by which *Hcfc1a* regulates RGC development. However, forced expression of murine *Asx/1* did not

result in changes to the NPC or RGC populations. These data are inconsistent with morpholino mediated knockdown of *asx1* in the *co60* allele, which led to a full restoration of the number of NPCs (126). At the present time we cannot explain the mechanism by which morpholino knockdown of *asx1* restored NPC phenotypes. But it is well-known that morpholinos can have off-target effects.

Here we found that heat shock directed expression of wildtype human HCFC1 caused an increase in *asx1* expression, and we detected human HCFC1 bound to the zebrafish *asx1* promoter. These data suggest that *asx1* is a bonafide target of human HCFC1. Since the *cb1X* mutation p.Ala115Val disrupted binding of HCFC1 to this promoter, we investigated whether HCFC1 regulated NPC and RGC phenotypes via modulation of *asx1* expression. However, forced expression of murine *asx1* did not affect the total numbers of NPCs or RGCs and had no effect on *gfap* expression. Interestingly, we also noted increased *asx1* expression upon over expression of wildtype HCFC1. In our previous study, we also observed decreased *sox2* and *gfap* expression after over expression of wildtype HCFC1 (126). Thus, *asx1* expression did not correlate with changes in *sox2* and *gfap* expression, which supports the data we observed after injection of murine *asx1* mRNA. Our collective data suggests that although *asx1* expression is disrupted in the *co60* and *co64* alleles, it is not likely to be the sole mediator of the Sox2+ NPC or Gfap+ RGC phenotypes in *cb1X* or related disorders. Hence, we did not attempt to restore the phenotypes present in the *co64* allele with forced *asx1* expression.

Our proteomics analysis of the *co60* allele uncovered increased expression of proteins essential for ribosome biogenesis (Supplementary Data File 1). These data are consistent with proteomics analysis using the *Tg(hsp701:HCFC1<sup>c.344C>T</sup>)* allele where we

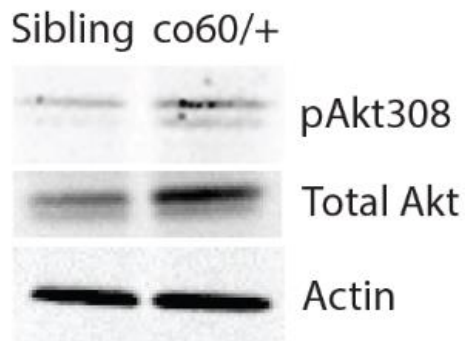
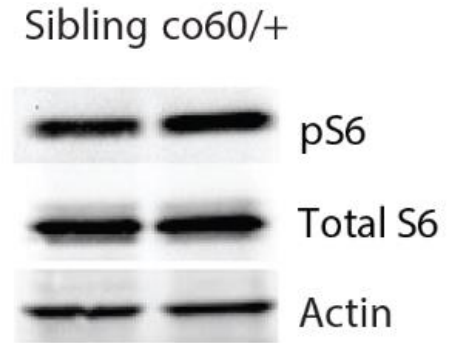
identified increased expression of several elongation initiation factor proteins (Supplementary File 2). Given that these two alleles demonstrate phenotypes consistent with the recent knock-in mouse models, we propose that both are valid systems to understand the mechanisms by which mutations in *cb1X* cause disease. We also identified a second putative regulator of zebrafish Akt signaling using proteomics, the 14-3-3-  $\beta/\alpha$  protein. 14-3-3 proteins have been implicated in brain development (137) and some members of the larger family have been shown to increase the number of NPCs (137) and inhibit AKT phosphorylation in cell lines (138). We found reduced expression of 14-3-3-  $\beta/\alpha$  in the co60 allele and increased expression in the co64 allele, which correspond with hyperactivated Akt/mTor and reduced Akt/mTor signaling, respectively. We validated through available data in the ENCODE database that human HCFC1 binds to the human *YWHAB* promoter. Future experiments to characterize the role of 14-3-3-  $\beta/\alpha$  in *cb1X* syndrome are warranted.

Collectively, our data suggest that distinct types of mutations, even in the same domain of *Hcfc1a*, can have contrasting phenotypes at the level of Akt/mTor, *asx1/1* expression, and *gfap* expression. Initially, the presence of contrasting phenotypes may call into question the physiological relevance of the co64 allele because the phenotypes in the co60 allele, such as increased synthesis of proteins required for ribosomal biogenesis, have been validated with recent patient derived models (62). However, cell type specific deletion of mouse *Hcfc1* in the *Nkx+2.1+* sub-compartment of progenitors is associated with reduced mouse *Gfap* expression (129), data that supports reduced zebrafish *gfap* expression in the co64 allele. Interestingly, the mouse *Thap11* p.F80L allele demonstrated decreased *Gfap* expression after knock-in. These data provide

additional evidence for the role of HCFC1 and its partner THAP11 in the regulation of *Gfap* expression. The mouse *Thap11* F80L mutation also has increased expression of proteins needed for ribosomal biogenesis. Interestingly, the mTor dependent regulation of *gfap* expression in the co60 allele combined with decreased mTor and *gfap* expression in the co64 allele further substantiates the validity for the co64 allele as a model to inform about *cb1X* syndrome. Unfortunately, the co64 could not be directly rescued because over expression of human *HCFC1* and heat shock induced expression of human HCFC1 cause independent phenotypes (126,127), complicating the interpretation of restoration assays. However, the co60 and co64 alleles have been outcrossed for 15-20 generations each, limiting the potential effects of off-target effects.

## **Conclusions**

In conclusion, our study uncovers differential regulation of zebrafish Akt/mTor across different types of germline mutations in the *hcfc1a* gene. Our data correlate contrasting levels of Akt/mTor to unique cellular defects of the Gfap+ RGC cellular compartment. Collectively, this work provides a fundamental mechanism (AKT/mTOR) by which increased synthesis of proteins required for ribosome biogenesis may occur in *cb1X* syndrome. However, our work also suggests that independent mutations with unique effects on overall protein expression/function could cause disease by unique mechanisms that may or may not include AKT/mTOR perturbation. Future studies characterizing the function of unique disease variants in various animal models are underway.

**A.****B.**

**Figure 1: Akt/mTor signaling is increased in the *hcfc1a<sup>co60/+</sup>* allele.** A-B. Western blot analysis was performed with anti-phospho Akt (thr308) antibodies (pAkt308), total Akt, anti-phospho p70S6kinase (pS6), total S6, or  $\beta$ -actin using brain homogenates from sibling wildtype or carriers of the *hcfc1a<sup>co60/+</sup>* (co60/+) allele. N=4/group/biological replicate and performed in 3 independent biological replicates.

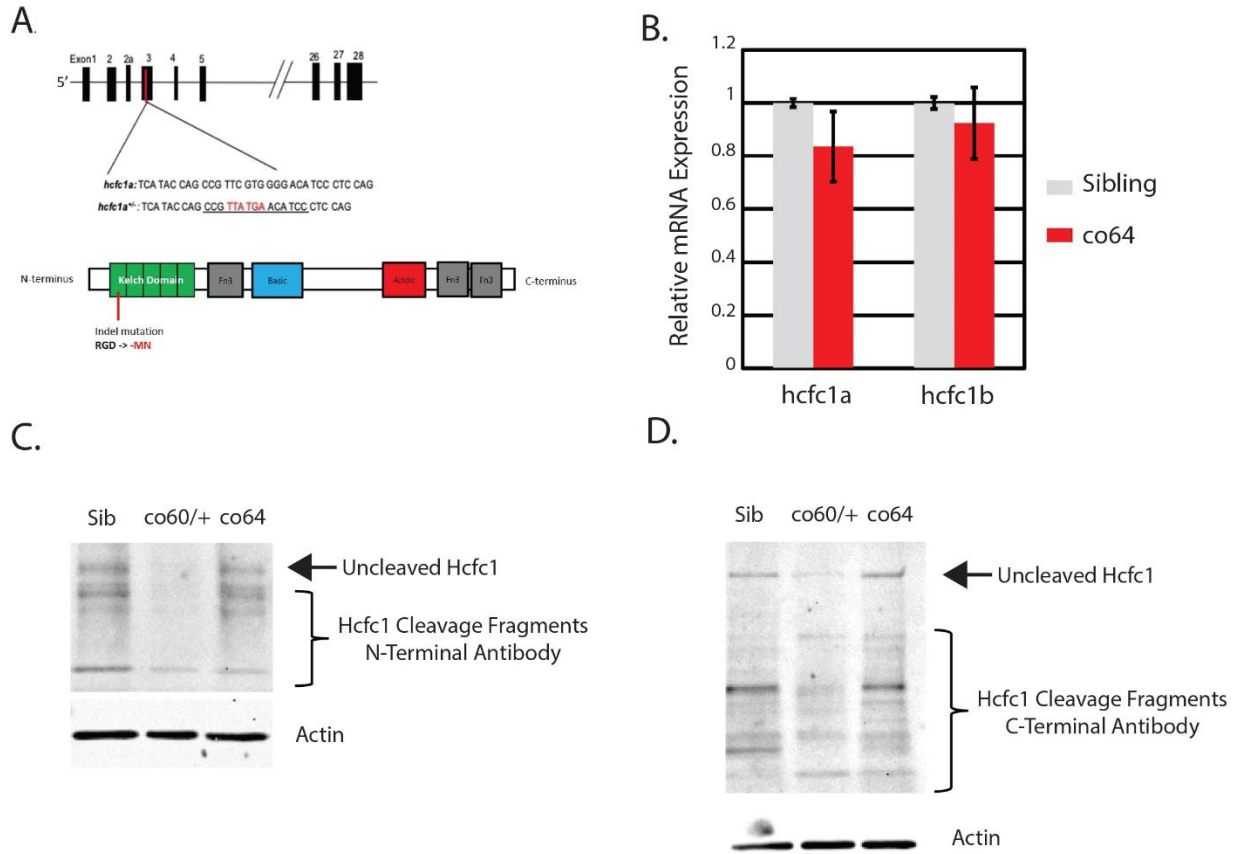
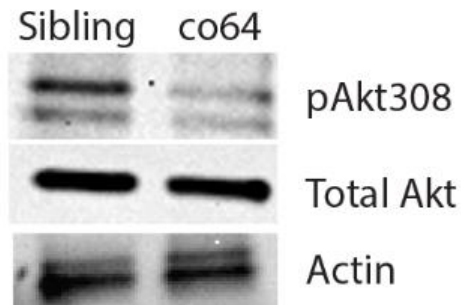


**Figure 2: Missense and nonsense alleles of the *hcfc1a* gene differentially affect Hcfc1 expression.** A. Schematic diagram for the location of the *hcfc1a*<sup>co64</sup> homozygous viable allele. CRISPR/Cas9 created an insertion/deletion in the genomic DNA that causes an in-frame deletion of arginine and a 2-amino acid base pair change (GD>MN) in the kelch domain. B. Quantitative PCR (qPCR) was performed with total RNA isolated from whole brain homogenates from wildtype siblings or homozygous carriers of the *hcfc1a*<sup>co64/co64</sup> allele (co64). The expression of *hcfc1a* and the *hcfc1b* paralog were analyzed. No significant difference in expression was observed, consistent with the effects of missense mutations in *cb1X* syndrome. A total of N=23 wildtype sibling and N=25 homozygous brains were used to measure *hcfc1a* expression. The expression of *hcfc1b* was analyzed with a total number of N=18 wildtype siblings and N=20

homozygous carriers. Numbers were obtained over the course of a minimum of 3 biological replicates. C-D. Western blot analysis was performed with N-terminal I or C-terminal (D) specific antibodies to the HCFC1 protein. Total protein was detected in brain homogenates from wildtype siblings, heterozygous carriers of the *hcfc1a*<sup>co60/+</sup> (co60/+), and homozygous carriers of the *hcfc1a*<sup>co64/co64</sup> (co64) allele. B-actin was used as a loading control. N=4/group/biological replicate and performed in 2 independent biological replicates were utilized for western blot analysis.

A.



B.

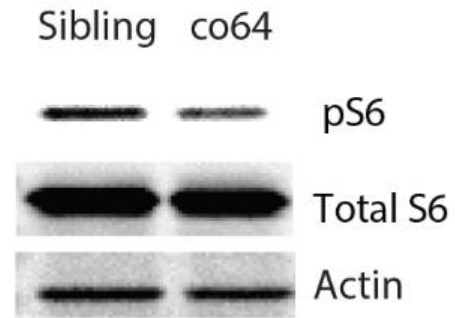


**Figure 3: Differential regulation of Akt/mTor in the *hcf1a<sup>co64</sup>* allele.** A-B. Western blot analysis was performed with anti-phospho Akt (thr308) (pAkt308), total Akt, anti-phospho-p70S6kinase (pS6), total S6, or  $\beta$ -actin antibodies using brain homogenates from sibling wildtype or carriers of the *hcf1a<sup>co64/co64</sup>* (co64) allele. N=4/group/biological replicate and performed in 3 independent biological replicates were utilized for western blot analysis.

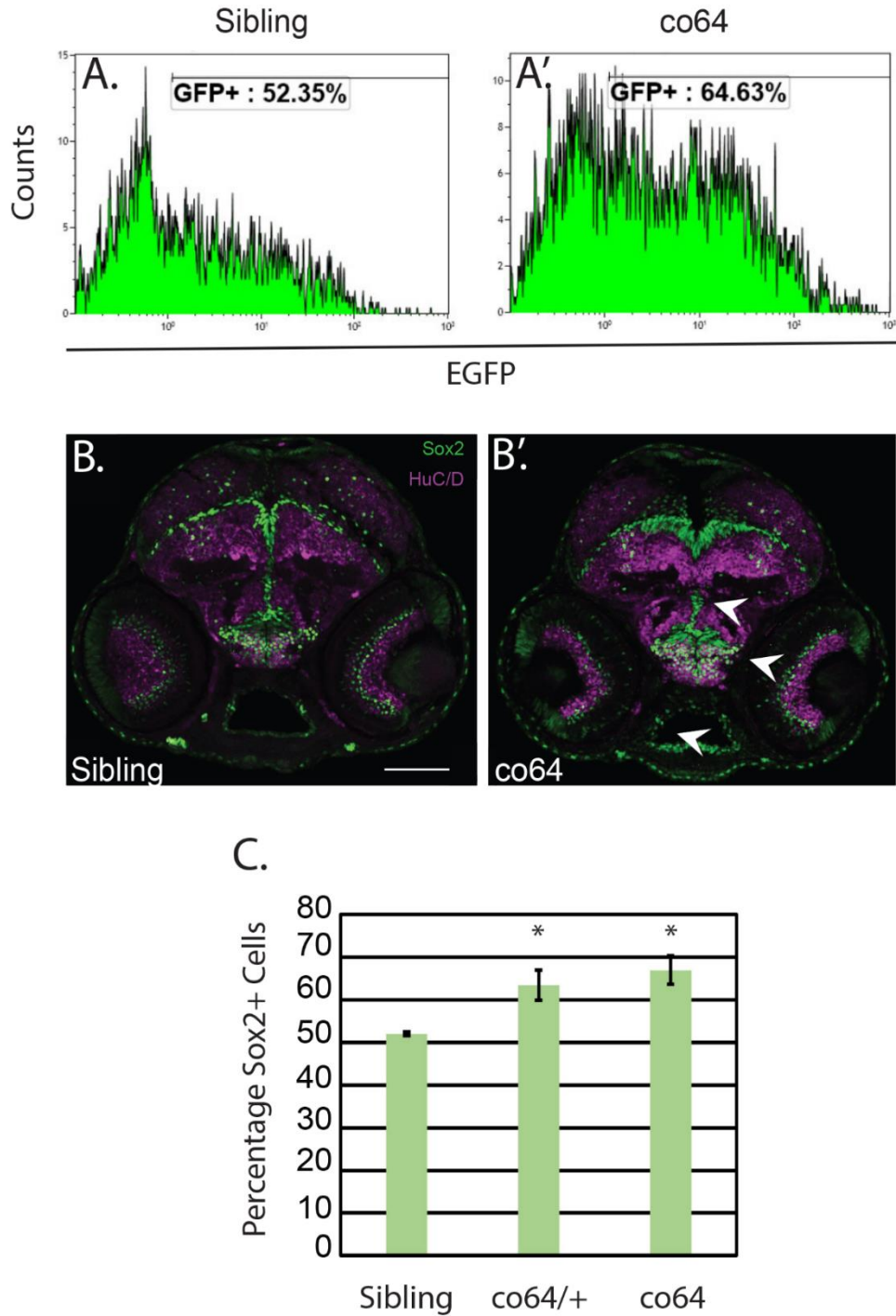


**Figure 4: Neural precursors (NPCs) are increased in the *co64* allele.** A&A'. Flow cytometry analysis was used to detect the number of Sox2+ cells in the *hcf1a<sup>co64</sup>* allele (*co64*) and wildtype siblings at 6 days post fertilization (DPF). Histograms represent a

single biological replicate with N=5/group. B&B'. Immunohistochemistry at 2 days post fertilization (DPF) was performed to detect Sox2+ (green) and Huc/D+ cells (magenta) in sibling wildtype and the co64 allele. N=6/group obtained from 2 biological replicates. C. Quantification of percentages obtained by flow cytometry from 3 biological replicates (N=5/replicate and performed in 3 biological replicates, one is shown in A&A'). The percentage of Sox2+ cells was quantified by flow cytometry and the average of 3 replicates is plotted. \*p<0.05.

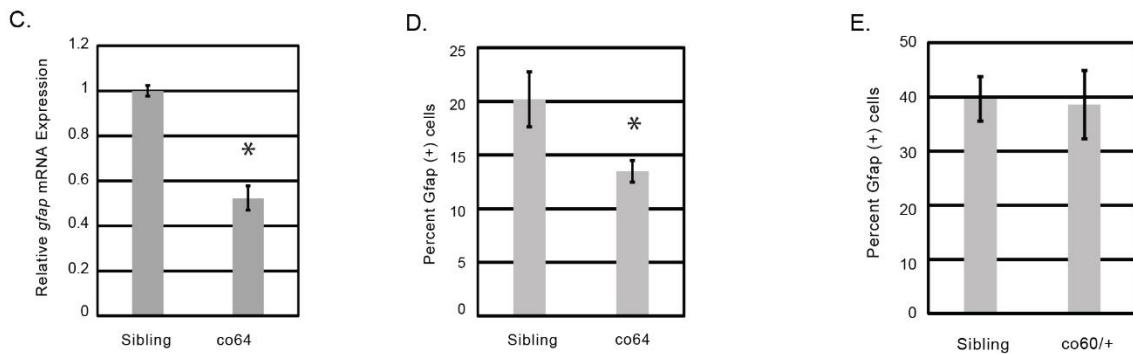
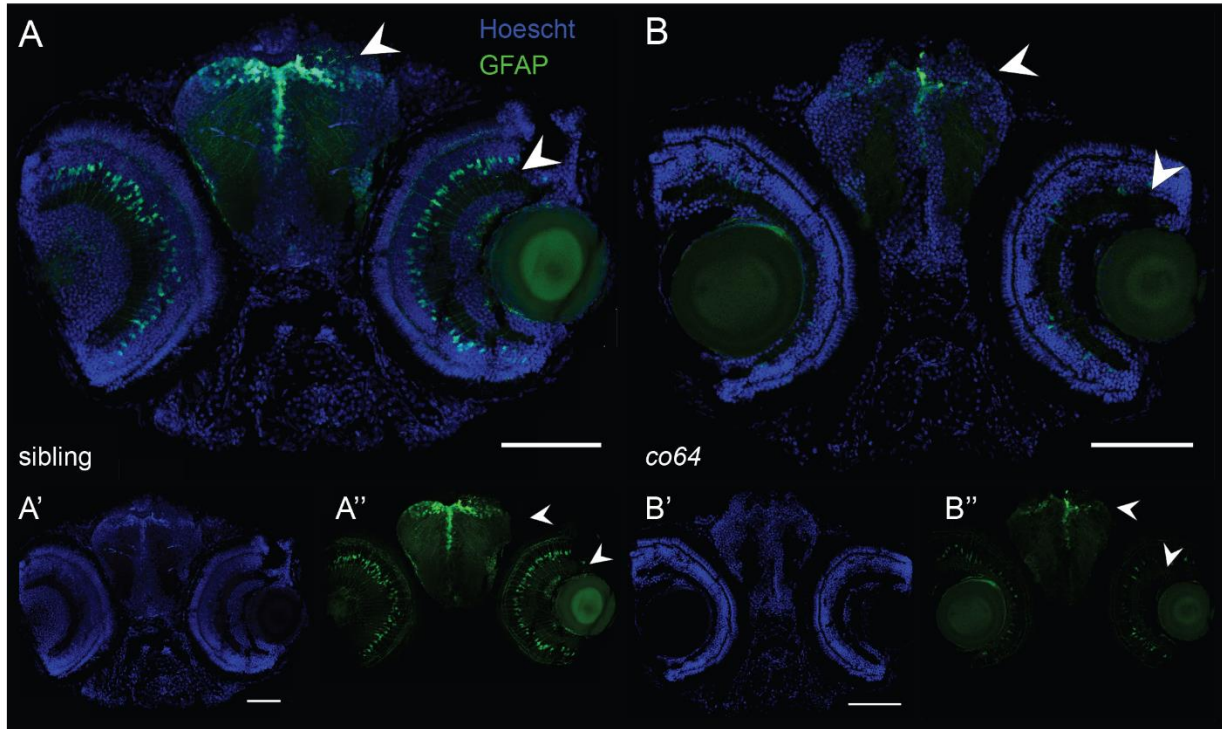


**Figure 5: Radial glial cells (RGCs) are reduced in number and expression in the *co64* allele.** A-B, A'-B', & A''-B''. Immunohistochemistry was used to detect the Gfap+ cells in wildtype sibling and homozygous carriers of the *hcf1a*<sup>co64/co64</sup> allele (*co64*) at 6 days post fertilization (DPF). The *co64* allele was crossed with the *Tg(gfap:EGFP)* reporter. Hoechst DNA content stain (A'-B') was used as a control. N=4 sibling and N=7 *co64*. Arrows indicate areas of decreased expression. C. Quantification of *gfap* expression in sibling wildtype and homozygous carriers of the *co64* allele. Total RNA was

isolated from whole brain homogenates and *gfap* expression was quantified by qPCR from 3 biological replicates (N=3/replicate) (\* $p < 0.05$ ). D. The number of Gfap+ cells was quantified at 5 DPF using flow cytometry in the *co64* allele and wildtype sibling. Analysis was performed in biological triplicate with a total N=14 and the average percentage of positive cells was plotted ( $p < 0.05$ ). E. The number of Gfap+ cells was quantified by flow cytometry in sibling wildtype and the *hcf1a<sup>co60/+</sup>* allele. Two biological replicates were performed with a total of N=6. The average percentage of cells in each biological replicate is plotted with error bars representing standard error of the mean between biological replicates. No significant difference was found.

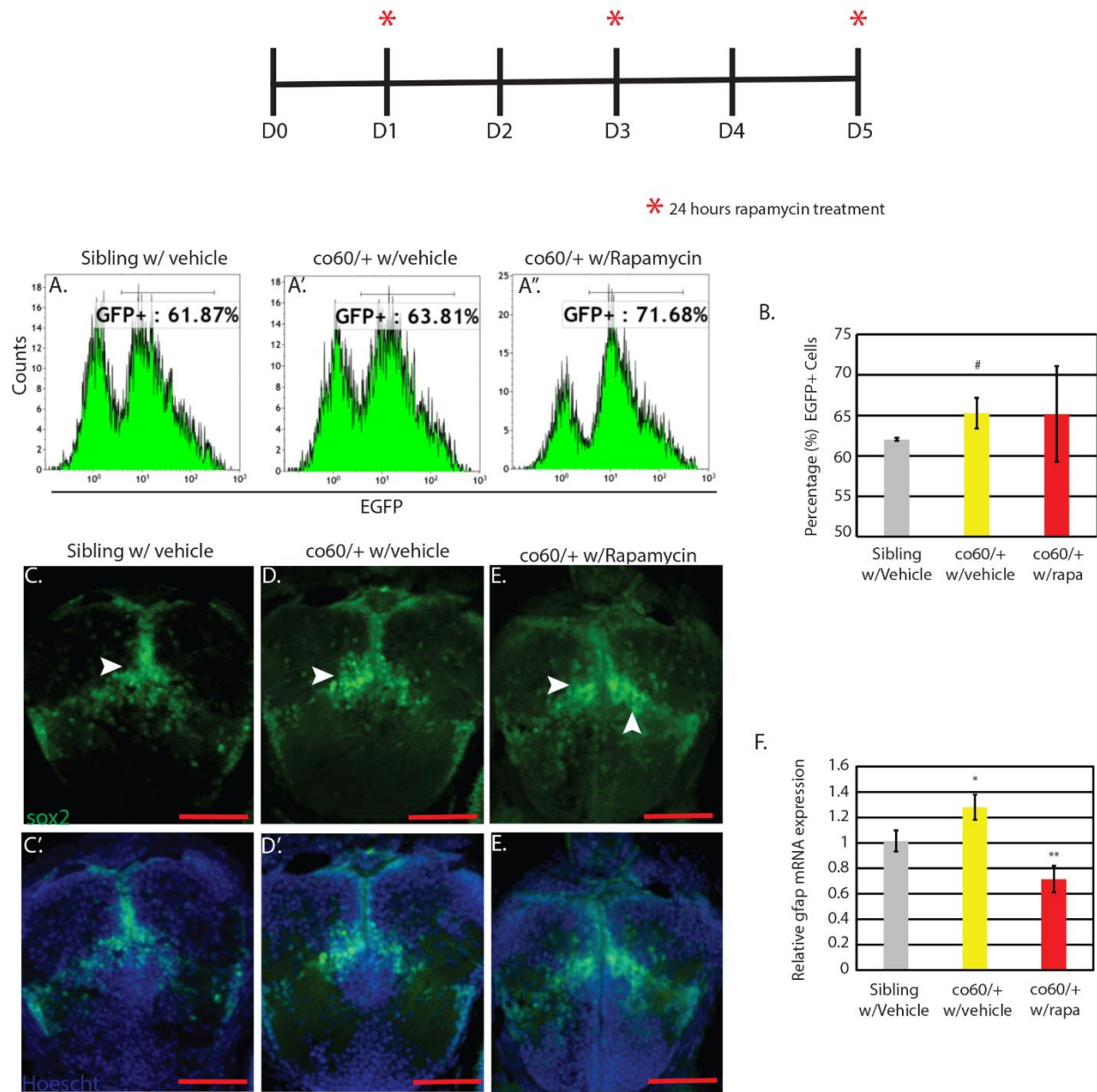


**Figure 6: *gfap* expression but not Sox2 cell number is mTor dependent.** Top: Schematic representing the onset of 0.8 micromolar (uM) rapamycin or vehicle dimethyl sulfoxide (DMSO) treatment. Each asterisk represents the onset of a 24- hour period of treatment. Days (D) without an asterisk are those where media did not contain 0.8 uM rapamycin or vehicle control. A-A''. Flow cytometry of the *hcf1a<sup>co60/+</sup>* (*co60/+*) and wildtype sibling was performed at 5 days post fertilization (DPF). The number of Sox2+

cells were quantified with the *Tg(sox2:2A:EGFP)* transgene. Flow cytometry shown here is a single representative replicate, but the assay was performed on 4 independent occasions with N=14/group. B. Graphical representation of the average percentage of Sox2+ cells obtained by flow cytometry across 4 biological replicates. # p=0.014959. The number of Sox2+ cells was not restored by treatment with 0.8uM rapamycin. C-E. Immunohistochemistry validation of A-A" analyzing Sox2+ cells using the *Tg(sox2:2A:EGFP)* reporter. Hoechst stain was performed as a control in C'-E'. F. Quantitative PCR (qPCR) was used to determine the expression of *gfap* in vehicle treated sibling wildtype, the *co60/+* allele treated with vehicle control (w/vehicle) or the *co60/+* allele treated with rapamycin (w/rapa). The level of *gfap* expression is increased in the *co60/+* allele (\*p<0.06) and restored by treatment with rapamycin (\*\*p<0.05).

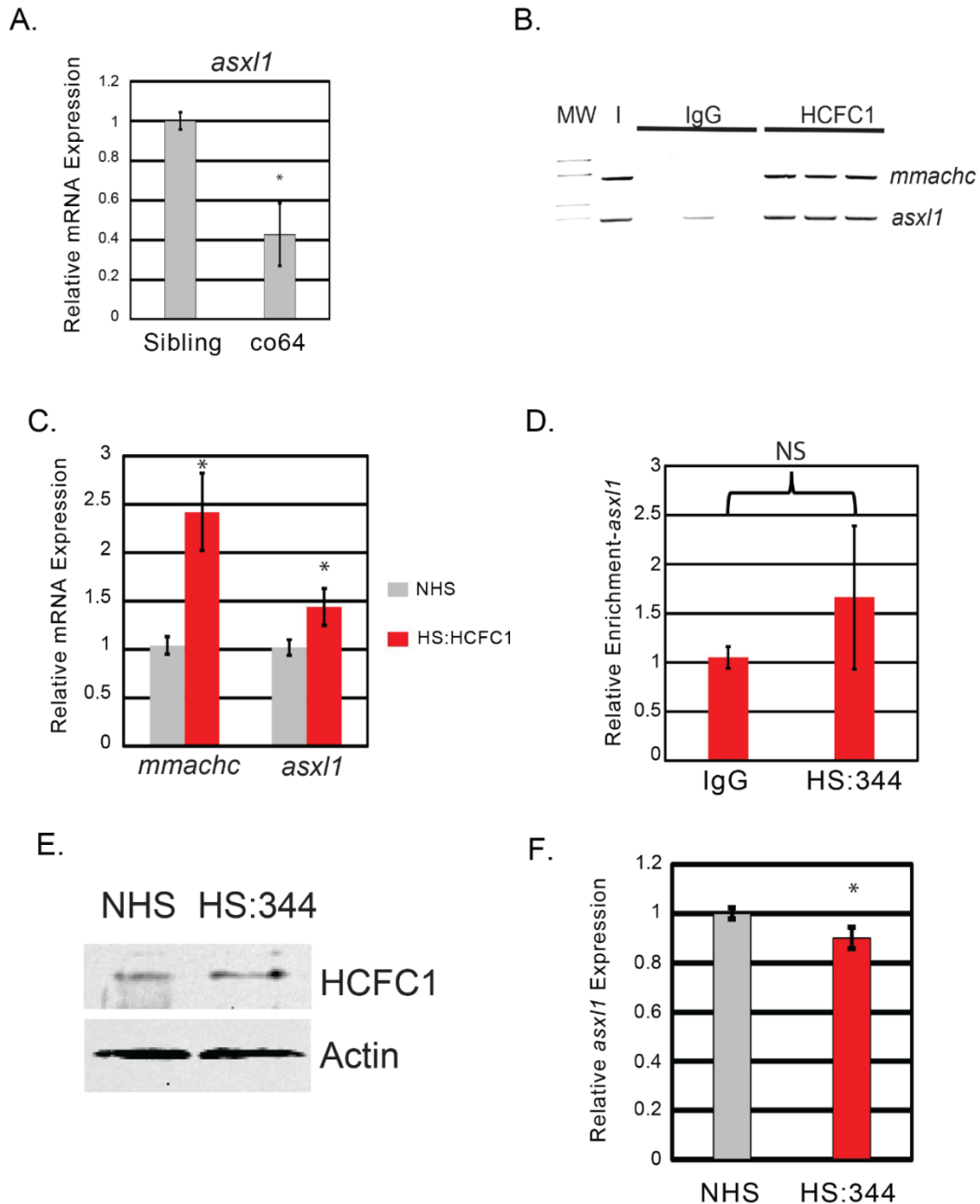


**Figure 7: *cbIX* mutations differentially regulate *asx1* expression.** A. Quantitative PCR (qPCR) was performed with total RNA isolated from whole brain homogenates of wildtype siblings or homozygous carriers of the *hcf1a*<sup>co64/co64</sup> allele (co64) to measure the expression level of *asx1*. A total of N=15 animals were used in two biological replicates. B. Chromatin Immunoprecipitation (ChIP) with semi-quantitative PCR was

used to detect binding to the endogenous *mmachc* (+ control) or *asx1* promoters. CHIP was performed using the *Tg(hsp701:HCFC1)*. Binding was detected with anti-HCFC1 antibodies (HCFC1) relative to the IgG control (IgG). Lanes represent triplicate PCR from one biological replicate. Additional replicates were performed and validated using qPCR. Approximately 10% of the lysate (I) was utilized as an input control. N=20 heads per group were isolated and used for analysis. Assay was repeated on 3 independent occasions for a total N=60. C. qPCR was used to measure the expression of *mmachc* and *asx1* in no heat shock (NHS) and heat shocked (HS:HCFC1) fish carrying the *Tg(hsp701:HCFC1)* transgene. Error bars represent standard error of the mean from biological replicates. Each biological replicate was performed with a pool of embryos from which total RNA was isolated. \*p<0.05. N=20 heads per group across all replicates. D. CHIP was performed with anti-HCFC1 antibodies (HS:344) or IgG control (IgG) following a heat shock protocol with *Tg(hsp701:HCFC1<sup>c.344C>T</sup>)* larvae. N=20 heads per group were isolated and used for analysis for each biological replicate (3 replicates were performed). E. Western blot was performed with anti-HCFC1 antibodies or  $\beta$ -actin in no heat shock (NHS) or heat shocked *Tg(hsp701:HCFC1<sup>c.344C>T</sup>)* larvae (HS:344). N=4/group/biological replicate and performed in 2 biological replicates. F. qPCR analysis was utilized to determine the expression of *asx1* in carriers of the *Tg(hsp701:HCFC1<sup>c.344C>T</sup>)* allele. \*p<0.05. N=20 heads per group were isolated and used for analysis. Error bars represent standard error of the mean between biological replicates as indicated in materials and methods.

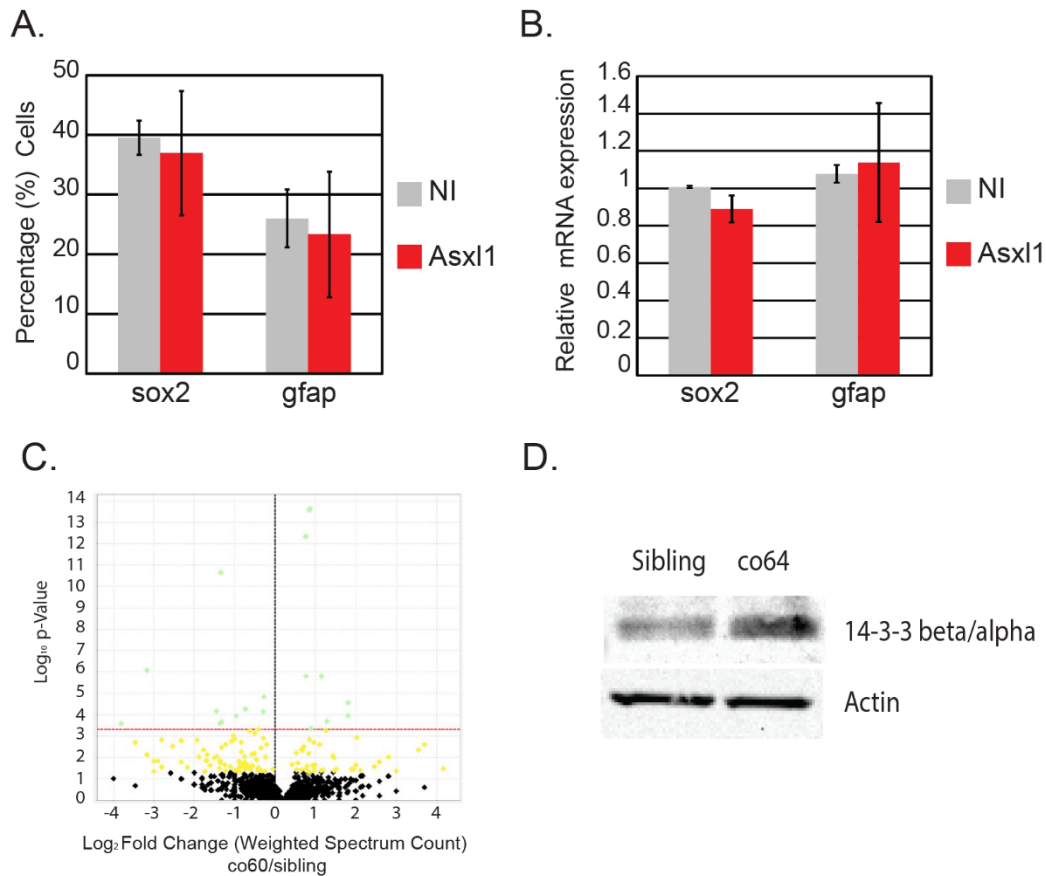


**Figure 8: Forced expression of *Asx1* does not drive NPC/RGC development but proteomics reveals differential expression of 14-3-3  $\beta\alpha$  in each *cb1X* allele.** A. The number of Gfap+ or Sox2+ cells were quantified by flow cytometry in non-injected (NI), *Tg(gfap:EGFP)*, or *Tg(sox2:2A:EGFP)* injected with mRNA encoding the murine *Asx1* gene (*Asx1*). Analysis was performed in two biological replicates. Error bars represent the standard error of the mean between biological replicates. N=14-20/group across 2 biological replicates. B. The relative expression of *gfap* or *sox2* was quantified in non-injected (NI) or wildtype embryos injected with mRNA encoding the murine *Asx1* gene (*Asx1*). N=12/group across 3 biological replicates. Error bars represent standard error of the mean from biological replicates. C. Mass spectrometry was performed to detect abnormal protein expression from N=13 brain homogenates obtained from sibling

wildtype or carriers of the *hcfc1a*<sup>co60/+</sup>. Volcano plot describes the proteins that were significantly different between groups. D. Western blot analysis was performed to determine the expression of 14-3-3  $\beta\alpha$  in total brain homogenates of the co64 allele or sibling control. B-actin was used as a loading control. N=4/group/biological replicate. A total of 2 biological replicates were performed.

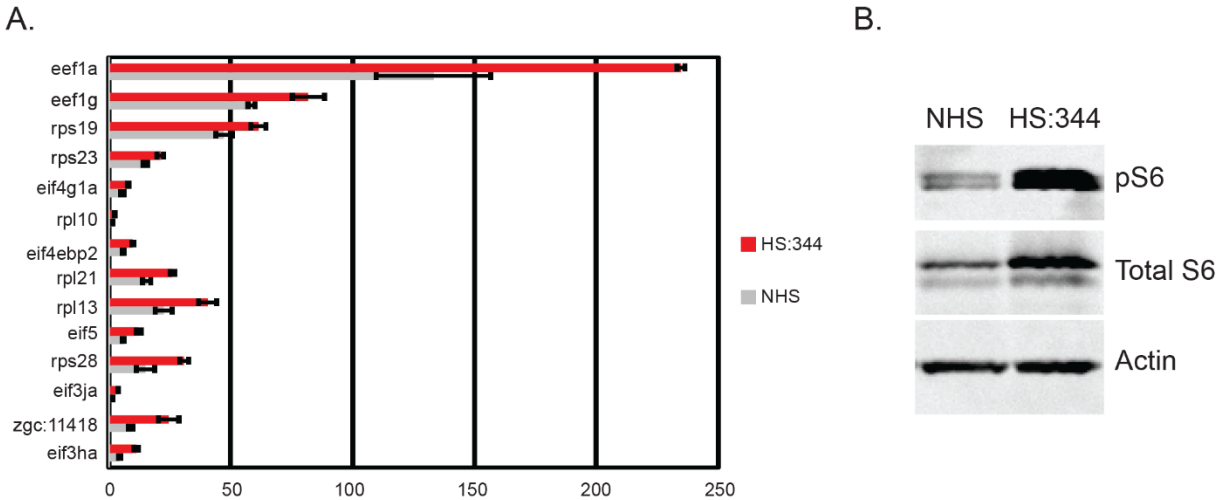


**Figure 9: Proteomics demonstrates abnormal expression of ribosomal proteins and activation of Akt/mTor in the *Tg(hsp701:HCFC1<sup>c.344C>T</sup>)*.** A. Graph depicting average spectral counts of genes encoding proteins associated with ribosomal biogenesis and translation initiation. Proteomics was performed in biological triplicates and average spectral count in non-heat shock (NHS) and heat shocked (HS:344) animals carrying the *Tg(hsp701:HCFC1<sup>c.344C>T</sup>)* allele were averaged and plotted. Proteins shown were statistically up regulated in the c.344C>T allele. Error bars represent standard deviation between spectral counts obtained from biological and technical replicates. A total of N=45 fish across 2 biological replicates were used for NHS and HS (HS:344) and N=46 fish across 2 biological replicates were used for NHS and HS *Tg(hsp701:HCFC1)* for analysis. B. Western blot was performed on whole brain homogenates with 104escribe-S6 kinase, total S6, or  $\beta$ -actin antibodies in no heat shock (NHS) or heat shocked animals carrying the *Tg(hsp701:HCFC1<sup>c.344C>T</sup>)* allele. Analysis was performed at 5 days post fertilization for both data in A and B. For western blot, a total N=4/group/biological replicate was utilized in 2 biological replicates.

## CHAPTER IV

### DISSERTATION SUMMARY AND CONCLUSIONS

Mutations in the HCFC1 transcriptional co-factor protein are the cause of *cbIX* syndrome (MIM 309541) and X-linked intellectual disability (XLID). *cbIX* is associated with intractable epilepsy, abnormal cobalamin metabolism, facial dysmorphia, cortical gyral malformations, and intellectual disability. *In vitro* studies were the first to pioneer investigations into the function of HCFC1 during neural development, pinpointing its regulation of neural precursor cell proliferation and differentiation. However, *in vivo* mouse models carrying missense mutations in the murine *Hcfc1* gene experienced early lethality, consequently leaving the mechanism for how HCFC1 regulates these neurodevelopmental processes unknown. Zebrafish have been put forward as a new model system to investigate these processes based on their ability to circumvent lethality of HCFC1 ortholog mutations, owing to early maternal contributions. Collectively, this dissertation describes independent studies using zebrafish as a model to study the function of HCFC1 and reveal a potential mechanism whereby HCFC1 regulates neural development.

#### ***Neural precursor cell development is independent of MMACHC function.***

HCFC1 interacts with the DNA-binding protein THAP11 to bind to the *MMACHC* promoter and activate transcription of the *MMACHC* gene, which encodes for of a vitamin B12 enzyme essential for breaking down cobalamin metabolites. *cbIX* syndrome is caused by mutations in the HCFC1 gene which induces cobalamin metabolic defects and severe neurological impairments. This raises the question of whether neurological deficits in *cbIX*

patients are due to MMACHC function or not. Data by Castro et al presented in this dissertation indicate that neural precursor cell (NPC) defects present in *hcfc1a* nonsense mutants are independent of *mmachc* expression (126). This is the first study to indicate that cellular phenotypes in HCFC1 mutants are not the result of abnormal MMACHC function. However, zebrafish carry two orthologs of the *HCFC1* gene, *hcfc1a* and *hcfc1b*, and the function of *hcfc1b* in NPC development has not been fully investigated. It has been well described that *hcfc1b* is essential for craniofacial development, but *hcfc1a* appears to be dispensable for this developmental process, indicating non-overlapping functions for these two paralogs. In addition, *mmachc* expression is not significantly decreased in *hcfc1a* morphants or germline mutants but is dramatically reduced in *hcfc1b* morphants. Whether *hcfc1a* and *hcfc1b* have an overlapping function in brain development is still unclear and has not been characterized to date.

Notably, studies by Chern and colleagues indirectly substantiate our NPC phenotype data suggesting cellular defects are independent of *mmachc* function. This study entailed analysis of a *cbIX* related disorder caused by mutations in THAP11 (p.F80L), which interacts with HCFC1. Here they find that this mutant causes increased expression of proteins associated with ribosome biogenesis and not *Mmachc* (62). These data indirectly corroborate our findings which show that neurodevelopmental phenotypes in loss of function *hcfc1a* mutants are independent of MMACHC function.

### ***Role of HCFC1 in radial glial cell and astrocytic development.***

Radial glial cells (RGCs) in zebrafish act as supporting cells for neurons that guide radial migration of neuronal populations from the ventricular zone to the mantle. Gfap-positive RGCs are neural stem cell-like progenitors in the developing nervous system and

have been shown to act as an essential progenitor population for late-born neurons and glia in the zebrafish spinal cord (160). In mice, RGCs also act as neural stem cells that give rise to glial cells such as, oligodendrocytes and astrocytes in late embryogenesis (161). However, in mice, RGCs express unique genes relative to zebrafish RGCs. For example, in zebrafish RGCs express *gfap*, which is an astrocytic marker in mice.

Our recent findings suggest that unique mutations in the same domain of *Hcfc1a* result in contrasting phenotypes of mRNA expression of *gfap*, a gene that encodes for proteins highly expressed in RGCs. These findings are consistent with two previous studies. The first was in a mouse with NPC cell-type specific deletion of *Hcfc1* that resulted in reduced mouse *Gfap* expression (129). The second was in mouse carrying mutations in the HCFC1 interacting partner, *Thap11* (p.F80L) which also demonstrated decreased *Gfap* expression. Collectively, these data provide profound evidence for the role of HCFC1 and its partner THAP11 in the regulation of *Gfap* expression. Our work demonstrates changes in *gfap* expression consistent with other mouse models, thus demonstrating high validity.

### ***HCFC1 regulation of ribosomal biogenesis via Akt/mTOR.***

Ribosome biogenesis is an essential process that cells undergo to generate ribosomes to synthesize and control protein abundance in the cell. Without this process cells cannot proliferate, grow, or survive. To produce the necessary ribosomal subunits, over 80 proteins and 4 different RNA species must be produced at the appropriate levels. Because this requires an abundance of amino acids and nucleotides, there are the requirement of secondary processes to facilitate this need. One of the more important mediators of this is the mTORC1 protein kinase. mTORC1 initiates many stages of

ribosomal biogenesis (162). For example, mTORC1 activates ribosomal RNA transcription and the synthesis of the necessary ribosomal proteins required to assemble subunits.

Recently, Chern and colleagues demonstrated the missense mutations in a HCFC1 interacting protein, THAP11, resulted in increased ribosomal biogenesis. This was the first study to reveal a potential mechanism underlying *cb1X* syndrome and HCFC1 function. However, because the HCFC1 mutants they created were sub-viable, it remained unknown whether this phenotype also occurred in a model of *cb1X* or what mechanism might be driving these ribosomal defects. Our analysis of a zebrafish haploinsufficient allele, revealed abnormal expression of *Asx11*, a protein that has been shown to drive the activation of Akt. Interestingly, we also demonstrated that inhibition of PI3K, an upstream regulator of Akt, restored NPC phenotypes in mutant zebrafish. Using this information combined with data from Chern et. Al. we honed in on the activity of Akt/mTor after mutation of *hcf1a* in zebrafish. We performed a comparison of two *hcf1a* mutant alleles that revealed abnormal Akt protein phosphorylation, disruption of downstream targets of mTOR, and atypical levels of ribosomal proteins (163). Because the function of mTOR has been widely shown to promote translation and ribosome biogenesis, our findings provide insight into the previous results from Chern and colleagues and reveal potential mechanisms for ribosomal dysregulation. Most notably, using an inhibitor to block mTOR activity, we effectively restored increased *gfap* levels in the nonsense *hcf1a* mutants. These data are the first to provide a putative mechanism for how neuronal phenotypes in *cb1X*-like models arise, establishing that glial cell phenotypes are mTOR dependent.

### ***cb1X* motor dysfunction and seizure phenotypes.**

Two common clinical manifestations of *cb1X* syndrome are intractable epileptic seizures and motor impairments. Both of which have little to no treatment or prevention options. In our work, we demonstrate that loss of function mutations of the *hcf1a* gene in zebrafish larvae induce hypolocomotion behavior. This deficit was correlated with increased production of NPCs and abnormal levels of markers associated with glial cells and neuronal differentiation. Future studies that are aimed at rescuing hypolocomotion behavior are highly warranted and can provide novel insight into *cb1X* motor impairments.

Although seizure phenotypes were not overtly detected in our *cb1X* model, additional protocols exist that can allow us to detect behavioral deficits and verify seizure like phenotypes. For example, sub-optimal doses of seizure inducing agents like pentylenetetrazol can be applied to the water of developing larvae. These doses would not induce seizures in wildtype siblings but could potentially increase susceptibility in *cb1X*. Preliminary studies for this protocol are underway and will help establish a model system with which mechanisms of seizure development in *cb1X* can be elucidated. Interestingly, increased levels of mTOR, namely mTORopathies, have been highly implicated in epilepsy (164). Based on hyperactivity of mTOR in our loss of function *hcf1a* mutants, it is plausible that future therapeutic strategies can be proposed, such as treatment with mTOR inhibitors. Moreover, it is possible that our work can establish mTOR as a biomarker for *cb1X*, whereby in utero, patients can be tested for elevated mTOR activity and specific treatments can be developed to help minimize seizures. Future studies that use multiple stimuli, including low dose convulsant agents will likely shed light on the epileptic phenotypes associated with mutations in *hcf1a*.

### **14-3-3- $\beta/\alpha$ protein as a regulator Akt/mTOR activity.**

Expressed early during brain development are highly conserved isoforms of the 14-3-3 proteins, which make up approximately 1% of total soluble brain protein. The 14-3-3 family of proteins play a large role in the development of the nervous system and cortical development, including neurogenesis and differentiation, neuronal migration and neuromorphogenesis, and synaptogenesis (137). Mutations in 14-3-3 proteins have been implicated in many neurological diseases including Parkinson's disease, Alzheimer's disease, schizophrenia, and bipolar disorder. The different isoforms of the 14-3-3 family have also been shown to increase the production of NPCs (137) and inhibit AKT phosphorylation in cell lines (138).

In our work, we applied proteomics analysis of our loss of function *hcfc1a* allele and found a highly significant reduction in the expression of the 14-3-3-  $\beta/\alpha$  protein. We found contrasting differences of this protein in our missense *hcfc1a* allele with increased levels of 14-3-3-  $\beta/\alpha$  protein compared to our haploinsufficient allele. Evidence suggesting that the 14-3-3-  $\beta/\alpha$  protein regulates and inhibits AKT phosphorylation and activity is substantiated in our nonsense and missense alleles based on hyperactivated Akt/mTOR and reduced Akt/mTOR signaling, respectively. We also validated through available data in the Encyclopedia of DNA Elements (ENCODE) database, that human HCFC1 directly binds to the human *YWHA B* promoter, which is the gene that encodes for the 14-3-3-  $\beta/\alpha$  protein. Based on these findings, we have established one putative downstream mediator of HCFC1 that may play a role in regulating both NPC and Akt/mTOR phenotypes in our *cb1X* models. Future experiments to characterize the role of 14-3-3-  $\beta/\alpha$  in *cb1X* syndrome are warranted.

### ***cbIX subtypes and patient specific mutations.***

Missense mutations of HCFC1 in humans cause varied presence and severity of neurological impairments. *cbIX* syndrome is caused by mutations in the kelch domain region of the HCFC1 protein. HCFC1 contains several domains in addition to the kelch domain including a basic and acidic region, fibronectin repeat region and proteolytic cleavage sites. There has been documentation of missense mutations across each of these regions, whereby no single study has investigated the mechanisms underlying the corresponding phenotypes. Interestingly, all individual mutations across HCFC1 cause defects in nervous system development, indicating that each domain of HCFC1, and not just the kelch domain and N-terminal region, may be important for brain development. Interestingly, patients with mutations along the C-terminal regions of the protein do not develop severe cobalamin metabolic disorders nor severe neurological impairments like intractable epilepsy and are limited to intellectual disability and autistic like disorders (165).

The work presented in this dissertation describes the neurological phenotypes and mechanisms associated with two different *hcf1a* alleles. The first is a mutant where all domains of *hcf1* are perturbed and little to no Hcfc1 protein is made. This is relevant to the *cbIX* field because no studies have yet described what disruption of other domains outside of the kelch region cause. Additionally, the second allele is a missense mutation in the kelch domain region which more directly mimics *cbIX* syndrome and is more representative of patient mutations. However, to date there are over 14 other unique mutations documented across the HCFC1 protein that have not yet been characterized (165). Thus, the future goals of our lab are to comprehensively understand *cbIX* and

related disorders by creating individual models of each variant and elucidate future therapeutic and patient specific treatment options.

### **Impact of these data to the field**

At the beginning of this research, very little was known about the role of HCFC1 in brain development except that changes in expression altered NPC function, number, and differentiation *in vitro*. An *in vivo* model did not exist. Whilst my research was ongoing multiple model systems were concurrently produced, each of them with limitations not observed in zebrafish. Despite the advent of these alleles, our work is the only work to date to characterize *in vivo* cellular phenotypes associated with missense and nonsense mutations of HCFC1 and provide a molecular mechanism (Akt/mTor) underlying unique cellular phenotypes. These data have provided a significant foundation for future research in mouse models and are currently the field standard, as no other system has been developed at the present time to understand these mechanisms.

## APPENDIX

### First and Middle-Author Publications (\* Indicates first-author)

1. \***Castro VL**, Quintana AM. The role of HCFC1 in syndromic and non-syndromic intellectual disability. Med Res Arch. 2020 Jun;8(6):10.18103/mra.v8i6.2122. doi: 10.18103/mra.v8i6.2122. Epub 2020 Jun 18. PMID: 34164576; PMCID: PMC8218923.
2. \***Castro VL**, Reyes JF, Reyes-Nava NG, Paz D, Quintana AM. Hcfc1a regulates neural precursor proliferation and asxl1 expression in the developing brain. BMC Neurosci. 2020 Jun 10;21(1):27. Doi: 10.1186/s12868-020-00577-1. PMID: 32522152; PMCID: PMC7288482.
3. \***Castro VL**, Reyes-Nava NG, Sanchez BB, Gonzalez CG, Paz D, Quintana AM. Activation of WNT signaling restores the facial deficits in a zebrafish with defects in cholesterol metabolism. Genesis. 2020 Dec;58(12):e23397. Doi: 10.1002/dvg.23397. Epub 2020 Nov 16. PMID: 33197123; PMCID: PMC7816230.
4. \***Castro VL**, Paz D, Virrueta V, Estevao IL, Grajeda BI, Ellis CC, Quintana AM. Missense and nonsense mutations of the zebrafish hcfc1a gene result in contrasting mTor and radial glial phenotypes. Gene. 2023 May 15;864:147290. Doi: 10.1016/j.gene.2023.147290. Epub 2023 Feb 17. PMID: 36804358.
5. \*Quintana AM, Yu HC, Brebner A, Pupavac M, Geiger EA, Watson A, **Castro VL**, Cheung W, Chen SH, Watkins D, Pastinen T, Skovby F, Appel B, Rosenblatt DS, Shaikh TH. Mutations in THAP11 cause an inborn error of cobalamin metabolism and developmental abnormalities. Hum Mol Genet. 2017 Aug 1;26(15):2838-2849. Doi: 10.1093/hmg/ddx157. PMID: 28449119; PMCID: PMC5886234.
6. \*Paz D, \*Pinales BE, \*Castellanos BS, Perez I, Gil CB, Jimenez Madrigal L, Reyes-Nava NG, **Castro VL**, Sloan JL, Quintana AM. Abnormal chondrocyte intercalation in a zebrafish model of *cb/C* syndrome restored by an MMACHC cobalamin binding mutant. bioRxiv [Preprint]. 2023 Jan 21:2023.01.20.524982. doi: 10.1101/2023.01.20.524982. PMID: 36711998; PMCID: PMC9882310.
7. \*Nayeli G. Reyes-Nava, Jose A. Hernandez, **Victoria L. Castro**, Joel F. Reyes, Barbara S. Castellanos, and Anita M. Quintana. (2018). Zebrafish: A Comprehensive Model to Understand the Mechanisms Underlying Neurodevelopmental Disorders. In A. Costa & E. Villalba (Eds.), Horizons in Neuroscience Research. Volume 36. Nova Science. ISBN: 978-1-53614-472-7.
8. \*Hernandez JA, \***Castro VL**, Reyes-Nava N, Montes LP, Quintana AM. Mutations in the zebrafish *hmgcs1* gene reveal a novel function for isoprenoids during red blood cell development. Blood Adv. 2019 Apr 23;3(8):1244-1254. Doi: 10.1182/bloodadvances.2018024539. PMID: 30987969; PMCID: PMC6482358.

## BIBLIOGRAPHY

1. Watkins D, Rosenblatt DS. Inborn errors of cobalamin absorption and metabolism. *Am J Med Genet C Semin Med Genet*. 2011 Feb 15;157C(1):33–44.
2. Kim J, Gherasim C, Banerjee R. Decyanation of vitamin B12 by a trafficking chaperone. *Proc Natl Acad Sci USA*. 2008 Sep 23;105(38):14551–4.
3. Froese DS, Krojer T, Wu X, Shrestha R, Kiyani W, von Delft F, et al. Structure of MMACHC reveals an arginine-rich pocket and a domain-swapped dimer for its B12 processing function. *Biochemistry*. 2012 Jun 26;51(25):5083–90.
4. Hannibal L, Kim J, Brasch NE, Wang S, Rosenblatt DS, Banerjee R, et al. Processing of alkylcobalamins in mammalian cells: A role for the MMACHC (cblC) gene product. *Mol Genet Metab*. 2009 Aug;97(4):260–6.
5. Froese DS, Kopec J, Fitzpatrick F, Schuller M, McCorvie TJ, Chalk R, et al. Structural Insights into the MMACHC-MMADHC Protein Complex Involved in Vitamin B12 Trafficking. *J Biol Chem*. 2015 Dec 4;290(49):29167–77.
6. Orphanet: Methylmalonic acidemia with homocystinuria, type cblC [Internet]. [cited 2016 May 9]. Available from: [http://www.orpha.net/consor/cgi-bin/OC\\_Exp.php?Expert=79282](http://www.orpha.net/consor/cgi-bin/OC_Exp.php?Expert=79282)
7. Coelho D, Suormala T, Stucki M, Lerner-Ellis JP, Rosenblatt DS, Newbold RF, et al. Gene identification for the cblD defect of vitamin B12 metabolism. *N Engl J Med*. 2008 Apr 3;358(14):1454–64.
8. Dobson CM, Wai T, Leclerc D, Wilson A, Wu X, Doré C, et al. Identification of the gene responsible for the cblA complementation group of vitamin B12-responsive methylmalonic acidemia based on analysis of prokaryotic gene arrangements. *Proc Natl Acad Sci USA*. 2002 Nov 26;99(24):15554–9.
9. Dobson CM, Wai T, Leclerc D, Kadir H, Narang M, Lerner-Ellis JP, et al. Identification of the gene responsible for the cblB complementation group of vitamin B12-dependent methylmalonic aciduria. *Hum Mol Genet*. 2002 Dec 15;11(26):3361–9.
10. Yu HC, Sloan JL, Scharer G, Brebner A, Quintana AM, Achilly NP, et al. An X-Linked Cobalamin Disorder Caused by Mutations in Transcriptional Coregulator HCFC1. *Am J Hum Genet*. 2013 Sep 5;93(3):506–14.
11. Michaud J, Praz V, Faresse NJ, Jnbaptiste CK, Tyagi S, Schütz F, et al. HCFC1 is a common component of active human CpG-island promoters and coincides with ZNF143, THAP11, YY1, and GABP transcription factor occupancy. *Genome Res*. 2013 Apr 25;

12. Huang L, Jolly LA, Willis-Owen S, Gardner A, Kumar R, Douglas E, et al. A Noncoding, Regulatory Mutation Implicates HCFC1 in Nonsyndromic Intellectual Disability. *Am J Hum Genet.* 2012 Oct 5;91(4):694–702.
13. Jolly LA, Nguyen LS, Domingo D, Sun Y, Barry S, Hancarova M, et al. HCFC1 loss-of-function mutations disrupt neuronal and neural progenitor cells of the developing brain. *Hum Mol Genet.* 2015 Jun 15;24(12):3335–47.
14. Koufaris C, Alexandrou A, Tanteles GA, Anastasiadou V, Sismani C. A novel HCFC1 variant in male siblings with intellectual disability and microcephaly in the absence of cobalamin disorder. *Biomed Rep.* 2016 Feb;4(2):215–8.
15. Gérard M, Morin G, Bourillon A, Colson C, Mathieu S, Rabier D, et al. Multiple congenital anomalies in two boys with mutation in HCFC1 and cobalamin disorder. *Eur J Med Genet.* 2015 Mar;58(3):148–53.
16. X-Linked Cobalamin Disorder (HCFC1) Mimicking Nonketotic Hyperglycinemia With Increased Both Cerebrospinal Fluid Glycine and Methylmalonic Acid. - PubMed - NCBI [Internet]. [cited 2020 Jan 27]. Available from: <https://www.ncbi.nlm.nih.gov/pubmed/28363510>
17. Dejosez M, Levine SS, Frampton GM, Whyte WA, Stratton SA, Barton MC, et al. Ronin/Hcf-1 binds to a hyperconserved enhancer element and regulates genes involved in the growth of embryonic stem cells. *Genes Dev.* 2010 Jul 15;24(14):1479–84.
18. Dejosez M, Levine SS, Frampton GM, Whyte WA, Stratton SA, Barton MC, et al. Ronin/Hcf-1 binds to a hyperconserved enhancer element and regulates genes involved in the growth of embryonic stem cells. *Genes Dev.* 2010 Jul 15;24(14):1479–84.
19. Mazars R, Gonzalez-de-Peredo A, Cayrol C, Lavigne AC, Vogel JL, Ortega N, et al. The THAP-zinc finger protein THAP1 associates with coactivator HCF-1 and O-GlcNAc transferase: a link between DYT6 and DYT3 dystonias. *J Biol Chem.* 2010 Apr 30;285(18):13364–71.
20. Quintana AM, Yu HC, Brebner A, Pupavac M, Geiger EA, Watson A, et al. Mutations in THAP11 cause an inborn error of cobalamin metabolism and developmental abnormalities. *Hum Mol Genet.* 2017 Aug 1;26(15):2838–49.
21. Pupavac M, Watkins D, Petrella F, Fahiminiya S, Janer A, Cheung W, et al. Inborn Error of Cobalamin Metabolism Associated with the Intracellular Accumulation of Transcobalamin-Bound Cobalamin and Mutations in ZNF143, Which Codes for a Transcriptional Activator. *Hum Mutat.* 2016 Sep;37(9):976–82.
22. Piton A, Gauthier J, Hamdan FF, Lafrenière RG, Yang Y, Henrion E, et al. Systematic resequencing of X-chromosome synaptic genes in autism spectrum disorder and schizophrenia. *Molecular Psychiatry.* 2011 Aug;16(8):867–80.

23. Tarpey PS, Smith R, Pleasance E, Whibley A, Edkins S, Hardy C, et al. A systematic, large-scale resequencing screen of X-chromosome coding exons in mental retardation. *Nat Genet.* 2009 May;41(5):535–43.
24. Daou S, Mashtalir N, Hammond-Martel I, Pak H, Yu H, Sui G, et al. Crosstalk between O-GlcNAcylation and proteolytic cleavage regulates the host cell factor-1 maturation pathway. *Proc Natl Acad Sci USA.* 2011 Feb 15;108(7):2747–52.
25. Capotosti F, Guernier S, Lammers F, Waridel P, Cai Y, Jin J, et al. O-GlcNAc transferase catalyzes site-specific proteolysis of HCF-1. *Cell.* 2011 Feb 4;144(3):376–88.
26. Luciano RL, Wilson AC. An activation domain in the C-terminal subunit of HCF-1 is important for transactivation by VP16 and LZIP. *Proc Natl Acad Sci USA.* 2002 Oct 15;99(21):13403–8.
27. Bhuiyan T, Waridel P, Kapuria V, Zoete V, Herr W. Distinct OGT-Binding Sites Promote HCF-1 Cleavage. *PLoS ONE.* 2015;10(8):e0136636.
28. Julien E, Herr W. Proteolytic processing is necessary to separate and ensure proper cell growth and cytokinesis functions of HCF-1. *EMBO J.* 2003 May 15;22(10):2360–9.
29. Wilson AC, Boutros M, Johnson KM, Herr W. HCF-1 amino- and carboxy-terminal subunit association through two separate sets of interaction modules: involvement of fibronectin type 3 repeats. *Mol Cell Biol.* 2000 Sep;20(18):6721–30.
30. Tyagi S, Chabes AL, Wysocka J, Herr W. E2F activation of S phase promoters via association with HCF-1 and the MLL family of histone H3K4 methyltransferases. *Mol Cell.* 2007 Jul 6;27(1):107–19.
31. Wilson AC, Parrish JE, Massa HF, Nelson DL, Trask BJ, Herr W. The gene encoding the VP16-accessory protein HCF (HCFC1) resides in human Xq28 and is highly expressed in fetal tissues and the adult kidney. *Genomics.* 1995 Jan 20;25(2):462–8.
32. Wilson AC, Freiman RN, Goto H, Nishimoto T, Herr W. VP16 targets an amino-terminal domain of HCF involved in cell cycle progression. *Mol Cell Biol.* 1997 Oct;17(10):6139–46.
33. Zhou P, Wang Z, Yuan X, Zhou C, Liu L, Wan X, et al. Mixed lineage leukemia 5 (MLL5) protein regulates cell cycle progression and E2F1-responsive gene expression via association with host cell factor-1 (HCF-1). *J Biol Chem.* 2013 Jun 14;288(24):17532–43.
34. Yokoyama A, Wang Z, Wysocka J, Sanyal M, Aufiero DJ, Kitabayashi I, et al. Leukemia proto-oncoprotein MLL forms a SET1-like histone methyltransferase

- complex with menin to regulate Hox gene expression. *Mol Cell Biol.* 2004 Jul;24(13):5639–49.
35. Misaghi S, Ottosen S, Izrael-Tomasevic A, Arnott D, Lamkanfi M, Lee J, et al. Association of C-terminal ubiquitin hydrolase BRCA1-associated protein 1 with cell cycle regulator host cell factor 1. *Mol Cell Biol.* 2009 Apr;29(8):2181–92.
  36. Machida YJ, Machida Y, Vashisht AA, Wohlschlegel JA, Dutta A. The deubiquitinating enzyme BAP1 regulates cell growth via interaction with HCF-1. *J Biol Chem.* 2009 Dec 4;284(49):34179–88.
  37. Yu H, Mashtalir N, Daou S, Hammond-Martel I, Ross J, Sui G, et al. The ubiquitin carboxyl hydrolase BAP1 forms a ternary complex with YY1 and HCF-1 and is a critical regulator of gene expression. *Mol Cell Biol.* 2010 Nov;30(21):5071–85.
  38. Tyagi S, Herr W. E2F1 mediates DNA damage and apoptosis through HCF-1 and the MLL family of histone methyltransferases. *EMBO J.* 2009 Oct 21;28(20):3185–95.
  39. Minocha S, Sung TL, Villeneuve D, Lammers F, Herr W. Compensatory embryonic response to allele-specific inactivation of the murine X-linked gene Hcfc1. *Developmental Biology.* 2016 Apr;412(1):1–17.
  40. Minocha S, Bessonard S, Sung TL, Moret C, Constam DB, Herr W. Epiblast-specific loss of HCF-1 leads to failure in anterior-posterior axis specification. *Dev Biol.* 2016 Oct 1;418(1):75–88.
  41. Minocha S, Herr W. Cortical and Commissural Defects Upon HCF-1 Loss in Nkx2.1-Derived Embryonic Neurons and Glia [Internet]. *Developmental Neurobiology.* 2019 [cited 2019 Jul 19]. Available from: <https://onlinelibrary.wiley.com/doi/abs/10.1002/dneu.22704>
  42. Minocha S, Villeneuve D, Praz V, Moret C, Lopes M, Pinatel D, et al. Rapid Recapitulation of Nonalcoholic Steatohepatitis upon Loss of Host Cell Factor 1 Function in Mouse Hepatocytes. *Mol Cell Biol.* 2019 15;39(5).
  43. Quintana AM. The necessity for in vivo functional analysis in human medical genetics. *MRA.* 2015 Nov 12;2(8).
  44. Quintana AM, Geiger EA, Achilly N, Rosenblatt DS, Maclean KN, Stabler SP, et al. Hcfc1b, a zebrafish ortholog of HCFC1, regulates craniofacial development by modulating mmachc expression. *Dev Biol.* 2014 Dec 1;396(1):94–106.
  45. Huning L, Kunkel GR. Two paralogous znf143 genes in zebrafish encode transcriptional activator proteins with similar functions but expressed at different levels during early development. *BMC Molecular and Cell Biology.* 2020 Jan 22;21(1):3.

46. Sloan JL, Achilly NP, Arnold ML, Catlett JL, Blake T, Bishop K, et al. The vitamin B12 processing enzyme, *mmachc*, is essential for zebrafish survival, growth and retinal morphology. *Hum Mol Genet*. 2020 Mar 18;
47. Bergsland M, Ramsköld D, Zaouter C, Klum S, Sandberg R, Muhr J. Sequentially acting Sox transcription factors in neural lineage development. *Genes Dev*. 2011 Dec 1;25(23):2453–64.
48. Liang Y, Vogel JL, Narayanan A, Peng H, Kristie TM. Inhibition of the histone demethylase LSD1 blocks alpha-herpesvirus lytic replication and reactivation from latency. *Nat Med*. 2009 Nov;15(11):1312–7.
49. Piluso D, Bilan P, Capone JP. Host cell factor-1 interacts with and antagonizes transactivation by the cell cycle regulatory factor Miz-1. *J Biol Chem*. 2002 Nov 29;277(48):46799–808.
50. Tyagi S, Herr W. E2F1 mediates DNA damage and apoptosis through HCF-1 and the MLL family of histone methyltransferases. *EMBO J*. 2009 Oct 21;28(20):3185–95.
51. Wysocka J, Myers MP, Laherty CD, Eisenman RN, Herr W. Human Sin3 deacetylase and trithorax-related Set1/Ash2 histone H3-K4 methyltransferase are tethered together selectively by the cell-proliferation factor HCF-1. *Genes Dev*. 2003 Apr 1;17(7):896–911.
52. Ellis P, Fagan BM, Magness ST, Hutton S, Taranova O, Hayashi S, et al. SOX2, a Persistent Marker for Multipotential Neural Stem Cells Derived from Embryonic Stem Cells, the Embryo or the Adult. *DNE*. 2004;26(2–4):148–65.
53. Amador-Arjona A, Cimadamore F, Huang CT, Wright R, Lewis S, Gage FH, et al. SOX2 primes the epigenetic landscape in neural precursors enabling proper gene activation during hippocampal neurogenesis. *PNAS*. 2015 Apr 14;112(15):E1936–45.
54. The Role of MeCP2 in Regulating Synaptic Plasticity in the Context of Stress and Depression - PMC [Internet]. [cited 2023 Mar 19]. Available from: <https://www.ncbi.nlm.nih.gov/pmc/articles/PMC8870391/>
55. Goto H, Motomura S, Wilson AC, Freiman RN, Nakabeppu Y, Fukushima K, et al. A single-point mutation in HCF causes temperature-sensitive cell-cycle arrest and disrupts VP16 function. *Genes Dev*. 1997 Mar 15;11(6):726–37.
56. Julien E, Herr W. Proteolytic processing is necessary to separate and ensure proper cell growth and cytokinesis functions of HCF-1. *EMBO J*. 2003 May 15;22(10):2360–9.
57. Reilly PT, Herr W. Spontaneous reversion of tsBN67 cell proliferation and cytokinesis defects in the absence of HCF-1 function. *Exp Cell Res*. 2002 Jul 1;277(1):119–30.

58. Parker JB, Yin H, Vinckevicius A, Chakravarti D. Host cell factor-1 recruitment to E2F-bound and cell-cycle-control genes is mediated by THAP11 and ZNF143. *Cell Rep*. 2014 Nov 6;9(3):967–82.
59. Wilson AC, Boutros M, Johnson KM, Herr W. HCF-1 amino- and carboxy-terminal subunit association through two separate sets of interaction modules: involvement of fibronectin type 3 repeats. *Mol Cell Biol*. 2000 Sep;20(18):6721–30.
60. Trimarchi JM, Lees JA. Sibling rivalry in the E2F family. *Nat Rev Mol Cell Biol*. 2002 Jan;3(1):11–20.
61. Capotosti F, Guernier S, Lammers F, Waridel P, Cai Y, Jin J, et al. O-GlcNAc Transferase Catalyzes Site-Specific Proteolysis of HCF-1. *Cell*. 2011 Feb 4;144(3):376–88.
62. Chern T, Achilleos A, Tong X, Hill MC, Saltzman AB, Reineke LC, et al. Mutations in Hcfc1 and Ronin result in an inborn error of cobalamin metabolism and ribosomopathy. *Nat Commun*. 2022 Jan 10;13(1):134.
63. Trazzi S, Mitrugno VM, Valli E, Fuchs C, Rizzi S, Guidi S, et al. APP-dependent up-regulation of Ptch1 underlies proliferation impairment of neural precursors in Down syndrome. *Hum Mol Genet*. 2011 Apr 15;20(8):1560–73.
64. Wang J, Weaver ICG, Gauthier-Fisher A, Wang H, He L, Yeomans J, et al. CBP histone acetyltransferase activity regulates embryonic neural differentiation in the normal and Rubinstein-Taybi syndrome brain. *Dev Cell*. 2010 Jan 19;18(1):114–25.
65. Dugani CB, Paquin A, Kaplan DR, Miller FD. Coffin-Lowry syndrome: a role for RSK2 in mammalian neurogenesis. *Dev Biol*. 2010 Nov 15;347(2):348–59.
66. Paronett EM, Meechan DW, Karpinski BA, LaMantia AS, Maynard TM. Ranbp1, Deleted in DiGeorge/22q11.2 Deletion Syndrome, is a Microcephaly Gene That Selectively Disrupts Layer 2/3 Cortical Projection Neuron Generation. *Cereb Cortex*. 2015 Oct;25(10):3977–93.
67. Roy A, Skibo J, Kalume F, Ni J, Rankin S, Lu Y, et al. Mouse models of human PIK3CA-related brain overgrowth have acutely treatable epilepsy. *Elife*. 2015;4.
68. Sugathan A, Biagioli M, Golzio C, Erdin S, Blumenthal I, Manavalan P, et al. CHD8 regulates neurodevelopmental pathways associated with autism spectrum disorder in neural progenitors. *Proc Natl Acad Sci USA*. 2014 Oct 21;111(42):E4468-4477.
69. Paquin A, Hordo C, Kaplan DR, Miller FD. Costello syndrome H-Ras alleles regulate cortical development. *Dev Biol*. 2009 Jun 15;330(2):440–51.
70. Cimadamore F, Amador-Arjona A, Chen C, Huang CT, Terskikh AV. SOX2-LIN28/let-7 pathway regulates proliferation and neurogenesis in neural precursors. *Proc Natl Acad Sci USA*. 2013 Aug 6;110(32):E3017-3026.

71. Pevny LH, Sockanathan S, Placzek M, Lovell-Badge R. A role for SOX1 in neural determination. *Development*. 1998 May;125(10):1967–78.
72. Mignone JL, Kukekov V, Chiang AS, Steindler D, Enikolopov G. Neural stem and progenitor cells in nestin-GFP transgenic mice. *J Comp Neurol*. 2004 Feb 9;469(3):311–24.
73. Curto GG, Gard C, Ribes V. Structures and properties of PAX linked regulatory networks architecting and pacing the emergence of neuronal diversity. *Semin Cell Dev Biol*. 2015 Aug;44:75–86.
74. Dejosez M, Krumenacker JS, Zitur LJ, Passeri M, Chu LF, Songyang Z, et al. Ronin is essential for embryogenesis and the pluripotency of mouse embryonic stem cells. *Cell*. 2008 Jun 27;133(7):1162–74.
75. Quintana AM, Yu HC, Brebner A, Pupavac M, Geiger EA, Watson A, et al. Mutations in THAP11 cause an inborn error of cobalamin metabolism and developmental abnormalities. *Human Molecular Genetics*. 2017 Aug;26(15):2838–49.
76. Michaud J, Praz V, Faresse NJ, Jnbaptiste CK, Tyagi S, Schütz F, et al. HCFC1 is a common component of active human CpG-island promoters and coincides with ZNF143, THAP11, YY1, and GABP transcription factor occupancy. *Genome Res*. 2013 Apr 25;
77. Minocha S, Sung TL, Villeneuve D, Lammers F, Herr W. Compensatory embryonic response to allele-specific inactivation of the murine X-linked gene Hcfc1. *Dev Biol*. 2016 Apr 1;412(1):1–17.
78. An S, Park UH, Moon S, Kang M, Youn H, Hwang JT, et al. Asxl1 ablation in mouse embryonic stem cells impairs neural differentiation without affecting self-renewal. *Biochem Biophys Res Commun*. 2019 Jan 15;508(3):907–13.
79. Youn HS, Kim TY, Park UH, Moon ST, An SJ, Lee YK, et al. Asxl1 deficiency in embryonic fibroblasts leads to cellular senescence via impairment of the AKT-E2F pathway and Ezh2 inactivation. *Sci Rep*. 2017 Jul 12;7(1):5198.
80. Ablain J, Durand EM, Yang S, Zhou Y, Zon LI. A CRISPR/Cas9 vector system for tissue-specific gene disruption in zebrafish. *Dev Cell*. 2015 Mar 23;32(6):756–64.
81. Hwang WY, Fu Y, Reyon D, Maeder ML, Tsai SQ, Sander JD, et al. Efficient genome editing in zebrafish using a CRISPR-Cas system. *Nat Biotechnol*. 2013 Mar;31(3):227–9.
82. Hwang WY, Fu Y, Reyon D, Maeder ML, Tsai SQ, Sander JD, et al. Efficient genome editing in zebrafish using a CRISPR-Cas system. *Nat Biotechnol*. 2013 Mar;31(3):227–9.

83. Kwan KM, Fujimoto E, Grabher C, Mangum BD, Hardy ME, Campbell DS, et al. The Tol2kit: a multisite gateway-based construction kit for Tol2 transposon transgenesis constructs. *Dev Dyn*. 2007 Nov;236(11):3088–99.
84. Atlas of Zebrafish Development [Internet]. Elsevier; 2012 [cited 2019 Nov 25]. Available from: <https://linkinghub.elsevier.com/retrieve/pii/C20090016171>
85. Atlas of Early Zebrafish Brain Development [Internet]. Elsevier; 2016 [cited 2019 Nov 25]. Available from: <https://linkinghub.elsevier.com/retrieve/pii/C20130006391>
86. Thisse C, Thisse B. High-resolution in situ hybridization to whole-mount zebrafish embryos. *Nat Protoc*. 2008;3(1):59–69.
87. Thisse C, Thisse B. High-resolution in situ hybridization to whole-mount zebrafish embryos. *Nat Protocols*. 2008 Jan;3(1):59–69.
88. Bolger AM, Lohse M, Usadel B. Trimmomatic: a flexible trimmer for Illumina sequence data. *Bioinformatics*. 2014 Aug 1;30(15):2114–20.
89. Kim D, Pertea G, Trapnell C, Pimentel H, Kelley R, Salzberg SL. TopHat2: accurate alignment of transcriptomes in the presence of insertions, deletions and gene fusions. *Genome Biol*. 2013 Apr 25;14(4):R36.
90. Trapnell C, Roberts A, Goff L, Pertea G, Kim D, Kelley DR, et al. Differential gene and transcript expression analysis of RNA-seq experiments with TopHat and Cufflinks. *Nat Protoc*. 2012 Mar 1;7(3):562–78.
91. Reyes-Nava N, Yu HC, Coughlin CR, Shaikh TH, Quintana AM. Abnormal expression of GABAA receptor sub-units and hypomotility upon loss of *gabra1* in zebrafish. *Biology Open* [Internet]. 2020 Jan 1 [cited 2020 Apr 9]; Available from: <https://bio.biologists.org/content/early/2020/03/20/bio.051367>
92. Ellis P, Fagan BM, Magness ST, Hutton S, Taranova O, Hayashi S, et al. SOX2, a persistent marker for multipotential neural stem cells derived from embryonic stem cells, the embryo or the adult. *Dev Neurosci*. 2004 Aug;26(2–4):148–65.
93. Hutton SR, Pevny LH. SOX2 expression levels distinguish between neural progenitor populations of the developing dorsal telencephalon. *Developmental Biology*. 2011 Apr 1;352(1):40–7.
94. Shen MC, Ozacar AT, Osgood M, Boeras C, Pink J, Thomas J, et al. Heat-shock-mediated conditional regulation of hedgehog/gli signaling in zebrafish. *Developmental Dynamics*. 2013;242(5):539–49.
95. Pinto D, Delaby E, Merico D, Barbosa M, Merikangas A, Klei L, et al. Convergence of genes and cellular pathways dysregulated in autism spectrum disorders. *American Journal of Human Genetics*. 2014 May;94(5):677–94.

96. Gou Y, Guo J, Maulding K, Riley BB. *sox2* and *sox3* cooperate to regulate otic/epibranchial placode induction in zebrafish. *Dev Biol.* 2018 Mar 1;435(1):84–95.
97. Pan X, Sittaramane V, Gurung S, Chandrasekhar A. Structural and Temporal Requirements of Wnt/PCP Protein Vangl2 Function for Convergence and Extension Movements and Facial Branchiomotor Neuron Migration in Zebrafish. *Mech Dev.* 2014 Feb;131:1–14.
98. Wong TT, Collodi P. Inducible Sterilization of Zebrafish by Disruption of Primordial Germ Cell Migration. *PLoS One* [Internet]. 2013 Jun 27 [cited 2019 Nov 25];8(6). Available from: <https://www.ncbi.nlm.nih.gov/pmc/articles/PMC3694954/>
99. Uni M, Kurokawa M. Role of ASXL1 mutation in impaired hematopoiesis and cellular senescence. *Oncotarget.* 2018 Dec 7;9(96):36828–9.
100. Hoischen A, van Bon BWM, Rodríguez-Santiago B, Gilissen C, Vissers LELM, de Vries P, et al. De novo nonsense mutations in ASXL1 cause Bohring-Opitz syndrome. *Nat Genet.* 2011 Aug;43(8):729–31.
101. Stainier DYR, Raz E, Lawson ND, Ekker SC, Burdine RD, Eisen JS, et al. Guidelines for morpholino use in zebrafish. *PLOS Genetics.* 2017 Oct 19;13(10):e1007000.
102. Kalueff AV, Stewart AM, Gerlai R. Zebrafish as an emerging model for studying complex brain disorders. *Trends Pharmacol Sci.* 2014 Feb;35(2):63–75.
103. Zebrafish Larvae as a Behavioral Model in Neuropharmacology [Internet]. [cited 2020 Jan 27]. Available from: <https://www.ncbi.nlm.nih.gov/pmc/articles/PMC6465999/>
104. Vinckevecius A, Parker JB, Chakravarti D. Genomic Determinants of THAP11/ZNF143/HCF1 Complex Recruitment to Chromatin. *Mol Cell Biol.* 2015 Dec;35(24):4135–46.
105. Mangone M, Myers MP, Herr W. Role of the HCF-1 basic region in sustaining cell proliferation. *PLoS ONE.* 2010;5(2):e9020.
106. Goto H, Motomura S, Wilson AC, Freiman RN, Nakabeppu Y, Fukushima K, et al. A single-point mutation in HCF causes temperature-sensitive cell-cycle arrest and disrupts VP16 function. *Genes Dev.* 1997 Mar 15;11(6):726–37.
107. Carrillo-Carrasco N, Chandler RJ, Venditti CP. Combined methylmalonic acidemia and homocystinuria, cblC type. I. Clinical presentations, diagnosis and management. *J Inher Metab Dis.* 2012 Jan;35(1):91–102.
108. Zhang P, Chen Z, Li R, Guo Y, Shi H, Bai J, et al. Loss of ASXL1 in the bone marrow niche dysregulates hematopoietic stem and progenitor cell fates. *Cell Discov.* 2018;4:4.

109. Yang H, Kurtenbach S, Guo Y, Lohse I, Durante MA, Li J, et al. Gain of function of ASXL1 truncating protein in the pathogenesis of myeloid malignancies. *Blood*. 2018 18;131(3):328–41.
110. Inoue D, Fujino T, Sheridan P, Zhang YZ, Nagase R, Horikawa S, et al. A novel ASXL1-OGT axis plays roles in H3K4 methylation and tumor suppression in myeloid malignancies. *Leukemia*. 2018;32(6):1327–37.
111. Reyes-Nava, Nayeli G., Hernandez, Jose A., Castro, Victoria L., Reyes, Joel F., Castellanos, Barbara S., Quintana, Anita M. Zebrafish: A Comprehensive Model to Understand the Mechanisms Underlying Neurodevelopmental Disorders. In: Costa, Andres., Villalba, Eugenio., editors. *Horizons in Neuroscience Research*. Nova Biomedical; 2018.
112. Afrikanova T, Serruys ASK, Buenafe OEM, Clinckers R, Smolders I, de Witte PAM, et al. Validation of the zebrafish pentylenetetrazol seizure model: locomotor versus electrographic responses to antiepileptic drugs. *PLoS ONE*. 2013;8(1):e54166.
113. Ciura S, Lattante S, Le Ber I, Latouche M, Tostivint H, Brice A, et al. Loss of function of C9orf72 causes motor deficits in a zebrafish model of amyotrophic lateral sclerosis. *Ann Neurol*. 2013 Aug;74(2):180–7.
114. Liu Y, Carmer R, Zhang G, Venkatraman P, Brown SA, Pang CP, et al. Statistical Analysis of Zebrafish Locomotor Response. *PLoS ONE*. 2015;10(10):e0139521.
115. Li F, Lin J, Liu X, Li W, Ding Y, Zhang Y, et al. Characterization of the locomotor activities of zebrafish larvae under the influence of various neuroactive drugs. *Ann Transl Med*. 2018 May;6(10):173.
116. Kalueff AV, Gebhardt M, Stewart AM, Cachat JM, Brimmer M, Chawla JS, et al. Towards a Comprehensive Catalog of Zebrafish Behavior 1.0 and Beyond. *Zebrafish*. 2013 Mar;10(1):70–86.
117. Lattante S, de Calbiac H, Le Ber I, Brice A, Ciura S, Kabashi E. Sqstm1 knock-down causes a locomotor phenotype ameliorated by rapamycin in a zebrafish model of ALS/FTLD. *Hum Mol Genet*. 2015 Mar 15;24(6):1682–90.
118. Bonnin E, Cabochette P, Filosa A, Jühlen R, Komatsuzaki S, Hezwani M, et al. Biallelic mutations in nucleoporin NUP88 cause lethal fetal akinesia deformation sequence. *PLoS Genet*. 2018;14(12):e1007845.
119. Gérard M, Morin G, Bourillon A, Colson C, Mathieu S, Rabier D, et al. Multiple congenital anomalies in two boys with mutation in HCFC1 and cobalamin disorder. *Eur J Med Genet*. 2015 Mar;58(3):148–53.
120. Yu HC, Sloan JL, Scharer G, Brebner A, Quintana AM, Achilly NP, et al. An X-Linked Cobalamin Disorder Caused by Mutations in Transcriptional Coregulator HCFC1. *Am J Hum Genet*. 2013 Sep 5;93(3):506–14.

121. Huang L, Jolly LA, Willis-Owen S, Gardner A, Kumar R, Douglas E, et al. A Noncoding, Regulatory Mutation Implicates HCFC1 in Nonsyndromic Intellectual Disability. *Am J Hum Genet.* 2012 Oct 5;91(4):694–702.
122. Jolly LA, Nguyen LS, Domingo D, Sun Y, Barry S, Hancarova M, et al. HCFC1 loss-of-function mutations disrupt neuronal and neural progenitor cells of the developing brain. *Hum Mol Genet.* 2015 Jun 15;24(12):3335–47.
123. Koufaris C, Alexandrou A, Tanteles GA, Anastasiadou V, Sismani C. A novel HCFC1 variant in male siblings with intellectual disability and microcephaly in the absence of cobalamin disorder. *Biomed Rep.* 2016 Feb;4(2):215–8.
124. Piton A, Gauthier J, Hamdan FF, Lafrenière RG, Yang Y, Henrion E, et al. Systematic resequencing of X-chromosome synaptic genes in autism spectrum disorder and schizophrenia. *Molecular Psychiatry.* 2011 Aug;16(8):867–80.
125. Piton A, Redin C, Mandel JL. XLID-Causing Mutations and Associated Genes Challenged in Light of Data From Large-Scale Human Exome Sequencing. *Am J Hum Genet.* 2013 Aug 8;93(2):368–83.
126. Castro VL, Reyes JF, Reyes-Nava NG, Paz D, Quintana AM. Hcfc1a regulates neural precursor proliferation and asxl1 expression in the developing brain. *BMC Neurosci.* 2020 Jun 10;21(1):27.
127. Quintana AM, Yu HC, Brebner A, Pupavac M, Geiger EA, Watson A, et al. Mutations in THAP11 cause an inborn error of cobalamin metabolism and developmental abnormalities. *Human Molecular Genetics.* 2017 Aug;26(15):2838–49.
128. Minocha S, Sung TL, Villeneuve D, Lammers F, Herr W. Compensatory embryonic response to allele-specific inactivation of the murine X-linked gene Hcfc1. *Developmental Biology.* 2016 Apr;412(1):1–17.
129. Minocha S, Herr W. Cortical and Commissural Defects Upon HCF-1 Loss in Nkx2.1-Derived Embryonic Neurons and Glia. *Dev Neurobiol.* 2019 Jun;79(6):578–95.
130. Mazars R, Gonzalez-de-Peredo A, Cayrol C, Lavigne AC, Vogel JL, Ortega N, et al. The THAP-zinc finger protein THAP1 associates with coactivator HCF-1 and O-GlcNAc transferase: a link between DYT6 and DYT3 dystonias. *J Biol Chem.* 2010 Apr 30;285(18):13364–71.
131. Dejosez M, Krumenacker JS, Zitur LJ, Passeri M, Chu LF, Songyang Z, et al. Ronin is essential for embryogenesis and the pluripotency of mouse embryonic stem cells. *Cell.* 2008 Jun 27;133(7):1162–74.
132. Dejosez M, Levine SS, Frampton GM, Whyte WA, Stratton SA, Barton MC, et al. Ronin/Hcf-1 binds to a hyperconserved enhancer element and regulates genes involved in the growth of embryonic stem cells. *Genes Dev.* 2010 Jul 15;24(14):1479–84.

133. Gabut M, Bourdelais F, Durand S. Ribosome and Translational Control in Stem Cells. *Cells*. 2020 Feb 21;9(2):497.
134. Parenti I, Rabaneda LG, Schoen H, Novarino G. Neurodevelopmental Disorders: From Genetics to Functional Pathways. *Trends in Neurosciences*. 2020 Aug 1;43(8):608–21.
135. Fleming A, Rubinsztein DC. Zebrafish as a model to understand autophagy and its role in neurological disease. *Biochim Biophys Acta*. 2011 Apr;1812(4):520–6.
136. An S, Park UH, Moon S, Kang M, Youn H, Hwang JT, et al. *Asxl1* ablation in mouse embryonic stem cells impairs neural differentiation without affecting self-renewal. *Biochem Biophys Res Commun*. 2019 Jan 15;508(3):907–13.
137. Cornell B, Toyo-oka K. 14-3-3 Proteins in Brain Development: Neurogenesis, Neuronal Migration and Neuromorphogenesis. *Front Mol Neurosci*. 2017 Oct 12;10:318.
138. Gómez-Suárez M, Gutiérrez-Martínez IZ, Hernández-Trejo JA, Hernández-Ruiz M, Suárez-Pérez D, Candelario A, et al. 14-3-3 Proteins regulate Akt Thr308 phosphorylation in intestinal epithelial cells. *Cell Death Differ*. 2016 Jun;23(6):1060–72.
139. Youn HS, Kim TY, Park UH, Moon ST, An SJ, Lee YK, et al. *Asxl1* deficiency in embryonic fibroblasts leads to cellular senescence via impairment of the AKT-E2F pathway and *Ezh2* inactivation. *Sci Rep*. 2017 Jul 12;7(1):5198.
140. Kwan KM, Fujimoto E, Grabher C, Mangum BD, Hardy ME, Campbell DS, et al. The Tol2kit: a multisite gateway-based construction kit for Tol2 transposon transgenesis constructs. *Dev Dyn*. 2007 Nov;236(11):3088–99.
141. Quintana AM, Geiger EA, Achilly N, Rosenblatt DS, Maclean KN, Stabler SP, et al. *Hcfc1b*, a zebrafish ortholog of HCFC1, regulates craniofacial development by modulating *mmachc* expression. *Dev Biol*. 2014 Dec 1;396(1):94–106.
142. Kosuta C, Daniel K, Johnstone DL, Mongeon K, Ban K, LeBlanc S, et al. High-throughput DNA Extraction and Genotyping of 3dpf Zebrafish Larvae by Fin Clipping. *J Vis Exp*. 2018 29;(136).
143. Bresciani E, Broadbridge E, Liu PP. An efficient dissociation protocol for generation of single cell suspension from zebrafish embryos and larvae. *MethodsX*. 2018 Oct 10;5:1287–90.
144. Quintana AM, Liu F, O'Rourke JP, Ness SA. Identification and regulation of c-Myb target genes in MCF-7 cells. *BMC Cancer*. 2011;11:30.
145. Hudish LI, Blasky AJ, Appel B. miR-219 regulates neural precursor differentiation by direct inhibition of apical par polarity proteins. *Dev Cell*. 2013 Nov 25;27(4):387–98.

146. Kapuria V, Röhrig UF, Bhuiyan T, Borodkin VS, van Aalten DMF, Zoete V, et al. Proteolysis of HCF-1 by Ser/Thr glycosylation-incompetent O-GlcNAc transferase:UDP-GlcNAc complexes. *Genes Dev.* 2016 Apr 15;30(8):960–72.
147. Dehaene H, Praz V, Lhôte P, Lopes M, Herr W. THAP11F80L cobalamin disorder-associated mutation reveals normal and pathogenic THAP11 functions in gene expression and cell proliferation. *PLoS One.* 2020;15(1):e0224646.
148. Gjini E, Jing CB, Nguyen AT, Reyon D, Gans E, Kesarsing M, et al. Disruption of *asxl1* results in myeloproliferative neoplasms in zebrafish. *Dis Model Mech.* 2019 May 7;12(5):dmm035790.
149. Uni M, Kurokawa M. Role of ASXL1 mutation in impaired hematopoiesis and cellular senescence. *Oncotarget.* 2018 Dec 7;9(96):36828–9.
150. ENCODE Project Consortium. An integrated encyclopedia of DNA elements in the human genome. *Nature.* 2012 Sep 6;489(7414):57–74.
151. Luo Y, Hitz BC, Gabdank I, Hilton JA, Kagda MS, Lam B, et al. New developments on the Encyclopedia of DNA Elements (ENCODE) data portal. *Nucleic Acids Res.* 2020 Jan 8;48(D1):D882–9.
152. Rouillard AD, Gundersen GW, Fernandez NF, Wang Z, Monteiro CD, McDermott MG, et al. The harmonizome: a collection of processed datasets gathered to serve and mine knowledge about genes and proteins. *Database (Oxford).* 2016;2016:baw100.
153. Scalais E, Osterheld E, Weitzel C, De Meirleir L, Mataigne F, Martens G, et al. X-Linked Cobalamin Disorder (HCFC1) Mimicking Nonketotic Hyperglycinemia With Increased Both Cerebrospinal Fluid Glycine and Methylmalonic Acid. *Pediatr Neurol.* 2017 Jun;71:65–9.
154. Minocha S, Bessonard S, Sung TL, Moret C, Constam DB, Herr W. Epiblast-specific loss of HCF-1 leads to failure in anterior-posterior axis specification. *Dev Biol.* 2016 Oct 1;418(1):75–88.
155. Julien E, Herr W. Proteolytic processing is necessary to separate and ensure proper cell growth and cytokinesis functions of HCF-1. *EMBO J.* 2003 May 15;22(10):2360–9.
156. Julien E, Herr W. A switch in mitotic histone H4 lysine 20 methylation status is linked to M phase defects upon loss of HCF-1. *Mol Cell.* 2004 Jun 18;14(6):713–25.
157. Luciano RL, Wilson AC. An activation domain in the C-terminal subunit of HCF-1 is important for transactivation by VP16 and LZIP. *Proc Natl Acad Sci USA.* 2002 Oct 15;99(21):13403–8.

158. Mangone M, Myers MP, Herr W. Role of the HCF-1 basic region in sustaining cell proliferation. *PLoS ONE*. 2010;5(2):e9020.
159. Johnston JJ, Olivos-Glander I, Killoran C, Elson E, Turner JT, Peters KF, et al. Molecular and Clinical Analyses of Greig Cephalopolysyndactyly and Pallister-Hall Syndromes: Robust Phenotype Prediction from the Type and Position of GLI3 Mutations. *Am J Hum Genet*. 2005 Apr;76(4):609–22.
160. Johnson K, Barragan J, Bashiruddin S, Smith CJ, Tyrrell C, Parsons MJ, et al. Gfap-Positive Radial Glial Cells Are an Essential Progenitor Population for Later-Born Neurons and Glia in the Zebrafish Spinal Cord. *Glia*. 2016 Jul;64(7):1170–89.
161. Li X, Liu G, Yang L, Li Z, Zhang Z, Xu Z, et al. Decoding Cortical Glial Cell Development. *Neurosci Bull*. 2021 Apr 1;37(4):440–60.
162. Iadevaia V, Liu R, Proud CG. mTORC1 signaling controls multiple steps in ribosome biogenesis. *Seminars in Cell & Developmental Biology*. 2014 Dec 1;36:113–20.
163. Castro VL, Paz D, Virrueta V, Estevao IL, Grajeda BI, Ellis CC, et al. Missense and nonsense mutations of the zebrafish *hcfc1a* gene result in contrasting mTor and radial glial phenotypes. *Gene*. 2023 May 15;864:147290.
164. Moloney PB, Cavalleri GL, Delanty N. Epilepsy in the mTORopathies: opportunities for precision medicine. *Brain Commun*. 2021 Sep 25;3(4):fcab222.
165. Castro VL, Quintana AM. The role of HCFC1 in syndromic and non-syndromic intellectual disability. *Medical Research Archives [Internet]*. 2020 Jun 18 [cited 2020 Dec 7];8(6). Available from: <https://esmed.org/MRA/mra/article/view/2122>

## BIOGRAPHICAL SKETCH

(contact: [vlcastro2@miners.utep.edu](mailto:vlcastro2@miners.utep.edu))

My name is Victoria Castro and my previous education includes receiving an Associate of Science Degree from El Paso Community College (EPCC) in 2017 and a Bachelor of Science in Biological Sciences Degree from the University of Texas at El Paso (UTEP) in 2017. In 2018, I joined as a doctoral student in the Biosciences PhD program at UTEP in the laboratory of Dr. Anita Quintana. My long-term future career goal is to become an independent investigator with my own research program to investigate the pathogenesis of neurodevelopmental disorders. I aim to become an academic faculty at a research-intensive institute and devote my career to educating and advancing the careers of underrepresented minorities (URMs) or persons excluded due to ethnicity and race (PEERs) in scientific research and academia. Below is a logical summary of my research and training experiences in support of my long-term career goal.

Throughout my PhD program I gained considerable experience instructing undergraduates with 1.5 years served as a teaching assistant in introductory biology topics and one summer as an assistant instructor in Developmental Neurobiology. Collectively over the course of five years, I published 4 first author and 2 middle-author manuscripts, 1 first-author review article, and 1 middle-author book chapter. In addition, I was invited on many occasions to present my research orally at national and international conferences (SACNAS 2018, SDB 2019, ZDMS 2022), with 1 best oral presentation award at the national level (SACNAS). I was awarded the UTEP Dodson Research Grant from 2019 to 2020 that helped fund preliminary data to support my initial F99 application. I was also granted the Keelung Hong Graduate Research Fellowship in January of 2022, which helped fully support my stipend and international travel (Sheffield, UK) to disseminate my work (ZDMS 2022) In addition, I was invited to conduct formal reviews for the Journal of Neuroscience Letters, and Genetics and G3 journals.

In June of 2022, I was awarded the National Institute of Neurological Disorders (NINDS) F99/K00 Diversity Specialized Predoctoral to Postdoctoral Advancement in Neuroscience (DSPAN) award. This award provided me funding for my last year of PhD and the next four years of my postdoctoral position. In my future work, I seek to broaden my knowledge of the epigenetic mechanisms that regulate neural precursor cell development in higher mammalian vertebrate systems. As a step towards this, I will take on a postdoctoral position in the laboratory of Dr. Jamy Peng at St. Jude Children's Research Hospital in the Department of Developmental Neurobiology beginning August 2023. In the future, I plan to extend my training and development into my own independent research program and secure a tenure-track teaching position at a competitive institution. Based on the well-rounded research and academic trajectory evidenced over the last six years, I believe I am well positioned to complete my overarching career goal of becoming an independent investigator and future assistant professor.